Analysis of the Quasicontinuum Method and Its Application

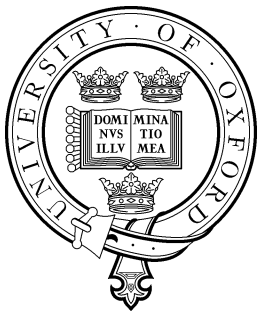

Hao Wang

Balliol College

University of Oxford

A thesis submitted for the degree of

Doctor of Philosophy

Trinity 2012

Acknowledgements

It has been four years of hard but inspiring work in Oxford, during which this thesis could be completed. I would like to take this opportunity to thank people for their support and help.

First of all, I would like to thank my supervisor Professor Christoph Ortner and Co-supervisor Professor Endre Süli for their heuristic and instructive supervision, especially the former one who I have closely worked with for four years and have changed the way I think in many aspects through our inspiring and interesting discussions, which definitely has a braoder impact on me than just academic.

I would like to address a special thanks to Professor Ping Lin, who was the advisor of my undergraduate project and the very first person brought me to the area that I have been working on for my DPhil. This initiation has greatly influenced the path of my life.

The Numerical Analysis Group have provided me the excellent research environment and support and I should thank all the members of the group.

Oxford is an magical place. It is especially true in my case as it has vastly broadened my vision and knowledge. So I'd like to thank the

university and everything in and around it for offering me such an amazing experience.

I would also like to thank Balliol College who has afforded me a lot of convenience for daily life as well as great opportunities for academic and working experiences. A special thanks should be given to Ms Glynis Price, the academic administrator of the college, who has provided me enormous amount of help since the very first day I became a member of the college.

My funding body China Scholarship Council and Sichuan University in which I did my undergraduate provide the financial support to me. I wish all the best to the future development of them and hope my country China will truly benefit from supporting the students and scholars to study and visit in different parts of the world.

Last but not the least, I would like to thank my wife Yue Cai, my parents Zeyun Wang and Xiaoyun Su for their love and support. I couldn't imagine what I have achieved so far without their continuous and tremendous help.

Abstract

The present thesis is on the error estimates of different energy based quasicontinuum (QC) methods, which are a class of computational methods for the coupling of atomistic and continuum models for micro- or nano-scale materials.

The thesis consists of two parts. The first part considers the a priori error estimates of three energy based QC methods. The second part deals with the a posteriori error estimates of a specific energy based QC method which was recently developed.

In the first part, we develop a unified framework for the a priori error estimates and present a new and simpler proof based on negative-norm estimates, which essentially extends previous results.

In the second part, we establish the a posteriori error estimates for the newly developed energy based QC method for an energy norm and for the total energy. The analysis is based on a posteriori residual and stability estimates. Adaptive mesh refinement algorithms based on these error estimators are formulated.

In both parts, numerical experiments are presented to illustrate the results of our analysis and indicate the optimal convergence rates.

The thesis is accompanied by a thorough introduction to the development of the QC methods and its numerical analysis, as well as an outlook of the future work in the conclusion.

Contents

List of Figures

Chapter 1

Introduction

The development of micro-scale technologies in recent decades has changed the focus of the research on materials to nano-scale systems. Systems like computer chips and micro-electromechanical devices that are typically on a micro- or nano-scale are often of great research interest. This change of focus has revealed the defect of continuum mechanics, in which a material is assumed to be comprised of an infinitely divisible continuous medium and the governing equations for deformation remain unchanged regardless of the size of the body.

However, while full atomistic models are necessary for the understanding of mechanism of certain deformation processes, it should also be noted that it is neither practical nor necessary to give up continuum mechanics. This is because the bulk of a material behaves according to continuum mechanics during a deformation process and the density of atoms in a typical material is about $10^{20}\text{atoms}/\text{mm}^3$, while the current limit of full atomistic simulation is only on the order of 10^9 atoms.

Therefore, researchers have been developing computational techniques that retain continuum mechanics in the bulk of a material but use atomistic modeling and computation to keep sufficient detail of a deformation process in regions of

interest. Quasicontinuum (QC) methods are a class of techniques that have been developed according to such principle. The philosophy of QC methods is to take the nonlocal discrete atomistic models as the 'correct' description of the material behavior, while applying continuum models together with finite element discretizations in the far field away from large deformations, where linear elasticity or Cauchy–Born rule could be good approximations to the original atomistic model, to reduce the computational cost. By applying such techniques, the important information on a deformation process is preserved while the computational cost is significantly reduced.

The present thesis is devoted to the numerical analysis, especially the error estimates, of different types of quasicontinuum methods in the zero temperature static setting. The first part (Chapter 2) considers the a priori error estimates of three energy based QC methods. The second part (Chapter 3) deals with the a posteriori error estimates of a specific energy based QC method that has recently been developed. Although the atomistic model considered in this work is relatively simple, we believe it is valuable to the full mathematical understanding of the QC methods as many aspects of a more general analysis are clearly revealed.

1.1 Atomistic Models

We restrict the modeling to atomistic systems consisting of atoms of the same species denoted by the set $\mathbb{L}$. It is often assumed, though rigorously proved in few cases, that the ground state of an atomistic system, which corresponds to the global minimizer of the energy of the system, is a Bravais lattice $\mathsf{B}\mathbb{Z}^d$, where d is the dimension of the atomistic system, $\mathsf{B} \in \mathbb{R}_+^{d\times d}$ and $\mathbb{R}_+^{d\times d}$ is the set of the d by d

matrices with positive determinants. Therefore, for the convenience of the presentation, we always assume that $\mathbb{L} \subset \mathbb{B}\mathbb{Z}^d$. The deformation $\boldsymbol{y}$ of the atomistic body is considered as a discrete map $\boldsymbol{y} : \mathbb{L} \to \mathbb{R}^d$.

Empirical molecular interaction models are often employed to compute the stored energy of the atomistic system. They consist of the contributions due to pair interactions of the atoms and contributions due to many body interactions. For pair interaction potentials, a typical example is given by

$$\mathcal{E}_{\mathrm{a}}(\boldsymbol{y}) = W_{pair}(\boldsymbol{y}) := \sum_{i \neq j} \phi(|y(i) - y(j)|), \tag{1.1.1}$$

where $i, j \in \mathbb{L}$, ϕ is a Lennard-Jones type interaction potential. This model has been extensively employed as the atomistic model for the QC methods and other atomistic to continuum coupling methods.

The many-body potentials can be written in an abstract form as

$$\mathcal{E}_{\mathrm{a}}(\boldsymbol{y}) = W_{pair}(\boldsymbol{y}) + W_{many-body}(\boldsymbol{y}). \tag{1.1.2}$$

Two typical example, named the Embedded Atom Method (EAM) model and Stillinger-Webber (SW) model, of this type of potentials can be found in [12] and [68].

In addition to the stored energy of the atomistic system, there may be energy due to the external loads $\mathcal{E}_{ext}$. In the simplest case where the external force is a dead load on the atoms or a linearization of a force field, $\mathcal{E}_{ext}$ is given by

$$\mathcal{E}_{ext}(\boldsymbol{y}) := -\boldsymbol{f} \cdot \boldsymbol{u}, \tag{1.1.3}$$

where $\boldsymbol{u} = \boldsymbol{y} - \mathbb{L}$ is the displacement of the atoms.

Therefore, the total energy of the atomistic system is given by

$$E_{\mathrm{a}}(\boldsymbol{y}) = \mathcal{E}_{\mathrm{a}}(\boldsymbol{y}) + \mathcal{E}_{ext}(\boldsymbol{y}), \tag{1.1.4}$$

and the full atomistic problem is to find $\boldsymbol{y}_{\mathrm{a}}$ such that

$$\boldsymbol{y}_{\mathrm{a}} \in \operatorname{argmin} E_{\mathrm{a}}(\mathcal{Y}^{\mathrm{a}}), \tag{1.1.5}$$

where $\mathcal{Y}^{\mathrm{a}}$ is an admissible set of deformation where we look for the solution and argmin denotes the set of local minimizers.

1.2 Continuum Models

Though (1.1.4) is considered to be accurate, its computational cost is normally of order $O(N)$ where N is the total number of the atoms in the system. Since N is often large, in real computations, we need to find an approximation to this energy.

Since Crystalline solids deform elastically without defects, i.e., the deformation $\boldsymbol{y}$ is locally close to Bravais lattices [36], a smooth deformation field $\boldsymbol{x} \to \boldsymbol{y}(\boldsymbol{x}), \boldsymbol{x} \in \Omega$ is often observed, where Ω is the continuous reference configuration and $\mathbb{L} \subset \Omega$. Under a smooth deformation, the stored energy can be approximated by the well-known Cauchy–Born elastic energy.

Here we remark that through out the thesis, we often identify a lattice function v with its continuous interpolation $v(\boldsymbol{x})$ and use the same notation to represent both objects in some cases.

The Cauchy–Born elastic energy essentially approximate the atomistic stored energy by the integration of an energy density functional which only depends

on the local deformation gradient, namely $\nabla \boldsymbol{y}(x)$. There are many different approaches to develop the Cauchy–Born energy density functional (c.f. [23, 36]), and here we briefly derive it following the approach adopted in [36].

From (1.1.1) in 1.1, we see that the stored energy could be written as

$$\mathcal{E}_{\mathrm{a}}(\boldsymbol{y}) = \sum_{i \in \mathbb{L}} \sum_{j \neq i, j \in \mathbb{L}} V^{\mathrm{a}}(y(j) - y(i)), \tag{1.2.1}$$

where V^{a} is the pair interaction potential. Under a homogeneous deformation, we could replace finite differences $y(j) - y(i)$ by the directional derivatives $\nabla_{j-i}\boldsymbol{y}$. Approximating the summations by integration, we may further approximate (1.2.1) by

$$\begin{aligned} \mathcal{E}_{\mathrm{a}}(\boldsymbol{y}) &= \sum_{i \in \mathbb{L}} \sum_{j \neq i, j \in \mathbb{L}} V^{\mathrm{a}}(y(j) - y(i)) \\ &\approx \sum_{i \in \mathbb{L}} \sum_{j \neq i, j \in \mathbb{L}} V^{\mathrm{a}}(\nabla_{j-i}\boldsymbol{y}) \approx \int_{\Omega} W(\nabla \boldsymbol{y}(x))\, \mathrm{d}x =: \mathcal{E}_c(\boldsymbol{y}), \end{aligned} \tag{1.2.2}$$

where $W(F) := \frac{1}{\det \mathsf{B}} V^{\mathrm{a}}(\{F\xi\}_{\xi \in B\mathbb{Z}^d \setminus \{0\}})$. $\mathcal{E}_c(\cdot)$ is often defined as the continuum energy functional. With suitable simplification of the external energy functional $\mathcal{E}_{ext}(\cdot)$, the total continuum energy of the system is given by

$$E_{\mathrm{c}}(\boldsymbol{y}) = \mathcal{E}_{\mathrm{c}}(\boldsymbol{y}) + \mathcal{E}_{ext}(\boldsymbol{y}), \tag{1.2.3}$$

and the full continuum problem is to find $\boldsymbol{y}_{\mathrm{c}}$ such that

$$\boldsymbol{y}_{\mathrm{c}} \in \operatorname{argmin} E_{\mathrm{c}}(\mathcal{Y}^{\mathrm{c}}), \tag{1.2.4}$$

where $\mathcal{Y}^{\mathrm{c}}$ is an admissible set of deformation where we look for the solution.

The Cauchy–Born energy approximation is in paricular efficient in real computations when it is used together with finite element method, as the integration

becomes a summation over elements whose computational cost is of order $O(K)$, where K is the number of the elements provided one can take $K \ll N$. However, since the Cauchy–Born energy is equal to the atomistic energy only under homogeneous deformation, we need to consider the accuracy of this approximation.

1.2.1 The Scaling Parameter and the Order of Accuracy

We introduce the scaling parameter and the order of accuracy before we present the error estimate of the Cauchy–Born approximation as these concepts are important throughout this thesis. In the atomistic model introduced above, the interatomic spacing of the Bravais lattice $\mathbb{L}$ is not defined. In the analysis and the computation of an atomistic system, $\varepsilon = 1/N^{1/d}$ is always assumed to be the interatomic spacing, where d is the dimension of the system and N is the total number of atoms in the system except for periodic boundary conditions, where N is the number of atoms in one period of the infinite system. Such ε is often taken to be the scaling parameter of the system and the length of the system is thus rescaled to be of order $O(1)$. Furthermore, if we multiply the energy E_{a} or E_{c} by ε^d, the total energy will also become of order $O(1)$.

Under this rescaling, the error estimate of an approximation with respect to its underlying atomistic model is often given by a product of a power of ε and a constant that depends on the derivatives of either the solution of the atomistic problem $\boldsymbol{y}_{\mathrm{a}}$ or that of its approximation $\boldsymbol{y}_{\mathrm{c}}$ as well as the energy functionals. The order of accuracy of an approximation is often considered to be the power of ε.

1.2.2 Accuracy of the Cauchy–Born approximation

Though the Cauchy–Born approximation is widely used [25], the accuracy of this approximation was not established mathematically until fairly recently.

Blanc et al. prove in [6] that for energy functionals consisting only of pair interaction potentials, the a priori error of the energy for a smooth deformation field $\boldsymbol{y}$ is estimated by

$$|\mathcal{E}_{\mathrm{c}}(\boldsymbol{y}) - \mathcal{E}_{\mathrm{a}}(\boldsymbol{y})| \leq C\varepsilon^2\big(\|D^2\boldsymbol{y}\|^2_{L^2(\Omega)} + \|D^3\boldsymbol{y}\|_{L^1(\Omega)}\big) \tag{1.2.5}$$

where D is the differential operator and C depends on the pair potential ϕ and $D\boldsymbol{y}$.

E and Ming analyze the convergence of the solution of the continuum problem and that of the corresponding atomistic problem under mild external deadload and with periodic boundary conditions [23, 22]. A sharp analysis of this problem is given by Ortner and Theil in [56] and the a posteriori error estimate could be summarized as

$$\|D\boldsymbol{y}_{\mathrm{a}} - D\boldsymbol{y}_{\mathrm{c}}\|_{L^2(\Omega)} \leq C\varepsilon^2(\|D^2\boldsymbol{y}_{\mathrm{c}}\|^2_{L^4(\Omega)} + \|D^3\boldsymbol{y}_{\mathrm{c}}\|_{L^2(\Omega)}), \tag{1.2.6}$$

for simple lattices, where C depends on the atomistic energy functional V^{a} and $D\boldsymbol{y}_c$. An order $O(\varepsilon)$ estimate of the deformation gradient in $L^2 - norm$ holds for complex lattices which consist of two species of atoms. As a result, we say the Cauchy–Born approximation is a second-order approximation for simple lattices and a first-order approximation for complex lattices. It should be noted that the estimates hold for V^{a} that is smooth in a the neighbourhood of the equilibrium state and the geometry of the lattice is very important in the stability which is a key component for this estimate to hold.

We see from the above estimates that if an atomistic system consists of a large number of atoms and experiences a smooth deformation relative to the atomistic scale, the Cauchy–Born model or even simpler models such as the linear elasticity models are good approximations of the atomistic model. This is the place where classical continuum mechanics plays an important role. However, since the number of atoms is limited in a micro-scale system and the deformation field may vary drastically in a certain region, the continuum approximation of the atomistic system may give a solution that is not comparable to that of the original atomistic problem. This motivates coupling the two models together to give a solution that retains the accuracy of the atomistic model while reducing the computational cost. This is the starting point of the development of the quasicontinuum methods and other atomistic to continuum methods, which we introduce in the next section.

1.3 The Quasicontinuum and Other Atomistic to Continuum Methods

We first give a mathematical description of the loss of validity of the continuum approximation. Theoretical analysis as well as numerical computations give that the deformation field near a defect is singular, for example, we have $|D^2\boldsymbol{y}_a| \sim r^{-2}$ for a dislocation and $|D^2\boldsymbol{y}_a| \sim r^{-3}$ for a vacancy in a two dimensional system (c.f. [26, 54]), where r is the distance to the core of the defect. Therefore, according to the error estimates, we would have $\varepsilon^2\|D^2\boldsymbol{y}_{\mathrm{a}}\|^2_{L^2(\Omega)}$ being of $O(1)$ near the defect core which implies that the error of the energy approximation may be uncontrolled. However, it is not necessary to use the full atomistic model as $|D^2\boldsymbol{y}_a|$ goes to 0 in the far field, which gives a perfect environment where the continuum

approximation can be employed with high accuracy.

Therefore, the model to couple the atomistic model and its continuum approximation becomes conceptually ideal for the accurate and efficient computation of the deformation of an atomistic system, where the atomistic model should be used near the defects while the continuum model in the far field.

Efforts have been made by a number of researchers over the last decades and here we give a brief summary of different atomistic to continuum coupling methods. Since our research is mainly in the numerical analysis of the quasicontinuum methods, we divide the methods to the class of quasicontinuum methods and that of other atomistic to continuum coupling methods. We note that this summary is by no means complete but only to give an introduction to the models we are working on.

1.3.1 The Quasicontinuum(QC) Methods

The first QC method was developed by Tadmor et al. in [48] in 1996. Several important ideas that have been adopted by the subsequent developments were initiated in this work.

The *first* idea is to use finite element discritization of the domain to reduce the number of degrees of freedom in the far field of the defects. Though simple and natural, this idea essentially leads to the *second* but the most important feature of all QC methods which is the simultaneous use of atomistic and continuum or continuum-like models. The computation of the energy of the representative crystallites which entirely lie in one linear element implicitly leads to the Cauchy–Born approximation of the energy, and the energy of the representative crystallites

which may cross several elements retain the atomistic model.

Another feature of this work is to formulate the problem as an energy minimization problem in a proper solution space, which is adopted by all the energy based QC methods as opposed to the force based QC methods which will be introduced in a following section.

Since its invention, there has been a great development and several variants of the original idea, some of which we introduce in the following sections.

1.3.1.1 The Original Energy Based QC method

As mentioned above, the orginal energy based QC method was first conceived in [48] and further developed in [65, 66]. The formulation of this QC method is best understood in the following way.

We first decompose the domain Ω into two different subdomains Ω_a and Ω_c such that $\Omega_a \cup \Omega_c = \Omega$ where Ω_a contains all the defects and Ω_c contains the far field. In most cases, $|\Omega_c| >> |\Omega_a|$.

We then construct a partition $\mathcal{T}$ of Ω, which is usually a mesh in 1D, a triangulation in 2D and a tetrahedral in 3D, such that $\mathcal{N}_\mathcal{T} \subset \mathbb{L}$ and $\mathbb{L} \cap \Omega_a \subset \mathcal{N}_\mathcal{T}$ which indicates that each atom in the atomistic region is a node in the partition. A continuous deformation field $\boldsymbol{y}_h : \Omega \to \mathbb{R}^d$ is then defined such that $\boldsymbol{y}_h$ is piecewise affine with respect to the partition $\mathcal{T}$. A corresponding displacement field $\boldsymbol{u}_h := \boldsymbol{y}_h - \mathbb{L}$ is immediately obtained. This process significantly reduces the number of degrees of freedom.

We finally consider the coupling of the stored energy. The stored energy of the atomistic system could be assigned to each atom and further decomposed accord-

ing to the location of the atoms as

$$\mathcal{E}_{\mathrm{a}}(\boldsymbol{y}_h) = \sum_i \mathcal{E}_i^{\mathrm{a}}(\boldsymbol{y}_h) = \sum_{i\in\Omega_a} \mathcal{E}_i^{\mathrm{a}}(\boldsymbol{y}_h) + \sum_{i\in\Omega_c} \mathcal{E}_i^{\mathrm{a}}(\boldsymbol{y}_h). \tag{1.3.1}$$

We then apply the Cauchy–Born rule to aprroximate the second sum. The procedure is to assign the volume of a Voronoi cell Ω_i^0, to a single atom i in the reference configuration [44] and then to approximate the site energy by the integration of an energy density $W(\cdot)$, which depends only on the local deformation gradient $\nabla \boldsymbol{y}$, over Ω_i^0. The Cauchy–Born site energy is then defined by

$$\mathcal{E}_i^{\mathrm{c}}(\boldsymbol{y}_h) = \int_{\Omega_i^0} W(\nabla \boldsymbol{y}_h)\,\mathrm{d}x, \tag{1.3.2}$$

and the atom based quasicontinuum formulation of the stored energy is given by

$$\mathcal{E}_{\mathrm{qce}}(\boldsymbol{y}_h) := \sum_i \mathcal{E}_i^{\mathrm{a}}(\boldsymbol{y}_h) = \sum_{i\in\Omega_a} \mathcal{E}_i^{\mathrm{a}}(\boldsymbol{y}_h) + \sum_{i\in\Omega_c} \int_{\Omega_i^0} W(\nabla \boldsymbol{y}_h)\,\mathrm{d}x. \tag{1.3.3}$$

This formulation reserves the distinguishing feature of this method, which is the association of energy with atoms that inherits from the original applications of this method to systems modeled by the Embedded Atom Method.

A further simplification of the model is obtained when the finite element method is used in the continuum region with piecewise linear elements. Let T be an element in the continuum region and V_T the area or the volume of the element. The original energy based QC stored energy is defined as

$$\mathcal{E}_{\mathrm{qce}}(\boldsymbol{y}_h) := \sum_{i\in\Omega_a} \mathcal{E}_i^{\mathrm{a}}(\boldsymbol{y}_h) + \sum_{T\subset\Omega_c} V_T W(\nabla \boldsymbol{y}_h|_T), \tag{1.3.4}$$

which is often called the element based formulation and is efficient in real computations.

We note that there are two steps in the transition from (1.3.1) to (1.3.4). However, since the inconsistency occuring in the transition from (1.3.1) to (1.3.3) is our main concern and the atom based and the element based formulations are equivalent if V_T is carefully constructed, we employ the atom based formulation (1.3.3) as the QCE energy as it is very useful in our analysis.

In the next section, we give a discussion of the issue of ghost force which is essentially the cause of the inconsistency in the first step of the transition and is often the main problem associated with the QCE formulation.

1.3.1.2 Ghost Force and Consistency

The issue of ghost force is best illustrated by a concrete example of a periodic one-dimensional atomistic chain with nearest neighbour and next nearest neighbour pair interaction potential.

It will be derived in detail in Chapter 2 that the atomistic stored energy functional for a period of this infinite chain is given by

$$\mathcal{E}_{\mathrm{a}}(\boldsymbol{y}) := \varepsilon \sum_{i=1}^{N} \left[\phi\Big(\frac{y_i - y_{i-1}}{\varepsilon}\Big) + \phi\Big(\frac{y_i - y_{i-2}}{\varepsilon}\Big) + \phi\Big(\frac{y_{i+1} - y_i}{\varepsilon}\Big) + \phi\Big(\frac{y_{i+2} - y_i}{\varepsilon}\Big) \right], \tag{1.3.5}$$

where N is the number of atoms in each period and $\varepsilon = 1/N$. For simplicity, we assume the partition $\mathcal{T}$ to coincide with the reference lattice $\mathbb{L}$. Let $\Omega_a := \{\ell_1, \ldots, \ell_2\}$ and $\Omega_c := \{1, \ldots, N\} \backslash \{\ell_1, \ldots, \ell_2\}$, then the QCE stored energy functional for a pe-

riod is given by

$$\begin{aligned}\mathcal{E}_{\mathrm{qce}}(\boldsymbol{y}) :=& \varepsilon \sum_{i\in\Omega_a}\left[\phi\Big(\frac{y_i-y_{i-1}}{\varepsilon}\Big)+\phi\Big(\frac{y_i-y_{i-2}}{\varepsilon}\Big)+\phi\Big(\frac{y_{i+1}-y_i}{\varepsilon}\Big)+\phi\Big(\frac{y_{i+2}-y_i}{\varepsilon}\Big)\right]\\ &+\varepsilon\sum_{i\in\Omega_c}\left[\phi\Big(\frac{y_i-y_{i-1}}{\varepsilon}\Big)+\phi\Big(2\frac{y_i-y_{i-1}}{\varepsilon}\Big)+\phi\Big(\frac{y_{i+1}-y_i}{\varepsilon}\Big)+\phi\Big(2\frac{y_{i+1}-y_i}{\varepsilon}\Big)\right].\end{aligned} \tag{1.3.6}$$

It can be checked that under a homogeneous deformation field $\boldsymbol{y}^F := Fx$,

$$\nabla\mathcal{E}_{\mathrm{a}}(\boldsymbol{y}^F)=0 \ \text{ but } \ \nabla\mathcal{E}_{\mathrm{qce}}(\boldsymbol{y}^F)\neq 0.$$

The problem lies on the interface atoms. If we take the partial derivative with respect to y_{ℓ_1-1} for $\mathcal{E}_{\mathrm{a}}$ and $\mathcal{E}_{\mathrm{qce}}$, we obtain

$$\begin{aligned}\frac{\partial\mathcal{E}_{\mathrm{a}}(\boldsymbol{y})}{\partial y_{\ell_1}} =&\phi'\Big(\frac{y_{\ell_1}-y_{\ell_1-1}}{\varepsilon}\Big)-\phi'\Big(\frac{y_{\ell_1+1}-y_{\ell_1}}{\varepsilon}\Big)\\ &+\phi'\Big(\frac{y_{\ell_1}-y_{\ell_1-2}}{\varepsilon}\Big)-\phi'\Big(\frac{y_{\ell_1+2}-y_{\ell_1}}{\varepsilon}\Big),\end{aligned}$$

and

$$\begin{aligned}\frac{\partial\mathcal{E}_{\mathrm{qce}}(\boldsymbol{y})}{\partial y_{\ell_1}} =&\phi'\Big(\frac{y_{\ell_1}-y_{\ell_1-1}}{\varepsilon}\Big)-\phi'\Big(\frac{y_{\ell_1+1}-y_{\ell_1}}{\varepsilon}\Big)\\ &+2\phi'\Big(2\frac{y_{\ell_1}-y_{\ell_1-1}}{\varepsilon}\Big)-\phi'\Big(2\frac{y_{\ell_1+1}-y_{\ell_1}}{\varepsilon}\Big)-\frac{1}{2}\phi'\Big(\frac{y_{\ell_1+2}-y_{\ell_1}}{\varepsilon}\Big).\end{aligned}$$

As a result,

$$\frac{\partial\mathcal{E}_{\mathrm{a}}(\boldsymbol{y}^F)}{\partial y_{\ell_1}}=0 \ \text{ but } \ \frac{\partial\mathcal{E}_{\mathrm{qce}}(\boldsymbol{y}^F)}{\partial y_{\ell_1}}=\frac{1}{2}\phi'(2F).$$

This unphysical residual force appearing in the QCE energy under homogeneous deformation field is conventionally called the *ghost force* and is caused by the unbalanced next nearest neighbor interactions at the interface [66]. The unbalanced interaction could be easily illustrated by Figure 1.1, where atom ℓ_1 and

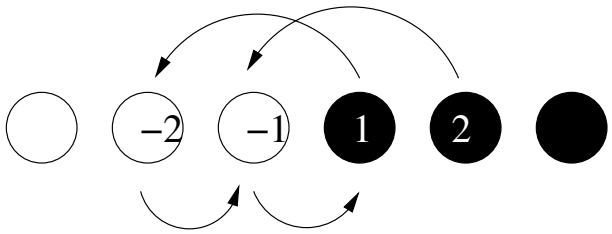

Figure 1.1: The unbalanced next nearest neighbor interactions.

$\ell_1 + 1$ interact with atom $\ell_1 - 2$ and $\ell_1 - 1$ respectively, however, atom $\ell_1 - 1$ and $\ell_1 - 2$ do not have the reverse interactions with their counterparts. The appearance of the ghost force implies that, even in the simplest case, namely the case without external forces, the solution to the minimization problem of the atomistic energy functional and that of the QCE energy functional may be significantly different.

Construction of methods that avoid the ghost force is the main motivation for the development of the QC methods which we will introduce immediately. The analysis of the effect of such an unphysical force, which is often the inconsistency between the deformation field of a QC method and its underlying atomistic model in the interface region, is one of the major topics of the numerical analysis for the QC methods as well as for our own research.

1.3.1.3 The Energy Based Ghost Force Removal Methods

Several alternative QC methods have been developed in order to preserve the energy conservation while avoiding the ghost forces, from which the name of the class 'Energy Based Ghost Force Removal' comes.

The first method was developed by Shimokawa et al. in [67] called the quasi-nonlocal (QNL) method, which is applied to the problem of the vacancy formation energy in Al and α iron, and the grain boundary energy of a tilt boundary in Cu.

The idea of the QNL method is to define a special site energy $\mathcal{E}_i^{\mathrm{i}}$ for a small layer of atoms at the interface region Ω_i between the atomistic region Ω_a and the continuum region Ω_c such that the stored energy functional is defined by

$$\mathcal{E}_{\mathrm{qnl}}(\boldsymbol{y}) = \sum_{i\in\Omega_a\setminus\Omega_i} \mathcal{E}_i^{\mathrm{a}}(\boldsymbol{y}) + \sum_{i\in\Omega_i} \mathcal{E}_i^{\mathrm{i}}(\boldsymbol{y}) + \sum_{i\in\Omega_c\setminus\Omega_i} \mathcal{E}_i^{\mathrm{c}}(\boldsymbol{y}), \tag{1.3.7}$$

and satisfies the condition

$$\mathcal{E}_i^{\mathrm{a}}(\boldsymbol{y}^F) = \mathcal{E}_i^{\mathrm{i}}(\boldsymbol{y}^F) = \mathcal{E}_i^{\mathrm{c}}(\boldsymbol{y}^F), \forall i \text{ and } \nabla\mathcal{E}_{\mathrm{qnl}}(\boldsymbol{y}^F) = 0, \tag{1.3.8}$$

for a homogeneous deformation field $\boldsymbol{y}^F$. The way to construct a proper site energy $\mathcal{E}_i^{\mathrm{i}}$ for the interface atoms is to let these atoms interact in a nonlocal way with the atoms in the atomistic region but interact locally with the atoms in the continuum region. It should be noted that an interaction of an atom to another in a nonlocal way is the interaction based on the physical distance of the two, while that in a local behaviour is based on the distance computed by using the positions of the nearest neighbour atoms to extrapolate the position of the other one.

While the original QNL method is in general consistent only for next nearest neighbour interaction models, the Geometrically Consistent Reconstruction Scheme developed by E et al. in [20], which is the extension of the original QNL method, is consistent for finite range interaction models. The consistency is achieved by reconstructing the distance of one atom to another to be a linear combination of the real distance between the two atoms and the Cauchy–Born distance which is extrapolated by the distance of the nearest neighbour atom with the cooefficients summing to 1 and being determined by solving certain system of equations [20, Equation 33]. However, the limitation of this method is that it may only be applied to the systems with flat atomistic to continuum interfaces.

A further extension of this method is given by Ortner and Zhang for a nearest neighbour interaction model in two dimension [58]. It provides a more general way to reconstruct the distance of one atom to another that could deal with the problem of the atomistic to continuum interfaces with corner.

The above approaches follow the two steps of transitioning from atomistic energy to continuum energy, i.e., the atom based summation rule is derived first and then the element based summation rule, which is better related to classic continuum mechanics. As a result, the geometrically consistent reconstruction schemes place two interface regions which are the atomistic to continuum interface and the atom based to element based interface which is inside the continuum region.

This complication is overcome by another QC method developed by Shapeev in [64], in one- and two- dimensional systems which have only pair interaction potentials and is often refered to as the ACC method. This QC method first formulate the stored energy as the summation of the energy of the interaction bonds, i.e.,

$$\mathcal{E}_{\mathrm{a}}(\boldsymbol{y}) = \sum_{b \in \mathcal{B}} e_b(\boldsymbol{y}), \tag{1.3.9}$$

where $\mathcal{B}$ denotes the set of all the interaction bonds and $e_b(\boldsymbol{y})$ is the energy contribution of the bond b under a deformation field $\boldsymbol{y}$. We then again decompose the region to be the atomistic region Ω_a and the continuum region Ω_c. The idea is to split the energy contribution of each bond b by

$$e_b(\boldsymbol{y}) = e_b^a(\boldsymbol{y}) + e_b^c(\boldsymbol{y}), \tag{1.3.10}$$

where $e_b^a(\boldsymbol{y})$ is the atomistic energy contribution which preserves the atom based formulation and depends on the interaction potential ϕ, the intersection of the bond and the atomistic region $b \cap \Omega_a$, and the deformation of this intersection

$\boldsymbol{y}(b \cap \Omega_a)$. $e_b^c(\boldsymbol{y})$ is the continuum energy contribution which is defined as a line integral that depends on ϕ, $b \cap \Omega_c$, and the local deformation gradient $\nabla \boldsymbol{y}(\boldsymbol{x})$. The most important feature of this method is the transformation of the summation of the line integrals to the summation of the energy on each element. In short, it was proved in [64] under certain conditions that

$$\sum_{b \in \mathcal{B}} e_b^c(\boldsymbol{y}) = \sum_{T \in \Omega_c} |T| W(\nabla \boldsymbol{y}|_T) \tag{1.3.11}$$

and consequently

$$\mathcal{E}_{\text{acc}}(\boldsymbol{y}) = \sum_{b \in \mathcal{B}} e_b^a(\boldsymbol{y}) + \sum_{T \in \Omega_c} |T| W(\nabla \boldsymbol{y}|_T), \tag{1.3.12}$$

is a consistent approximation of $\mathcal{E}^{\text{a}}(\boldsymbol{y})$, i.e., the second equation of (1.3.8) holds for $\mathcal{E}_{\text{acc}}(\cdot)$.

The detailed formulation of this method will be introduced in Chapter 3 and the numerical analysis of this method will be covered in Section 1.4 as well as in Chapter 3 as it is another major part of our research.

1.3.1.4 Other QC Methods

We briefly introduce three important QC methods for reference purpose only.

The force based QC (QCF) method, which was developed in [66, 13], is the first variant of the original QC method which avoids the presence of the ghost force. This method follows a very simple idea that the formulation of the force experienced by each atom depends on the region where the atom locates. It can be easily checked that no ghost force exists under a homogeneous deformation field.

The simplicity of the formulation and the fast convergence speed in real computation may be the biggest advantages of the QCF method [44, 13]. However, since

the QC problem is then no longer to find a configuration that minimize an energy but to find a configuration that drives the forces on each degree of freedom to be zero and the system of the QCF method is not energy conservative, it sometimes finds unphysical 'equilibrium' solutions that correspond to saddle points or local maxima of the energy functional corresponding to the underlying atomistic model [44]. The QCF method is rigorously analyzed in [13] and in [18], it is pointed out that instability of the QCF method exists in certain norms. Moreover, for many real applications of the QC method where energy is an important quantity of interest, the QCF method is obviously not a proper method to employ.

Further development of the force based QC method based on the idea of stress can be found in [40].

The cluster based QC method which was first introduced in [29] is another variant of the original QC method. The idea is to approximate the average energy of each atom in the system by the energy of the atoms in clusters near the finite element nodes. The approximation gains better accuracy when the size of the clusters gets larger while the computational cost becomes more expensive. The method is further analyzed in [43] and [27] but is pointed out in [39] that the method introduces new types of error that are especially large in non-uniform meshes.

The blended QC method was conceived orginally in [75]. The idea of this method is to create a region where the energy of each atom is defined to be a linear combination of the atomistic energy and the continuum energy. The linear combination is determined by solving a minimization problem. By doing this, the transition of the atomistic energy to the continuum energy formulation is less abrupt and the effect of the ghost force is thus smoothed out. This method is an-

alyzed in [71] and [38] and a force based variant of this method can be found in [30, 35]. However, it should be noted that this method does not remove the effect of the ghost force as opposed to the ghost force removal methods.

1.3.2 Other Atomistic to Continuum Coupling Methods

Besides the QC methods, there are other atomistic to continuum coupling methods proposed under different names. Some methods essentially share similar construction steps with the QC methods, such as Coupling of Length Scales (CLS) method developed in [9] to solve the problem in the fracture of nano scale system of silicon whose atomistic model is the Stillinger-Webber empirical model which we introduced in Section 1.1.

However, there are other methods which are conceptionally different from the QC methods. A typical example for such methods is the Bridging Scale Method (BSM), which was developed in [73] for dynamic problems and in [61] for static problems. It assumes a coarse-scale displacement field $\boldsymbol{u}^c$ and a fine-scale displacement field $\boldsymbol{u}^a$ and the total displacement field $\boldsymbol{u}$ is defined to be the summation of the two.

In static problems, the coarse-scale displacement field $\boldsymbol{u}^c$ exists everywhere and is computed as the solution of the finite element discretization of the atomistic model with least-squares fit, while the fine-scale displacement field $\boldsymbol{u}^a$ is assumed to exist only in the atomistic region and to be defined on every atom in the atomistic region which serves as a correction of the coarse-scale displacement field so that the equillibrium of a fine-scale problem in the atomistic region is obtained.

The method essentially solves two energy minimization problems iteratively

with the solution of one being the constrain or boundary condition for another. The iteration terminates when the change of energy is below certain tolerance. The main disadvantage of this method is that the convergence rate could be very slow when the problem is nonlinear [44].

1.4 The Numerical Analysis of the Quasicontinuum Methods

Since it was conceived, the QC method has been extensively employed for various problems by a number of material scientists [65, 66, 29, 43, 67, 44]. However, the mathematical analysis of the QC method has not been fully developed. In this section, we give a review of the analysis of the energy based QC methods which are the object of our research.

The first analysis that is worth noting is by Lin [32]. He analyzes a finite one dimensional atomistic chain who poccesses the Lennard-Jones pair interaction potential with no external forces being applied. In this work, the correct atomistic model is the one with full range atomistic interactions, i.e., every pair of atoms interact to contribute to the total energy. The two simplified models are the one that has a cut-off radius for the pair interactions and the one that has both a cut-off radius and is coarse grained by a uniform mesh in the entire domain with piecewise linear functions used on each element. He first proves the existence and the uniqueness of the solutions of these models, which are the displacements and equivalently the interatomic distances that corresponds to the global minima of the total energy, and then gives the a priori error estimates between the solutions in an ℓ^∞- and a weighted ℓ^2- norm, where the estimates depend on the cut-off radius

and are of first order of the mesh size when the finite element solution is involved. An asymptotic technique is used for the analysis as a result of explicitly knowing the formulation of the interaction potential.

A further development can be found in Ortner and Süli [55]. The models they analyze are almost the same as the first and the third model in [32], which is the full atomistic model and the model with cut-off radius and coarse graining but with several relaxations that make the analysis more general. The first relaxation is that pointwise defined applied forces are allowed in the problem. The second one is that general pair interaction potentials may be employed if certain properties are satisfied (see, e.g., [55, Equation 4, 7, 8, 9]). The third one is that a Dirichlet boundary condition is applied to the deformation field. In addition, it substantially differs from Lin's work in the two aspects: the variational formulations of the atomistic and the QC problems and the solutions being the local minima rather than the global minima as a result of the external force. They first prove the existence of the elastic atomistic deformation under certain conditions (see [55, Theorem 3.1]) and then answered two important questions: 'under what conditions does a QC solution exist which approximates a given exact solution of the atomistic model' (see [55, Theorem 3.2]) and 'given a computed QC solution, does an exact solution of the atomistic model approximated by the QC solution exist' (see [55, Theorem 5.1]), which are essentially the a priori existence of the QC solution and the a posteriori existence of the atomistic solution. They develop both the a priori error estimates and the a posteriori error estimates for elastic deformation gradient in the discrete $w^{1,\infty}$-norm and also extend the a priori analysis to the configuration of a single fracture, which is another stable configuration in one dimension.

The above QC method is named the Projected QC method (QCP) and is further analyzed and compared with other QC methods in [34]. This method is analyzed in a two dimensional system without defect under external loads by Lin in [33], where a variational formulation is employed for the modeling as well as the analysis. The limitation there is the strong hypothesis adopted [33, Assumptions 1 and 2] which are difficult to verify and may not hold in general lattice domains.

The QCP method essentially uses the full atomistic model with finite element discretizations of the domain and does not use the continuum approximation. As a result, none of the above works considered the coupling of the models and did not see the important error that occurs in the atomistic to continuum interface.

The first rigorous analysis of the effect of the ghost force, which is caused by the coupling of different models, is given by Dobson and Luskin in [15]. In this work, they consider an infinite periodic chain with nearest and next nearest neighbour pair interaction and the original QC approximation defined in (1.3.6). The models are further simplified by a linearization of the energy functional at a macro scopic deformation gradient F and assuming the external force to be zero. They essentially give an error estimate of the QC solution, in terms of the displacement, in weighted ℓ^p- and $W^{1,p}$-norms. As a result of the linearization of the problem, the explicit solutions of the atomistic model and that of the QC model are obtained as the solutions of some recurrence equations corresponding to some systems of linear equations. The effect of the ghost force is explicitly computable.

The above work was extended by the same authors in [16]. In this work, the same linearized problem with a periodic nonzero external force, which is assumed to be mean zero and odd around the center of each period, is analyzed through the

same approach. In addition, the QNL approximation (1.3.7) is formulated and analyzed. Again the error estimates are given in weighted ℓ^p- and $W^{1,p}$-norms with optimal order with respect to the interatomic spacing in the reference lattice ε (the scaling parameter), which is of zero order for the QCE method and of first order for the QNL method as opposed to second order for the pure Cauchy–Born approximation. The QC methods have lower order error because of the coupling of different models in the atomistic to continuum interface region. The estimates also show the dependence of the error on the derivatives of the displacement which could also be interpreted as the curvature of the deformation field in the continuum region, which is an important factor that has been ignored by previous works but reveals the necessity of having the atomistic region in the part of the system where deformation is large. It should be noted that the errors they analyze in this work are actually the difference between the solutions of the QC models and that of the pure continuum model, which is different from the definition of the error employed in [55] and in the present work.

The nearest and next nearest neighbour pair potential model is analyzed through a different approach in [51, 45] and [57], where the last one forms the major part of Chapter 2. The two works extend the analysis of the model to a nonlinear setting, where the energy functionals are nonlinear with respect to the deformation fields, and variational formulations of the problems which are simliar to those in [55] are used to define the solutions. The approach they employ to analyze the QC methods are a consistency analysis based on negative $w^{-1,p}$- Sobolev norms and a stability analysis based on the coercivity of the energy functionals. The errors are estimated in a weighted H^1-norm and have the same order as pointed out in [16]

but are shaper in the dependence of the deformation in the continuum region. The emphasis of the two works are different. [51] concentrates on the rigorous analysis of the a priori and a posteriori existence of the QNL model and the atomistic model in one dimension, whereas [57] apply the same techniques to the local QC model (QCL) which is essentially the pure Cauchy–Born model, the QCE model as well as the QNL model, with the emphasis on the a priori error estimates. [57] also includes the analysis of the coarse graining (finie element approximation) for the first time, which has been omitted by previous works that only concentrated on the coupling error. The detail could be found in Chapter 2.

The above works are all on one dimensional problems except [33], which is essentially the analysis of the QCP method that has no coupling of models. The reason for this exlusion is that energy based ghost force free QC methods are hard to construct in higher dimensions as we metioned in Section 1.3.1.

Such difficulty has been tackled through different approaches [20, 64, 63] with certain limitations. We note that these literatures consider the first order consistency of a QC method for simple lattices to be equivalent to the ghost force free condition under uniform deformation. However, this assumption is not rigorously proved for two-dimensional case until recently by Ortner in [52]. This gives a significant theoretical basis for constructing energy based ghost force free QC methods. The author rigorously answered the important question that under what condition, the patch test condition [52, Equation 14], which is often used to test the consistency of the finite element methods [5, 69] and is equivalent to the ghost force free condition in most QC methods, implies first order consistency of a QC method. This work essentially uses the negative norm consistency analysis

approach which is first introduced in [51].

Based on the patch test consideration, Ortner and Shapeev give an a priori error analysis for the Consistent Energy Based Atomistic to Continuum Coupling (ACC) method [64] for pair interaction potentials as introduced in Section 1.3.1 applying to a periodic two dimensional atomistic system with a single vacancy in each period. Besides the consistency analysis, the stability of the system is also analyzed with a great effort as such condition is in general hard to establish in higher dimensions.

The most recent work on the construction and a priori error analysis for the energy based ghost force free QC methods for multi body interactions in two and three dimensional spaces can be found in [58]. It has been shown in this work that there might be no explicit formulations for the interface energy for such QC methods but one may construct such interface energy numerically.

In the works listed above, considerable effort has been devoted to the a priori error analysis of the QC methods. However, since the QC methods are always used with finite element discretization in the continuum region, the a posteriori error control, which has attracted relatively little attention, is another aspect of the research of the QC methods and forms the second part of the thesis.

The adaptive finite element method was applied to the QC methods shortly after the method was developed. The very first literature on such topic is [66], where the orginal QC method is formulated and applied to several dislocation model and a simple Zienkiewicz-Zhu error indicator [76] is used for mesh refinement without rigorous a posteriori error estimates.

Prudhomme et al. provide an a posteriori error analysis for the original QC

method applied to a nano indentation problem and a shear deformation problem in a two dimensional setting in [59, 60]. They adopt the goal-oriented approach and construct the dual problems with respect to the quantities of interests, which are the reaction force on the indenter in [59] and certain linear functionals of the deformation in [60]. However, the omission of the higher order remainders of the residual, which are [59, Equation 33], and [60, Equation 28] and certain simplications that are applied to the computation of the residuals without theoretical proof of the validity make the estimates less rigorous.

Arndt and Luskin conduct the a posteriori error estimates for the original QC method applied to one dimensional Frenkel-Kontorova model in a series of papers [2, 3, 4]. They follow the same methodology as [59, 60], which is the goal-oriented approach and the construction of the dual problems with respect to the quantity of interests. In [3] and [2], they derive the error estimators for the correct choice of atomistic region with the quantity of interest being the size of the dislocation and with a Dirichlet boundary condition, and with the quantity of interest being any linear functional of the deformation and with a periodic boundary condition respectively. In [4], they derive the error estimator for the mesh refinement in the continuum region. Since the models they analyze are linear, the error estimators are rigorously derived.

In the present work, we use the residual-based approach [72, Chapter 2] to derive a posteriori error estimates for the Consistent Energy Based Atomistic to Continuum Coupling (ACC) method [64] for the QC solution both in the H^1-norm and for the energy itself. A similar approach is employed by Ortner and Süli in [55] and Ortner in [51], and the present work differs itself from the two by employing a

different coupling mechanism and taking coarse graining in the continuum region into account. The details can be found in Chapter 3.

1.5 The Structure of the Thesis

The rest of the thesis is structured as follows:

In Chapter 2, we give the a priori error estimates for three different QC methods (QCL, QCE and QNL) for a nearest and next nearest neighbour pair interaction model in one dimension and a nonlinear setting. The major contribution of the content of this chapter is to propose a unified framework, which is based on a variation of the proof of the First Lemma of Strang in finite element analysis (see, e.g., [7, Chapter 3, §1]), to the a priori error analysis for the energy-based QC methods, and refine and extend the previous analyses. While previous results on estimating the modelling error exist, we give a new and simpler proof based on negative-norm estimates. Our stability analysis extends the sharp estimates in [17] to the nonlinear setting. Finally, we present numerical experiments to illustrate the results of our analysis.

In Chapter 3, we give the a posteriori error estimates for the Consistent Energy Based Atomistic to Continuum Coupling (ACC) method developed in [64] in the setting of one dimensional nearest and next nearest neighbour pair interaction. We establish a posteriori error estimates for the energy norm and for the energy, based on a posteriori residual and stability estimates. We formulate adaptive mesh refinement algorithms based on these error estimators. Our numerical experiments indicate optimal convergence rates of these algorithms.

In Chapter 4, we give the conclusion of the thesis and mention briefly the application of the framework we have presented in more complicated situations. An outlook of potential development of the QC methods is also given.

Chapter 2

The A Priori Error Analysis For Energy Based Quasicontinuum Approximations

This chapter is devoted to the a priori error analysis of several energy based quasicontinuum methods. The error analysis of energy based quasicontinuum methods has received considerable attention in recent years [32, 21, 33, 45, 55, 16, 15, 51]. The purpose of the present chapter is to refine and extend previous results [16, 45, 18, 51], in a unified framework in one dimension and a nonlinear setting.

The framework we employ here in the a priori error analysis is based on a variation of the proof of the First Lemma of Strang (see, e.g., [7, Chapter 3, §1]) in non-conforming finite element analysis. By following the steps of the proof of a variation of the lemma, we are able to clearly separate the generalized consistency error into three parts, which are the error due to the coupling of different energy, the error due to the coarse-graining of the solution space and the error due to the external forces.

In particular, in the analysis of the modeling and coupling errors, we use the negative-norm techniques developed in [51] for the quasinonlocal QC method and

extend it to the local and original energy-based QC method, obtaining new and sharper estimates. In Section 2.3.5 we will comment on the differences and similarities of our analysis with previous efforts. In the analysis of the error due to the coarse-graining of the solution space, we fully use the one-dimensional feature of the problem and obtain the same superconvergence result as obtained for the force-based QC method in [41]. The analysis of the external force essentially follows the one in [55] with necessary modifications to accommodate this particular problem. We remark here that coarse-graining is included for the first time in the error analysis of these energy-based QC methods. (We note, however, that E and Ming [21] analyze a 1D local QC method within the framework of the *heterogeneous multiscale method* and Lin [33] analyzes a different 2D coarse-graining scheme in the framework of non-conforming finite element methods.)

Our analysis is restricted to a second-neighbour pair interaction model in one dimension, since this simple model problem contains much of the structure of more complicated situations. Indeed, the analysis [54] of a recently proposed QC method for 2D problems with finite range interaction [64] largely follows a similar framework put forward in the next section. The similarity of the analysis will be discussed in detail in Chapter 4.

In the following section, we will give the detail of the First Lemma of Strang as well as the proof of its variation, and the outline of the analysis in the current chapter.

2.1 Framework and Outline of the Analysis

The First Lemma of Strang is a generalization of Céa's Lemma in nonconforming finite element analysis. It is useful when the bilinear forms and the linear functionals of the variational formulations of the problem are different while the finite element solution space is a subspace of the original one. For future reference, we write out this lemma and give the proof of it which largely follows [7, Chapter 3, §1].

Lemma 2.1. ***First Lemma of Strang.*** *Let the original variational problem be*

$$a(u,v) = \langle l, v\rangle \quad \forall v \in V,$$

and the finite element problem be

$$a_h(u_h, v_h) = \langle l_h, v_h\rangle \quad \forall v_h \in S_h,$$

where $a(\cdot,\cdot)$ and $a_h(\cdot,\cdot)$ are two bilinear forms defined on V and S_h respectively and $S_h \subset V$. If we have the continuity condition of $a(\cdot,\cdot)$ on V

$$a(u,v) \leq C\|u\|\|v\| \ \forall v \in V,$$

and the stability condition of $a_h(\cdot,\cdot)$ on S_h

$$a_h(v_h, v_h) \geq \alpha\|v_h\|^2 \ \forall v_h \in V,$$

then there exists a constant c independent of h such that

$$\|u - u_h\| \leq c\Bigg(\inf_{v_h \in S_h} \Big\{ \|u - v_h\| + \sup_{w_h \in S_h} \frac{|a(v_h, w_h) - a_h(v_h, w_h)|}{\|w_h\|} \Big\} + \sup_{w_h \in S_h} \frac{\langle l, w_h\rangle - \langle l_h, w_h\rangle}{\|w_h\|} \Bigg) \tag{2.1.1}$$

Proof. Let $v_h \in S_h$ and $v_h - u_h = e_h$, by the stability of $a_h(\cdot,\cdot)$ and the continuity of $a(\cdot,\cdot)$, we have

$$\begin{aligned}
\alpha\|u_h - v_h\|^2 \leq & a_h(v_h, v_h - u_h) - a_h(u_h, v_h - u_h) \\
\leq & \big[a_h(v_h, e_h) - a(v_h, e_h)\big] + \big[a(v_h, e_h) - a(u, e_h)\big] \\
& + \big[a(u, e_h) - a_h(u_h, e_h)\big] \\
\leq & \big|a_h(v_h, e_h) - a(v_h, e_h)\big| + C\|v_h - u\|\|e_h\| + \big|\langle l, e_h\rangle - \langle l_h, e_h\rangle\big|. \quad (2.1.2)
\end{aligned}$$

Dividing both sides through by $\|e_h\|$ and making use of the arbitrariness of $v_h \in S_h$ and the triangle inequality

$$\|u - u_h\| \leq \|u - v_h\| + \|u_h - v_h\|,$$

we obtain the estimate. □

Our problem differs from the above one mainly in two aspects:

The first one is the nonlinearity, which leads $a(\cdot;\cdot)$ and $a_h(\cdot;\cdot)$ to be semilinear forms. As a result, the stability and the continuity may be defined differently.

The second difference is that the approximate semilinear form $a_h(\cdot;\cdot)$ is also well defined on the original solution space V. This does not hold for finite element approximations for PDEs as $a_h(\cdot,\cdot)$ often approximate $a(\cdot,\cdot)$ using quadrature and an element v in V, which is often a Sobolev space $W^{p,q}$, is not always pointwise defined. This feature allows us to estimate the consistency error of the QC problems in terms of the regularity of the original solution u rather than its interpolant.

For these two reasons, we switch the framework of our analysis to a variation of the proof of this Lemma which we introduce immediately.

Suppose we write the exact problem as

$$a(u;v) = \langle \ell, v \rangle \quad \forall v \in V, \tag{2.1.3}$$

and the approximate problem as

$$a_h(u_h;v_h) = \langle \ell_h, v_h \rangle \quad \forall v_h \in S_h, \tag{2.1.4}$$

where $a(\cdot;\cdot)$ and $a_h(\cdot;\cdot)$ are two semilinear forms and are defined on $V \times V$ and $V \times S_h$ respectively where $S_h \subset V$.

If we have the stability condition of $a_h(\cdot;\cdot)$ at $I_h u$, u and $I_h u - u$, where $I_h u \in S_h$ is an interpolant of u in S_h, such that

$$a_h(I_h u; I_h u - u_h) - a_h(u_h; I_h u - u_h) \geq \alpha \|u_h - I_h u\|^2, \tag{2.1.5}$$

for some $\alpha > 0$, then by letting $e_h = I_h u - u_h$, we may obtain

$$\begin{aligned}
\alpha \|e_h\|^2 \leq & a_h(I_h u; e_h) - a_h(u_h; e_h) \\
= & \big[\langle \ell, e_h \rangle - a(u; e_h)\big] + \big[a_h(u; e_h) - a_h(u; e_h)\big] + \big[a_h(I_h u; e_h) - a_h(u_h; e_h)\big] \\
= & a_h(u; e_h) - a(u; e_h) && (2.1.6) \\
& + a_h(I_h u; e_h) - a_h(u; e_h) && (2.1.7) \\
& + \langle \ell, e_h \rangle - \langle \ell_h, e_h \rangle. && (2.1.8)
\end{aligned}$$

(2.1.6) (2.1.7) and (2.1.8) respectively corresponds to the consistency error for the semilinear forms which is defined on the original solution u as we mentioned, the error caused by coarse graining of the solution space and the consistency error for linear functional on the right hand side. By further estimating the three parts

by

$$|a_h(u;e_h) - a(u;e_h)| \leq \mathscr{E}_{\mathrm{CO}}(u)\|e_h\|, \tag{2.1.9}$$

$$|a_h(I_h u;e_h) - a_h(u;e_h)| \leq \mathscr{E}_{\mathrm{CG}}(u)\|e_h\|, \text{ and} \tag{2.1.10}$$

$$|\langle \ell, e_h\rangle - \langle \ell_h, e_h\rangle| \leq \mathscr{E}_{\mathrm{VC}}(\ell)\|e_h\|, \tag{2.1.11}$$

where $\mathscr{E}_{\mathrm{CO}}(\cdot)$ and $\mathscr{E}_{\mathrm{CG}}(\cdot)$ are functionals on V and $\mathscr{E}_{\mathrm{VC}}(\cdot)$ is a functional on V^* which is the dual space of V, we obtain an a priori error estimate for e_h. Using the triangle inequality

$$\|u - u_h\| \leq \|u - I_h u\| + \|I_h u - u_h\|,$$

and an estimate of $\|u - I_h u\|$ using u, we may establish the a priori error estimate of $u - u_h$ in certain norms.

This chapter gives the a priori error estimates of the QC methods by making the above steps concrete. We give the outline of the analysis as follows.

In Section 2.2 we formulate the atomistic model and the three different QC methods. We will also introduce some notation that will be used throughout this chapter.

In Section 2.3, we first formulate the atomistic and the QC problems in variational formulations, i.e., to construct $a(\cdot;\cdot)$ and $a_h(\cdot;\cdot)$ respectively and then derive the consistency error estimates for the three different QC methods, which corresponds to (2.1.9). Since the most natural norms in which to measure the error are discrete Sobolev norms, we use similar techniques as in [45, 51] to derive the estimates in corresponding negative Sobolev norms. Our estimates will clearly show the error sources for each method.

In Section 2.4, we coarse grain the original solution space and define a new linear functional to formulate the full QC problems.

In Section 2.5, we first estimate $\|u - I_h u\|$ in a suitable norm and then analyze the error caused by the coarse-graining of the solution space which corresponds to (2.1.10), since the previous estimate $\|u - I_h u\|$ is used in the later one. A superconvergence estimate of coarse-graining error is derived as a result of the one dimensional feature of our underlying problem.

In Section 2.6, the estimate of the error due to the external force is given. This error essentially corresponds to the variational crimes (2.1.8).

In Section 2.7, we give a stability analysis for the three QC methods, extending the sharp results in [17] to nonlinear deformations. This analysis provides sufficient conditions under which (2.1.5) may hold.

In Section 2.8, we combine all the estimates derived previously to give an a priori error estimates for the QC methods following the steps of the proof of the variation given earlier.

In Section 2.9, we present numerical experiments to complement our analysis.

2.2 The Atomistic Model and its QC Approximations

2.2.1 The atomistic model

To avoid technical difficulties with boundaries we formulate a model problem with periodic boundary conditions. To this end, let $N \in \mathbb{N}$ and $\varepsilon = 1/2N$, and define the space of $2N$-periodic zero mean displacements as

$$\mathcal{U} = \left\{ u \in \mathbb{R}^{\mathbb{Z}} : u_{\ell+2N} = u_\ell, \sum_{\ell=-N+1}^{N} u_\ell = 0 \right\}. \tag{2.2.1}$$

The set of admissible deformations is given by

$$\mathcal{Y} = \{y \in \mathbb{R}^{\mathbb{Z}} : y_\ell = \varepsilon F\ell + u_\ell,\ u \in \mathcal{U}\}, \tag{2.2.2}$$

where $\varepsilon = 1/2N$ is chosen to rescale the computational domain to unit length, and $F > 0$ is a macroscopic deformation gradient.

Remark 2.1. Throughout the thesis, we identify a lattice function $v \in \mathbb{R}^{\mathbb{Z}}$ with its continuous and piecewise affine interpolant with nodal values $v(\varepsilon\ell) = v_\ell$. Vice-versa, if $g \in C^0(\mathbb{R})$ then we always identify it with its vectors of nodal values $(g_\ell)_{\ell\in\mathbb{Z}} = (g(\varepsilon\ell))_{\ell\in\mathbb{Z}}$.

We observe that $y \in \mathcal{Y}$ if and only if $y = Fx + u$ for some $u \in \mathcal{U}$.

For simplicity of the presentation and analysis, we adopt a pair interaction model and assume that only nearest neighbours and the next-nearest neighbours interact. The *stored atomistic energy* (per period) of an admissible deformation is then given by

$$\begin{aligned}\mathcal{E}_{\mathrm{a}}(y) :=\ & \varepsilon \sum_{\ell=-N+1}^{N} \phi\Big(\frac{y_\ell - y_{\ell-1}}{\varepsilon}\Big) + \varepsilon \sum_{\ell=-N+1}^{N} \phi\Big(\frac{y_\ell - y_{\ell-2}}{\varepsilon}\Big) \\ =\ & \varepsilon \sum_{\ell=-N+1}^{N} \phi(y'_\ell) + \varepsilon \sum_{\ell=-N+1}^{N} \phi(y'_\ell + y'_{\ell-1}),\end{aligned} \tag{2.2.3}$$

where $y'_\ell = \frac{y_\ell - y_{\ell-1}}{\varepsilon}$, and where $\phi \in C^3((0,+\infty))$ is a Lennard-Jones type interaction potential: We assume that there exists $r_* > 0$ such that ϕ is convex in $(0, r_*)$ and concave in $(r_*, +\infty)$.

For $v, w \in \mathbb{R}^{\mathbb{Z}}$, we define

$$\langle v, w\rangle_\varepsilon := \varepsilon \sum_{\ell=-N+1}^{N} v_\ell w_\ell.$$

Given a dead load $f \in \mathcal{U}$, the *external energy* (per period) is defined by

$$-\langle f, u\rangle_\varepsilon := -\varepsilon \sum_{\ell=-N+1}^{N} f_\ell u_\ell, \tag{2.2.4}$$

where $u = y - Fx$. Thus, the *total energy* (per period) of a deformation $y \in \mathcal{Y}$ is given by

$$E_{\rm a}(y) := \mathcal{E}_{\rm a}(y) - \langle f, y - Fx\rangle_\varepsilon = \mathcal{E}_{\rm a}(y) - \langle f, u\rangle_\varepsilon.$$

The problem we wish to solve is to find

$$y_{\rm a} \in \operatorname{argmin} E_{\rm a}(\mathcal{Y}), \tag{2.2.5}$$

where argmin denotes the set of local minimizers.

Remark 2.2. 1. The external energy (2.2.4) can be thought of as the linearisation of a nonlinear external energy about the state Fx.

2. We have included the external forces primarily to render the problem non-trivial. In realistic applications in 2D/3D, defects or forces applied on a boundary are the cause of deformation of the crystal, however, in 1D such complex behaviour cannot be described directly.

2.2.2 The local QC method (QCL)

For 1-periodic functions $u, f \in C^\infty(\mathbb{R})$ we define $y^{(\varepsilon)} \in \mathcal{Y}$ as $y_\ell^{(\varepsilon)} = \varepsilon F\ell + u(\varepsilon\ell)$. It is then easy to see (e.g., [6, 56]) that, as $N \to \infty$,

$$E_{\rm a}(y^{(\varepsilon)}) \to \int_{-\frac{1}{2}}^{\frac{1}{2}} \big(\phi(y'(x)) + \phi(2y'(x)) - f(x)y(x)\big)\,{\rm d}x, \tag{2.2.6}$$

the so-called *Cauchy–Born approximation* of $E_{\rm a}$. The stored energy density $W(r) = \phi(r) + \phi(2r)$ is called the *Cauchy–Born stored energy function*.

The local QC (QCL) energy functional on the atomistic grid is obtained by applying a P1 finite element discretization to (2.2.6) with ε being the size of the finite element mesh and the reference atom positions being the nodes. The total QCL energy (per period) is given by

$$E_{\mathrm{qcl}}(y) = \mathcal{E}_{\mathrm{qcl}}(y) - \langle f, u \rangle_{\varepsilon}, \tag{2.2.7}$$

where

$$\mathcal{E}_{\mathrm{qcl}}(y) = \varepsilon \sum_{\ell=-N+1}^{N} W(y'_{\ell}) = \varepsilon \sum_{\ell=-N+1}^{N} \phi(y'_{\ell}) + \varepsilon \sum_{\ell=-N+1}^{N} \phi(2y'_{\ell}), \tag{2.2.8}$$

and $u = y - Fx$.

An alternative argument to derive (2.2.8) from (2.2.3) is to assume that $y'_{\ell} \approx y'_{\ell-1}$ for all ℓ, that is, the local deformation gradients vary slowly everywhere.

In the QCL model, we wish to compute

$$y_{\mathrm{qcl}} \in \operatorname{argmin} E_{\mathrm{qcl}}(\mathcal{Y}). \tag{2.2.9}$$

2.2.3 The original energy-based QC method (QCE)

When a material contains a defect, i.e., when the deformation y is not globally smooth, then the Cauchy–Born / local QC approximation is inaccurate. The full atomistic model should be used at the defect while the simpler local QC model (which allows for coarse graining) may be used to describe the far field.

As we mentioned in Section 1.3.1.1, the original energy-based QC method (QCE), introduced in [48], is a particularly simple example of a method coupling an atomistic model to its Cauchy–Born approximation. To motivate it in our setting, we

note that the atomistic and the QCL stored energies may be written in terms of contributions to each atom,

$$\mathcal{E}_{\rm a}(y) = \varepsilon \sum_{\ell=-N+1}^{N} \mathcal{E}_\ell^{\rm a}(y), \quad \text{and} \quad \mathcal{E}_{\rm qcl}(u) = \varepsilon \sum_{\ell=-N+1}^{N} \mathcal{E}_\ell^{\rm c}(y),$$

where

$$\mathcal{E}_\ell^{\rm a}(y) = \frac{1}{2}\big\{\phi(y'_\ell) + \phi(y'_{\ell+1}) + \phi(y'_{\ell-1} + y'_\ell) + \phi(y'_{\ell+1} + y'_{\ell+2})\big\}, \quad \text{and} \tag{2.2.10}$$

$$\mathcal{E}_\ell^{\rm c}(y) = \frac{1}{2}\big\{\phi(y'_\ell) + \phi(y'_{\ell+1}) + \phi(2y'_\ell) + \phi(2y'_{\ell+1})\big\} = \tfrac{1}{2}\big\{W(y'_\ell) + W(y'_{\ell+1})\big\}. \tag{2.2.11}$$

Next, we decompose the reference lattice into an atomistic region $\mathcal{A}$, which should contain any "defects", and a continuum region $\mathcal{C}$ where the solution is expected to be a "smooth" deformation from the reference lattice. For the sake of simplicity, we assume that

$$\mathcal{A} := \{\ell_1, \dots, \ell_2\}, \quad \text{and} \quad \mathcal{C} := \{1, ..., N\} \backslash \mathcal{A}, \tag{2.2.12}$$

where $-N+3 < \ell_1 < \ell_1 + 2 < \ell_2 < N-2$, which essentially locate the atomistic region away from the boundary and make it large enough to to avoid unnecessary notational complication. The stored energy functional for the *energy-based QC (QCE) method* [48] is then defined as

$$\mathcal{E}_{\rm qce}(y) = \varepsilon \sum_{\ell \in \mathcal{A}} \mathcal{E}_\ell^{\rm a}(y) + \varepsilon \sum_{\ell \in \mathcal{C}} \mathcal{E}_\ell^{\rm c}(y), \tag{2.2.13}$$

and the corresponding total energy (per period) as

$$E_{\rm qce}(y) = \mathcal{E}_{\rm qce}(y) - \langle f, u \rangle_\varepsilon,$$

where $u = y - Fx$.

In the QCE method, we aim to compute

$$y_{\text{qce}} \in \text{argmin} E_{\text{qce}}(\mathcal{Y}). \tag{2.2.14}$$

The original motivation behind the QCE method was that it exactly reproduces the energy under uniform strain (Cauchy–Born rule), however, it was later discovered [66, 16] that certain inconsistency occurs for the QCE solution due to the ghost force on the atomistic to continuum interface which we briefly described in Section 1.3.1.2 and whose effect will be analyzed in later sections.

2.2.4 The quasinonlocal QC method (QNL)

As we mentioned in Section 1.3.1.3, To avoid the ghost forces but preserve the energy conservation, the Energy Based Ghost Force Removal coupling methods were sought. One of the alternative approaches to couple the atomistic and continuum energy that was first proposed in [67], is to associate the energy with interaction bonds. In our model, the interaction bonds are the nearest neighbour bonds and the next-nearest neighbour bonds. The energy of the nearest neighbour bonds need not be modified, as they are already sufficiently localized. The atomistic energy of the next-nearest neighbour bonds built by atom $\ell - 1$ and $\ell + 1$ is

$$\phi(y'_\ell + y'_{\ell+1}).$$

In the region where the deformation gradients varies slowly, this energy can be approximated by

$$\frac{1}{2}\{\phi(2y'_\ell) + \phi(2y'_{\ell+1})\}.$$

If we perform the same decomposition to the whole domain as before, this leads to an approximation of (2.2.3) by

$$\mathcal{E}_{\mathrm{qnl}}(y) = \varepsilon \sum_{\ell \in \mathcal{A}\cup\mathcal{C}} \phi(y'_\ell) + \varepsilon \sum_{\ell \in \mathcal{A}} \phi(y'_\ell + y'_{\ell+1}) + \varepsilon \sum_{\ell \in \mathcal{C}} \frac{1}{2}\{\phi(2y'_\ell) + \phi(2y'_{\ell+1})\}. \tag{2.2.15}$$

It is fairly easy to see that in the 'interior' of the continuum region, $\mathcal{E}_{\mathrm{qnl}}$ reduces to the local QC method while in the 'interior' of the atomistic region, it reduces to the atomistic model. To be more precise, if we define an *interface region* $\mathcal{I}$ as

$$\mathcal{I} = \{\ell_1 - 1, \ell_1, \ell_2, \ell_2 + 1\},$$

then this stored energy can be written as

$$\mathcal{E}_{\mathrm{qnl}}(y) = \varepsilon \sum_{\ell \in \mathcal{A}\setminus\mathcal{I}} \mathcal{E}^{\mathrm{a}}_\ell(y) + \varepsilon \sum_{\ell \in \mathcal{C}\setminus\mathcal{I}} \mathcal{E}^{\mathrm{c}}_\ell(y) + \varepsilon \sum_{\ell \in \mathcal{I}} \mathcal{E}^{\mathrm{i}}_\ell(y),$$

where $\mathcal{E}^{\mathrm{a}}_\ell(y)$ and $\mathcal{E}^{\mathrm{c}}_\ell(y)$ are defined in (2.2.10) and (2.2.11) and $\mathcal{E}^{i}_\ell(y)$ is appropriately defined as [16]

$$\mathcal{E}^{i}_\ell = \frac{1}{2}\big[\phi(y'_\ell) + \phi(y'_{\ell+1}\big] + \begin{cases} \frac{1}{2}\big[\phi(2y'_\ell) + \phi(y'_{\ell+1} + y'_{\ell+2})\big], & \ell \in \{\ell_1 - 1, \ell_1\}, \\ \frac{1}{2}\big[\phi(y'_{\ell-1} + y'_\ell) + \phi(2y'_{\ell+1})\big], & \ell \in \{\ell_2, \ell_2 + 1\}. \end{cases} \tag{2.2.16}$$

This is the special treatment of the interface in the one dimensional case [67, 20, 58]. The above coupling method is conventionally named the *quasinonlocal QC (QNL) method*.

The total QNL energy functional is then given by

$$E_{\mathrm{qnl}}(y) = \mathcal{E}_{\mathrm{qnl}}(y) - \langle f, u\rangle_\varepsilon, \tag{2.2.17}$$

where $u = y - Fx$.

In the QNL method, we aim to find

$$y_{\mathrm{qnl}} \in \operatorname{argmin} E_{\mathrm{qnl}}(\mathcal{Y}). \tag{2.2.18}$$

2.2.5 Notation

Before we begin the detailed analysis in the next section, we define some notation that will be used throughout.

For $v \in \mathbb{R}^{\mathbb{Z}}$, besides the first order finite difference $v' := \varepsilon^{-1}(v_\ell - v_{\ell-1})$, we define the second and third order finite differences by

$$v''_\ell = \frac{v'_{\ell+1} - v'_\ell}{\varepsilon} = \frac{v_{\ell+1} - 2v_\ell + v_{\ell-1}}{\varepsilon^2}, \qquad \text{and}$$
$$v'''_\ell = \frac{v''_\ell - v''_{\ell-1}}{\varepsilon} = \frac{v_{\ell+1} - 3v_\ell + 3v_{\ell-1} - v_{\ell-2}}{\varepsilon^3}.$$

In general, the odd differences are associated with bonds, while even differences are associated with nodes. It should be noted that, for $v \in \mathcal{U}$, higher order differences, for example v' , v'' and v''', are all N-periodic and with mean zero in each period. Thus, all these higher order differences belong to $\mathcal{U}$. It can be checked that, for $y \in \mathcal{Y}$, finite differences of order higher than one, for example y'' and y''', also belong to $\mathcal{U}$.

For $v \in \mathcal{U}$, we define the weighted ℓ^p_ε-norms by

$$\|v\|_{\ell^p_\varepsilon} = \begin{cases} \left(\varepsilon \sum_{\ell=-N+1}^{N} |v_\ell|^p\right)^{1/p}, & 1 \le p < \infty, \\ \max_{\ell=-N+1,\dots,N} |v_\ell|, & p = \infty. \end{cases}$$

The space $\mathcal{U}$ is usually equipped with the discrete Sobolev norms

$$\|u\|_{\mathcal{U}^{1,p}} := \|u'\|_{\ell^p_\varepsilon} = \|u'\|_{L^p(-1/2,1/2)}, \quad \text{for } u \in \mathcal{U} \text{ and } p \in [1,\infty],$$

as we identify a lattice function $v \in \mathbb{R}^{\mathbb{Z}}$ with its continuous and piecewise affine interpolant with respect to the lattice nodes. When $\mathcal{U}$ is equipped with the $\mathcal{U}^{1,p}$-norm, it is denoted by $\mathcal{U}^{1,p}$. If $\mathcal{D}$ is a subset of $\mathbb{Z}$, for $v \in \mathbb{R}^{\mathbb{Z}}$, we also define the

(semi-)norms

$$\|v\|_{\ell^p_\varepsilon(\mathcal{D})} := \Big(\varepsilon \sum_{\ell\in\mathcal{D}} |v_\ell|^p\Big)^{1/p}.$$

For $p' = p/(p-1)$, the norm on the dual $\mathcal{U}^{-1,p} := (\mathcal{U}^{1,p})^*$ is defined by

$$\|F\|_{\mathcal{U}^{-1,p}} := \sup_{\substack{v\in\mathcal{U} \\ \|v\|_{\mathcal{U}^{1,p'}}=1}} F[v], \quad \text{for } F \in \mathcal{U}^{-1,p}.$$

In particular, let $\mathcal{E}$ be a functional on $\mathcal{Y}$, for $y \in \mathcal{Y}$ and $v \in \mathcal{U}$, we define

$$\mathcal{E}'(y)[v] := \lim_{t\to 0} \frac{\mathcal{E}(y+tv) - \mathcal{E}(y)}{t}. \tag{2.2.19}$$

We can then consider $\mathcal{E}'(y)$ as an element in $(\mathcal{U}^{1,p})^*$.

Finally, we introduce a function we will use in our analysis to bound derivatives of ϕ. For any $\mathcal{S} \subset \mathbb{R}$, we define

$$M_i(\mathcal{S}) := \sup_{s\in\mathcal{S}} |\phi^{(i)}(s)|, \tag{2.2.20}$$

where $\phi^{(i)}$ denotes the ith derivative of ϕ.

2.3 Consistency Error Analysis

In this section, we present the consistency error analysis of the three QC methods introduced in Section 2.2, which corresponds to (2.1.9) in Section 2.1.

In general, a numerical method is called consistent if the truncation error tends to zero as some discretization parameters tend to zero. However, this definition is not suitable for the QC methods as the atomistic model which we are approximating is a discrete model itself where the "grid size" ε is fixed. As we mentioned in Section 1.2.1, the order of consistency and the smoothness of the solution to the

atomistic model in certain regions are of great importance for the consistency of a QC method. Another key ingredient in the consistency error analysis is the norm in which the consistency error is estimated. We will make a further discussion on it after presenting our analysis where we estimate the consistency error in some special chosen norms, namely the $\mathcal{U}^{-1,p}$-norm.

2.3.1 The variational formulation and the consistency error

Let y_{a} be a solution of the atomistic model problem (2.2.5). If $\min_\ell (y_{\mathrm{a}})'_\ell > 0$, then E is differentiable at y_{a}, and the first-order necessary optimality condition for (2.2.5), in variational form, is

$$\mathcal{E}'_{\mathrm{a}}(y_{\mathrm{a}})[v] = \langle f, v\rangle_\varepsilon \qquad \forall v \in \mathcal{U}, \tag{2.3.1}$$

where

$$\begin{aligned}\mathcal{E}'_{\mathrm{a}}(y)[v] =& \lim_{t\to 0} \frac{\mathcal{E}_a(y+tv) - \mathcal{E}_a(y)}{t} \\ =& \varepsilon \sum_{\ell=-N+1}^{N} \phi'(y'_\ell) v'_\ell + \varepsilon \sum_{\ell=-N+1}^{N} \{\phi'(y'_{\ell-1} + y'_\ell) + \phi'(y'_\ell + y'_{\ell+1})\} v'_\ell.\end{aligned} \tag{2.3.2}$$

It is easily observed that (2.3.1) corresponds to the original variational problem $a(\cdot;\cdot) = \langle \ell, v\rangle$ in Section 2.1.

When using a QC method we are looking for

$$y_{\mathrm{qc}} \in \operatorname{argmin} E_{\mathrm{qc}}(\mathcal{Y}), \tag{2.3.3}$$

where $\mathrm{qc} \in \{\mathrm{qcl}, \mathrm{qce}, \mathrm{qnl}\}$. As above, if $\min_\ell (y_{\mathrm{qc}})'_\ell > 0$, then E_{qc} is differentiable at y_{qc}, and the first order necessary optimality condition for (2.3.3) in variational form is

$$\mathcal{E}'_{\mathrm{qc}}(y)[v] = \langle f, v\rangle_\varepsilon \qquad \forall v \in \mathcal{U}, \tag{2.3.4}$$

where

$$\mathcal{E}'_{\rm qc}(y)[v] = \lim_{t\to 0} \frac{\mathcal{E}_{\rm qc}(y+tv) - \mathcal{E}_{\rm qc}(y)}{t}, \tag{2.3.5}$$

whose formulation depends on the particular QC method we choose and will be given in detail in later sections. It is also easy to observe that (2.3.4) corresponds to the abstract approximation $a_h(\cdot;\cdot) = \langle \ell, v\rangle$ in Section 2.1. We do not modify the linear form $\langle \ell, v\rangle$ on the right hand side at this moment as the consistency analysis is independent of the choice of the linear form.

The *consistency error* (for the solution $y_{\rm a}$) of a QC method is

$$\begin{aligned} T_{\rm qc}(y_{\rm a}) :=&\ E'_{\rm qc}(y_{\rm a}) \\ =&\ E'_{\rm qc}(y_{\rm a}) - E'_{\rm a}(y_{\rm a}) \\ =&\ \mathcal{E}'_{\rm qc}(y_{\rm a}) - \mathcal{E}'_{\rm a}(y_{\rm a}), \end{aligned}$$

which is understood as a functional $T_{\rm qc}(y_{\rm a}) \in \mathcal{U}^*$ and corresponds to $a_h(u;\cdot) - a(u;\cdot)$ in the abstract formulation.

In our error analysis in Section 2.8, we will only need the estimates on the consistency error $T_{\rm qc}$ in the negative Sobolev norm $\|\cdot\|_{\mathcal{U}^{-1,2}}$. However, since it requires no modifications of our analysis we will in fact produce estimates in all $\mathcal{U}^{-1,p}$-norms, where $1 \le p \le \infty$.

2.3.2 The consistency error of the QCL method

For $y \in \mathcal{Y}$ with $\min_\ell y'_\ell > 0$, the first variation of $\mathcal{E}_{\rm qcl}$ at y reads

$$\mathcal{E}'_{\rm qcl}(y)[v] = \varepsilon \sum_{\ell=-N+1}^{N} \phi'(y'_\ell) v'_\ell + \varepsilon \sum_{\ell=-N+1}^{N} \phi'(2y'_\ell)\,(2v'_\ell). \tag{2.3.6}$$

Theorem 2.2. *For $y \in \mathcal{Y}$ with $\min_\ell y'_\ell > 0$, and for $1 \le p \le \infty$, we have*

$$\begin{aligned}\big\|T_{\rm qcl}(y)\big\|_{\mathcal{U}^{-1,p}} =& \big\|\mathcal{E}'_{\rm qcl}(y) - \mathcal{E}'_{\rm a}(y)\big\|_{\mathcal{U}^{-1,p}} && (2.3.7)\\ \le& \varepsilon^2\big\{M_2(\mathcal{S}_1)\|y'''\|_{\ell^p_\varepsilon} + M_3(\mathcal{S}_2)\|y''\|^2_{\ell^{2p}_\varepsilon}\big\} =: \mathscr{E}^{\rm qcl}_{\rm model}(y), && (2.3.8)\end{aligned}$$

where $\mathcal{S}_1 := \{2y'_1, \dots, 2y'_N\}$, $\mathcal{S}_2 := [\min_\ell 2y'_\ell, \max_\ell 2y'_\ell]$, and where $M_i(\mathcal{S})$ is defined in (2.2.20)*.*

Proof. Since $\min_\ell y'_\ell > 0$, $\mathcal{E}_{\rm a}$ and $\mathcal{E}_{\rm qcl}$ are differentiable at y. The difference between $\mathcal{E}'_{\rm a}(y)[v]$ and $\mathcal{E}'_{\rm qcl}(y)[v]$, which are written out in (2.3.2) and (2.3.6), respectively, can be written in the form

$$\mathcal{E}'_{\rm qcl}(y)[v] - \mathcal{E}'_{\rm a}(y)[v] = \varepsilon \sum_{\ell=-N+1}^{N} \big\{2\phi'(2y'_\ell) - \phi'(y'_{\ell-1} + y'_\ell) - \phi'(y'_\ell + y'_{\ell+1})\big\} v'_\ell.$$

From this second difference structure, we can already expect a second-order consistency error. To make this precise, we first note that the second neighbour interactions can be rewritten in terms of nearest neighbour interactions and a strain gradient correction,

$$\begin{aligned} y'_{\ell-1} + y'_\ell =&\ 2y'_\ell - \varepsilon\frac{y'_\ell - y'_{\ell-1}}{\varepsilon} = 2y'_\ell - \varepsilon y''_{\ell-1}, \quad \text{and}\\ y'_{\ell+1} + y'_\ell =&\ 2y'_\ell + \varepsilon\frac{y'_{\ell+1} - y'_\ell}{\varepsilon} = 2y'_\ell + \varepsilon y''_\ell. \end{aligned}$$

Hence, expanding $\phi'(y'_{\ell-1} + y'_\ell)$ and $\phi'(y'_\ell + y'_{\ell+1})$ at $2y'_\ell$ we obtain

$$\begin{aligned}\phi'(y'_{\ell-1} + y'_\ell) =&\ \phi'(2y'_\ell) - \varepsilon y''_{\ell-1}\phi''(2y'_\ell) + \tfrac{1}{2}(\varepsilon y''_{\ell-1})^2\phi'''(\eta^\ell_1), \quad \text{and} && (2.3.9)\\ \phi'(y'_\ell + y'_{\ell+1}) =&\ \phi'(2y'_\ell) + \varepsilon y''_\ell\phi''(2y'_\ell) + \tfrac{1}{2}(\varepsilon y''_\ell)^2\phi'''(\eta^\ell_2), && (2.3.10)\end{aligned}$$

where $\eta^\ell_1 \in \operatorname{conv}\{2y'_\ell, y'_\ell + y'_{\ell-1}\}$ and $\eta^\ell_2 \in \operatorname{conv}\{2y'_\ell, y'_\ell + y'_{\ell+1}\}$. We note that $\eta^\ell_k \in \mathcal{S}_2$ for $k = 1, 2$ and $\ell = 1, \dots, N$.

Adding these expansions together gives

$$\begin{aligned}
&2\phi'(2y'_\ell) - \phi'(y'_{\ell-1} + y'_\ell) - \phi'(y'_\ell + y'_{\ell+1}) \\
=\ & -\{-\varepsilon y''_{\ell-1}\phi''(2y'_\ell) + \tfrac{1}{2}(\varepsilon y''_{\ell-1})^2\phi'''(\eta_1^\ell)\} - \{\varepsilon y''_\ell\phi''(2y'_\ell) + \tfrac{1}{2}(\varepsilon y''_\ell)^2\phi'''(\eta_2^\ell)\} \\
=\ & -\varepsilon^2 y'''_\ell\phi''(2y'_\ell) - \tfrac{1}{2}\varepsilon^2\{y''^2_{\ell-1}\phi'''(\eta_1^\ell) + y''^2_\ell\phi'''(\eta_2^\ell)\}. \qquad (2.3.11)
\end{aligned}$$

Thus, we can bound $\mathcal{E}'_{\mathrm{qcl}}(y)[v] - \mathcal{E}'_{\mathrm{a}}(y)[v]$ by

$$\begin{aligned}
&\left|\mathcal{E}'_{\mathrm{qcl}}(y)[v] - \mathcal{E}'_{\mathrm{a}}(y)[v]\right| \\
&\qquad \le \varepsilon^3 \sum_{\ell=-N+1}^{N} \{|\phi''(2y'_\ell)||y'''_\ell| + \frac{1}{2}|\phi'''(\eta_1^\ell)||y''_{\ell-1}|^2 + \frac{1}{2}|\phi'''(\eta_2^\ell)||y''_\ell|^2\}|v'_\ell|.
\end{aligned}$$

Using the fact that $y'', v' \in \mathcal{U}$, and the bounds

$$|\phi''(2y'_\ell)| \le M_2(\mathcal{S}_1), \quad \text{and} \quad |\phi'''(\eta_k^\ell)| \le M_3(\mathcal{S}_2),$$

we further estimate

$$\begin{aligned}
&\left|\mathcal{E}'_{\mathrm{qcl}}(y)[v] - \mathcal{E}'_{\mathrm{a}}(y)[v]\right| \\
=&\left|\varepsilon\Big\{ \sum_{\ell=-N+1}^{N} \big(-\varepsilon^2\phi''_2(2y'_\ell)y'''_{\ell+1} + \frac{1}{2}\varepsilon^2[\phi'''_2(\eta_1^\ell)y''^2_\ell + \phi'''_2(\eta_2^\ell)y''^2_{\ell+1}]\big)v'_\ell\Big\}\right| \\
\le&\varepsilon^2\Big\{M_2(\mathcal{S}_1)\varepsilon \sum_{\ell=-N+1}^{N} |y'''_\ell||v'_\ell| + M_3(\mathcal{S}_2)\tfrac{1}{2}\varepsilon \sum_{\ell=-N+1}^{N} |y''_\ell|^2\big(|v'_\ell| + |v'_{\ell+1}|\big)\Big\}
\end{aligned}$$

By Hölder's inequality and periodicity of y_ℓ

$$\varepsilon^3 \sum_{\ell=-N+1}^{N} |y'''_{\ell+1}||v'_\ell| \le \varepsilon^2 \|y'''\|_{\ell^p_\varepsilon}\|v'\|_{\ell^q_\varepsilon},$$

and

$$\begin{aligned}
\varepsilon^3 \sum_{\ell=-N+1}^{N} |y''_\ell|^2|v'_\ell| &\le \varepsilon^2\Big(\sum_{\ell=-N+1}^{N} \varepsilon|y''_\ell|^{2p}\Big)^{\frac{1}{p}}\Big(\sum_{\ell=-N+1}^{N} \varepsilon|v'_\ell|^q\Big)^{\frac{1}{q}} \\
&= \varepsilon^2\|y''\|^2_{\ell^{2p}_\varepsilon}\|v'\|_{\ell^q_\varepsilon}, \qquad (2.3.12)
\end{aligned}$$

$$\varepsilon^3 \sum_{\ell=-N+1}^{N} |y''_{\ell+1}|^2 |v'_\ell| \le \varepsilon^2 \Big(\sum_{\ell=-N+1}^{N} \varepsilon |y''_{\ell+1}|^{2p} \Big)^{\frac{1}{p}} \Big(\sum_{\ell=-N+1}^{N} \varepsilon |v'_\ell|^q \Big)^{\frac{1}{q}}$$
$$= \varepsilon^2 \|y''\|^2_{\ell^{2p}_\varepsilon} \|v'\|_{\ell^q_\varepsilon}, \tag{2.3.13}$$

where $1/p + 1/q = 1$. We then have

$$\big|\mathcal{E}'_{\rm qcl}(y)[v] - \mathcal{E}'_{\rm a}(y)[v]\big| \le \varepsilon^2 \big\{ M_2(\mathcal{S}_1) \|y'''\|_{\ell^p_\varepsilon} \|v'\|_{\ell^{p'}_\varepsilon} + M_3(\mathcal{S}_2) \|y''\|^2_{\ell^{2p}_\varepsilon} \|v'\|_{\ell^{p'}_\varepsilon} \big\}.$$

In view of the definition of the negative norm $\|\cdot\|_{\mathcal{U}^{-1,p}}$, this last estimate establishes the stated result.

We note that, to obtain this last estimate, upon setting $w_\ell = (y''_\ell)^2$ and $\hat{w}_\ell = (y''_{\ell-1})^2$, we used that,

$$\varepsilon \sum_{\ell=-N+1}^{N} \frac{1}{2} \big(|y''_\ell|^2 + |y''_{\ell-1}|^2 \big) |v'_\ell| \le \big\| \frac{1}{2}(w + \hat{w}) \big\|_{\ell^p_\varepsilon} \|v'\|_{\ell^{p'}_\varepsilon} \le \frac{1}{2} \big(\|w\|_{\ell^p_\varepsilon} + \|\hat{w}\|_{\ell^p_\varepsilon} \big) \|v'\|_{\ell^{p'}_\varepsilon}.$$

Finally, since $w_\ell = \hat{w}_{\ell+1}$ we have $\|w\|_{\ell^p_\varepsilon} = \|\hat{w}\|_{\ell^p_\varepsilon} = \|y''\|^2_{\ell^{2p}_\varepsilon}$. □

Remark 2.3. As we mentioned in Section 1.2.2, it is well-known (see [23, 56] for instance) that the Cauchy–Born approximation is second-order accurate for simple lattices. This can also be seen in the above result. We note that our estimate is slightly sharper in that we require lower differentiability than the pointwise estimates in [23] (see also [16, Lemma 6.1] for a similar result in a linear setting).

2.3.3 The consistency error of the QCE method

The algebraic expressions for the QCE method can become relatively complex, and hence, in some parts of our following analysis, we will only write out the right half of the atomistic chain in detail, namely, from $\ell = \ell_0$ to $\ell = N$ where $\ell_1 + 1 < \ell_0 < \ell_2 - 1$, and indicate the remaining terms by dots.

To highlight the source of inconsistency of the QCE method on the interface, we first explicitly give the QCE stored energy from (2.2.13):

$$\begin{aligned}\mathcal{E}_{\mathrm{qce}}(y) = \varepsilon\Big\{ &\sum_{\ell=-N+1}^{N} \phi(y'_\ell) + \sum_{\ell=-N+1}^{\ell_1-1} \frac{1}{2}[\phi(2y'_\ell) + \phi(2y'_{\ell+1})] \\ &+\frac{1}{2}\phi(y'_{\ell_1-1} + y'_{\ell_1}) + \frac{1}{2}\phi(y'_{\ell_1} + y'_{\ell_1+1}) \\ &+ \sum_{l=\ell_1+1}^{\ell_2-1} \phi(y'_\ell + y'_{\ell+1}) \\ &+\frac{1}{2}\phi(y'_{\ell_2} + y'_{\ell_2+1}) + \frac{1}{2}\phi(y'_{\ell_2+1} + u'_{\ell_2+2}) + \sum_{\ell=\ell_2+2}^{N} \frac{1}{2}[\phi(2y'_\ell) + \phi(2y'_{\ell+1})]\Big\}\end{aligned}$$

for $y \in \mathcal{Y}$ with $\min_\ell y'_\ell > 0$, we can compute the first variation of $\mathcal{E}_{\mathrm{qce}}$ at y as follows:

$$\begin{aligned}\mathcal{E}'_{\mathrm{qce}}(y)\,[v] = \ldots + \varepsilon\Big\{ &\sum_{\ell=\ell_0}^{N} \phi'(y'_\ell)v'_\ell + \sum_{\ell=\ell_0}^{\ell_2-1} \big[\phi'(y'_{\ell-1} + y'_\ell) + \phi'(y'_\ell + y'_{\ell+1})\big]v'_\ell \\ &+ \Big[\tfrac{1}{2}\phi'(y'_{\ell_2} + y'_{\ell_2+1}) + \phi'(y'_{\ell_2-1} + y'_{\ell_2})\Big]v'_{\ell_2} \\ &+ \Big[\phi'(2y'_{\ell_2+1}) + \tfrac{1}{2}\phi'(y'_{\ell_2} + y'_{\ell_2+1}) + \tfrac{1}{2}\phi'(y'_{\ell_2+1} + y'_{\ell_2+2})\Big]v'_{\ell_2+1} \\ &+ \Big[2\phi'(2y'_{\ell_2+2}) + \tfrac{1}{2}\phi'(y'_{\ell_2+1} + y'_{\ell_2+2})\Big]v'_{\ell_2+2} \\ &+ \sum_{\ell=\ell_2+3}^{N} 2\phi'(2y'_\ell)v'_\ell\Big\}.\end{aligned} \tag{2.3.14}$$

In the following theorem we estimate the consistency error for the QCE method in the $\mathcal{U}^{-1,p}$-norm. In its formulation we use the following notation:

$$\mathcal{C}_{K_1,K_2} := \{1, \ldots, K_1, K_2, \ldots, N\}, \tag{2.3.15}$$

for any $1 < K_1 < K_2 < N$.

Theorem 2.3. *For $y \in \mathcal{Y}$ with $\min_\ell y'_\ell > 0$, and for $1 \le p \le \infty$, we have*

$$\begin{aligned}\|T_{\rm qce}(y)\|_{\mathcal{U}^{-1,p}} =& \|\mathcal{E}'_{\rm qce}(y) - \mathcal{E}'_{\rm a}(y)\|_{\mathcal{U}^{-1,p}} \\ \le& 2\varepsilon^{1/p} M_1(\mathcal{S}_1) + \tfrac{1}{2}\varepsilon M_2(\mathcal{S}_1)\|y''\|_{\ell^p_\varepsilon(\mathcal{I}_{\rm qce})} \\ &+ \varepsilon^2 M_2(\mathcal{S}_2)\|y'''\|_{\ell^p_\varepsilon(\mathcal{C}_{\ell_1,\ell_2+1})} + \varepsilon^2 M_3(\mathcal{S}_3)\|y''\|^2_{\ell^{2p}_\varepsilon(\mathcal{C}_{\ell_1,\ell_2})} =: \mathscr{E}^{\rm qce}_{\rm model}(y),\end{aligned}$$

where

$$\begin{aligned}\mathcal{S}_1 =& \ \{2y'_{\ell_1-1}, 2y'_{\ell_1+1}, 2y'_{\ell_2}, 2y'_{\ell_2+2}\} \\ \mathcal{S}_2 =& \ \{2y'_1, \dots, 2y'_{\ell_1}, 2y'_{\ell_2+1}, \dots, 2y'_N\}, \\ \mathcal{S}_3 =& \ [\min_{\ell\in\mathcal{C}_{\ell_1+1,\ell_2}} 2y'_\ell, \max_{\ell\in\mathcal{C}_{\ell_1+1,\ell_2}} 2y'_\ell], \quad \textit{and} \\ \mathcal{I}_{\rm qce} =& \ \{\ell_1 - 1, \ell_1, \ell_2, \ell_2 + 1\}.\end{aligned}$$

Proof. Using (2.3.14) and (2.3.2) we write the consistency error $\mathcal{E}'_{\rm qce}(y)[v] - \mathcal{E}'_{\rm a}(y)[v]$ as

$$\mathcal{E}'_{\rm qce}(y)[v] - \mathcal{E}'_{\rm a}(y)[v] =: \varepsilon \sum_{\ell=-N+1}^{N} Q_\ell v'_\ell$$

where

$$\begin{aligned}&Q_\ell = 0, \quad \text{for } \ell \in \mathcal{A}\backslash\mathcal{I}, \\ &Q_\ell = 2\phi'(2y'_\ell) - \phi'(y'_{\ell-1} + y'_\ell) - \phi'(y_\ell + y'_{\ell+1}) \quad \text{for } \ell \in \mathcal{C}\backslash(\mathcal{I} \cup \{\ell_1 + 1, \ell_2 + 2\}).\end{aligned}$$

On the interface, we have

$$\begin{aligned}
Q_{\ell_1-1} &= 2\phi'(2y'_{\ell_1-1}) - \frac{1}{2}\phi'(y'_{\ell_1-1}+y'_{\ell_1}) - \phi'(y'_{\ell_1-2}+y'_{\ell-1}))\\
Q_{\ell_1} &= \phi'(2y'_{\ell_1}) - \frac{1}{2}\phi'(y'_{\ell_1-1}+y'_{\ell_1}) - \frac{1}{2}\phi'(y'_{\ell_1}+y'_{\ell_1+1})\\
Q_{\ell_1+1} &= -\frac{1}{2}\phi'(y'_{\ell_1-1}+y'_{\ell_1}),
\end{aligned} \tag{2.3.16}$$

$$\begin{aligned}
Q_{\ell_2} &= -\frac{1}{2}\phi'(y'_{\ell_2}+y'_{\ell_2+1}),\\
Q_{\ell_2+1} &= \phi'(2y'_{\ell_2+1}) - \frac{1}{2}\phi'(y'_{\ell_2}+y'_{\ell_2+1}) - \frac{1}{2}\phi'(y'_{\ell_2+1}+y'_{\ell_2+2}),\\
Q_{\ell_2+2} &= 2\phi'(2y'_{\ell_2+2}) - \frac{1}{2}\phi'(y'_{\ell_2+1}+y'_{\ell_2+2}) - \phi'(y'_{\ell_2+2}+y'_{\ell_2+3}),
\end{aligned} \tag{2.3.17}$$

The estimate of Q_ℓ for $\ell \in \mathcal{C}\backslash(\mathcal{I}\cup\{\ell_1+1,\ell_2+2\})$ is already contained in the proof of Theorem 2.2.

Using the expansions (2.3.9) and (2.3.10), we can rewrite $Q_\ell, \ell \in \{\ell_1-1,\ell_1,\ell_1+1,\ell_2,\ell_2+1,\ell_2+2\}$, in the form

$$\begin{aligned}
Q_{\ell_1-1} &= \frac{1}{2}\phi'(2y'_{\ell_1-1}) - \varepsilon^2 y'''_{\ell_1-1}\phi''(2y'_{\ell_1-1}) + \frac{1}{2}\varepsilon y''_{\ell_1-1}\phi''(2y'_{\ell_1-1})\\
&\quad - \frac{1}{4}\varepsilon^2 y''_{\ell_1-1}\phi'''(\eta_1^{\ell_1-1}) - \frac{1}{2}\varepsilon^2 {y''_{\ell_1-2}}^2\phi'''(\eta_2^{\ell_1-1})\\
Q_{\ell_1} &= -\frac{1}{2}\varepsilon^2 y'''_{\ell_1}\phi''(2y'_{\ell_2}) - \frac{1}{4}\varepsilon^2\left[{y''_{\ell_1-1}}^2\phi'''(\eta_1^{\ell_1}) + {y''_{\ell_1}}^2\phi'''(\eta_2^{\ell_1})\right]\\
Q_{\ell_1+1} &= -\frac{1}{2}\phi'(2y'_{\ell_1+1}) - \frac{1}{2}\varepsilon y''_{\ell_1}\phi''(2y'_{\ell_1+1}) - \frac{1}{4}\varepsilon^2 {y''_{\ell_1}}^2\phi'''(\eta^{\ell_1+1}),
\end{aligned}$$

$$\begin{aligned}
Q_{\ell_2} &= -\frac{1}{2}\phi'(2y'_{\ell_2}) - \tfrac{1}{2}\varepsilon y''_{\ell_2}\phi''(2y'_{\ell_2}) - \tfrac{1}{4}\varepsilon^2 {y''_{\ell_2}}^2\phi'''(\eta^{\ell_2}),\\
Q_{\ell_2+1} &= -\tfrac{1}{2}\varepsilon^2 y'''_{\ell_2+1}\phi''(2y'_{\ell_2+1}) - \tfrac{1}{4}\varepsilon^2\left[{y''_{\ell_2}}^2\phi'''(\eta_1^{\ell_2+1}) + {y''_{\ell_2+1}}^2\phi'''(\eta_2^{\ell_2+1})\right],\\
Q_{\ell_2+2} &= \tfrac{1}{2}\phi'(2y'_{\ell_2+2}) - \tfrac{1}{2}\varepsilon y''_{\ell_2+1}\phi''(2y'_{\ell_2+2}) - \varepsilon^2 y'''_{\ell_2+2}\phi''_2(2y'_{\ell_2+2})\\
&\quad - \tfrac{1}{4}\varepsilon^2 {y''_{\ell_2+1}}^2\phi'''(\eta_1^{\ell_2+2}) - \tfrac{1}{2}\varepsilon^2 {y''_{\ell_2+2}}^2\phi'''(\eta_2^{\ell_2+2}),
\end{aligned}$$

where

$$\eta^{\ell_1+1} \in \operatorname{conv}\{2y'_{\ell_1}, y'_{\ell_1}+y'_{\ell_1+1}\}, \qquad \eta^{\ell_2} \in \operatorname{conv}\{2y'_{\ell_2}, y'_{\ell_2}+y'_{\ell_2+1}\},$$
$$\eta_1^{\ell_1} \in \operatorname{conv}\{2y'_{\ell_1}, y'_{\ell_1-1}+y'_{\ell_1}\}, \qquad \eta_2^{\ell_1} \in \operatorname{conv}\{2y'_{\ell_1}, y'_{\ell_1}+y'_{\ell_1+1}\},$$
$$\eta_1^{\ell_2+1} \in \operatorname{conv}\{2y'_{\ell_2+1}, y'_{\ell_2}+y'_{\ell_2+1}\}, \qquad \eta_2^{\ell_2+1} \in \operatorname{conv}\{2y'_{\ell_2+1}, y'_{\ell_2+1}+y'_{\ell_2+2}\},$$
$$\eta_1^{\ell_1-1} \in \operatorname{conv}\{2y'_{\ell_1-1}, y'_{\ell_1-1}+y'_{\ell_1}\}, \qquad \eta_2^{\ell_1-1} \in \operatorname{conv}\{2y'_{\ell_1-1}, y'_{\ell_1-2}+y'_{\ell_1-1}\},$$
$$\eta_1^{\ell_2+2} \in \operatorname{conv}\{2y'_{\ell_2+2}, y'_{\ell_2+1}+y'_{\ell_2+2}\}, \qquad \eta_2^{\ell_2+2} \in \operatorname{conv}\{2y'_{\ell_2+2}, y'_{\ell_2+2}+y'_{\ell_2+3}\}.$$

After regrouping the terms, using corresponding estimates on the left half of the domain, and using the constants we defined in the statement of the theorem, we get the following estimate:

$$\begin{aligned}
|\mathcal{E}'_{\mathrm{qce}}(y)[v] - \mathcal{E}'_{\mathrm{a}}(y)[v]| \leq\ & M_1(\mathcal{S}_1)\Big\{\tfrac{1}{2}\varepsilon|v'_{\ell_1-1}| + \tfrac{1}{2}\varepsilon|v'_{\ell_1+1}| + \tfrac{1}{2}\varepsilon|v'_{\ell_2}| + \tfrac{1}{2}\varepsilon|v'_{\ell_2+2}|\Big\} \\
& + M_2(\mathcal{S}_1)\Big\{\tfrac{1}{2}\varepsilon^2|y''_{\ell_1-1}||v'_{\ell_1-1}| + \tfrac{1}{2}\varepsilon^2|y''_{\ell_1}||v'_{\ell_1+1}| \\
& \qquad + \tfrac{1}{2}\varepsilon^2|y''_{\ell_2}||v'_{\ell_2}| + \tfrac{1}{2}\varepsilon^2|y''_{\ell_2+1}||v'_{\ell_2+2}|\Big\} \\
& + M_2(\mathcal{S}_2)\Big\{\varepsilon^3 \sum_{\ell=-N+1}^{\ell_1} |y'''_\ell||v'_\ell| + \varepsilon^3 \sum_{\ell=\ell_2+1}^{N} |y'''_\ell||v'_\ell|\Big\} \\
& + M_3(\mathcal{S}_3)\Big\{\tfrac{1}{2}\varepsilon^3 \sum_{\ell=-N+1}^{\ell_1} |y''_\ell|^2\big(|v'_\ell| + |v'_{\ell+1}|\big) \\
& \qquad + \tfrac{1}{2}\varepsilon^3 \sum_{\ell=\ell_2}^{N} |y''_\ell|^2\big(|v'_\ell| + |v'_{\ell+1}|\big)\Big\}.
\end{aligned}$$

It then holds by a weighted Hölder inequality that

$$\varepsilon^3 \sum_{\ell=-N+1}^{\ell_1} |y'''_\ell||v'_\ell| + \varepsilon^3 \sum_{\ell=\ell_2+1}^{N} |y'''_\ell||v'_\ell| \leq \varepsilon^2 \|y'''\|_{\ell_\varepsilon^p(\mathcal{C}_{\ell_1-1,\ell_2+1})} \|v'\|_{\ell_\varepsilon^{p'}},$$

$$\varepsilon^3 \sum_{\ell=-N+1}^{\ell_1} |y''_\ell|^2|v'_\ell| + \varepsilon^3 \sum_{\ell=\ell_2}^{N} |y''_\ell|^2|v'_\ell| \leq \varepsilon^2 \|y''\|^2_{\ell_\varepsilon^{2p}(\mathcal{C}_{\ell_1,\ell_2})} \|v'\|_{\ell_\varepsilon^{p'}},$$

where $1/p + 1/p' = 1$.

For the interface terms, we have

$$\varepsilon^2 |y''_\ell||v'_\ell| \le \varepsilon \|y'\|_{\ell^p_\varepsilon(\mathcal{I}_{\rm qce})} \|v'\|_{\ell^{p'}_\varepsilon},$$

and

$$\varepsilon |v'_\ell| \le \varepsilon^{1/p} \|v'\|_{\ell^{p'}_\varepsilon}.$$

Thus we can estimate the consistency error by

$$\begin{aligned}|\mathcal{E}'_{\rm qce}(y)[v] - \mathcal{E}'_{\rm a}(y)[v]| \le \Big\{ & 2\varepsilon^{1/p} M_1(\mathcal{S}_1) + \tfrac{1}{2}\varepsilon \|y'\|_{\ell^p_\varepsilon(\mathcal{I}_{\rm qce})} + \varepsilon^2 M_2(\mathcal{S}_1) \|y'''\|_{\ell^p_\varepsilon(\mathcal{C}_{\ell_1+1,\ell_2+2})} \\ & + 2\varepsilon^2 M_3(\mathcal{S}_2) \|y''\|^2_{\ell^{2p}_\varepsilon(\mathcal{C}_{\ell_1+1,\ell_2+1})} \Big\} \|v'\|_{\ell^{p'}_\varepsilon}.\end{aligned}$$

In view of the definition of the negative norm $\|\cdot\|_{\mathcal{U}^{-1,p}}$, this estimate establishes the stated result. □

2.3.4 The consistency error of the QNL method

We again explicitly give the formulation of the QNL stored energy

$$\begin{aligned}\mathcal{E}_{\rm qnl}(y) = \varepsilon \Big\{ & \sum_{\ell=-N+1}^{N} \phi_1(y'_\ell) \\ & + \sum_{\ell=-N+1}^{\ell_1-1} \frac{1}{2}[\phi_2(2y'_\ell) + \phi_2(2y'_{\ell+1})] \\ & + \sum_{\ell=\ell_1}^{\ell_2} \phi_2(y'_\ell + y'_{\ell+1}) \\ & + \sum_{\ell=\ell_2+1}^{N} \frac{1}{2}[\phi_2(2y'_\ell) + \phi_2(2y'_{\ell+1})] \Big\}\end{aligned}$$

From the above expression, we obtain, for $y \in \mathcal{Y}$ with $\min_\ell y'_\ell > 0$, and for $v \in \mathcal{U}$,

$$\begin{aligned}\mathcal{E}'_{\rm qnl}(y)\,[v] = \ldots + \varepsilon\Big\{ \sum_{\ell=\ell_0}^{N} \phi'(y'_\ell) v'_\ell + \sum_{\ell=\ell_0}^{\ell_2} \big[\phi'(y'_{\ell-1}+y'_\ell) + \phi'(y'_\ell + y'_{\ell+1})\big] v'_\ell \\ + \Big[\phi'(2y'_{\ell_2+1}) + \phi'(y'_{\ell_2}+y'_{\ell_2+1})\Big] v'_{\ell_2+1} \\ + \sum_{\ell=\ell_2+2}^{N} 2\phi'(2y'_\ell) v'_\ell \Big\}. \end{aligned} \tag{2.3.18}$$

Using this representation, it is easy to establish a consistency error estimate for the QNL method in the $\mathcal{U}^{-1,p}$-norm. A similar estimate was given in [51, Theorem 3.1]; for the sake of completeness we nevertheless include a proof here as well.

Theorem 2.4. *For any $y \in \mathcal{Y}$ with $\min_\ell y'_\ell > 0$, and for $1 \le p \le \infty$, we have*

$$\begin{aligned}\|T_{\rm qnl}(y)\|_{\mathcal{U}^{-1,p}} &= \|\mathcal{E}'_{\rm qnl}(y) - \mathcal{E}'_{\rm a}(y)\|_{\mathcal{U}^{-1,p}} && (2.3.19)\\ &\le \varepsilon M_2(\mathcal{S}_1)\|y''\|_{\ell^p_\varepsilon(\mathcal{I}_{\rm qnl})} + \varepsilon^2 M_2(\mathcal{S}_2)\|y'''\|_{\ell^p_\varepsilon(\mathcal{C}_{\ell_1-1,\ell_2+2})} \\ &\quad + \varepsilon^2 M_3(\mathcal{S}_3)\|y''\|^2_{\ell^{2p}_\varepsilon(\mathcal{C}_{\ell_1-1,\ell_2+1})} =: \mathscr{E}^{\rm qnl}_{\rm model}(y), && (2.3.20)\end{aligned}$$

where

$$\begin{aligned}\mathcal{S}_1 &= {\rm conv}\{2y'_{\ell_1}, y'_{\ell_1-1}+y'_{\ell_1}\} \cup {\rm conv}\{2y'_{\ell_2+1}, y'_{\ell_2+1}+y'_{\ell_2+2}\},\\ \mathcal{S}_2 &= \{2y'_1, \ldots, 2y'_{\ell_1-1}, 2y'_{\ell_2+2}, \ldots, 2y'_N\},\\ \mathcal{S}_3 &= [\min_{\ell\in\mathcal{C}_{\ell_1,\ell_2+1}} 2y'_\ell, \max_{\ell\in\mathcal{C}_{\ell_1,\ell_2+1}} 2y'_\ell],\\ \mathcal{I}_{\rm qnl} &= \{\ell_1-1, \ell_2+1\},\end{aligned}$$

and where the sets $\mathcal{C}_{K_1,K_2}$ are defined in (2.3.15).

Proof. As in the proof of Theorem 2.3 we write the consistency error as

$$\mathcal{E}'_{\text{qnl}}(y)[v] - \mathcal{E}'_{\text{a}}(y)[v] =: \varepsilon \sum_{\ell=-N+1}^{N} Q_\ell v'_\ell,$$

where

$$\begin{aligned} Q_\ell &= 0, \qquad \text{for } \ell = \ell_0, \dots, \ell_2, \\ Q_\ell &= 2\phi'(2y'_\ell) - \phi'(y'_{\ell-1} + y'_\ell) - \phi'(y'_\ell + y'_{\ell+1}), \quad \text{for } \ell \in \mathcal{C}\backslash\mathcal{I}. \end{aligned}$$

On the interface, we have

$$Q_{\ell_1} = \phi'(2y'_{\ell_1}) - \phi'(y'_{\ell_1-1} + y'_{\ell_1}), \tag{2.3.21}$$

$$Q_{\ell_2+1} = \phi'(2y'_{\ell_2+1}) - \phi'(y'_{\ell_2+1} + y'_{\ell_2+2}), \tag{2.3.22}$$

Using the expansions (2.3.9) and (2.3.10), we can write Q_{ℓ_1} and Q_{ℓ_2+1} as

$$\begin{aligned} Q_{\ell_1} &= \phi'(2y'_{\ell_1}) - \phi'(2y'_{\ell_1} - \varepsilon y''_{\ell_1-1}) \\ &= \varepsilon y''_{\ell_1-1}\phi''(\eta^{\ell_1}) \\ Q_{\ell_2+1} &= \phi'(2y'_{\ell_2+1}) - \phi'(2y'_{\ell_2+1} + \varepsilon y''_{\ell_2+1}) \\ &= -\varepsilon y''_{\ell_2+1}\phi''(\eta^{\ell_2}), \end{aligned}$$

where $\eta^{\ell_1} \in \text{conv}\{2y'_{\ell_1+1}, y'_{\ell_1+1} + y'_{\ell_1+2}\}$ and $\eta^{\ell_2} \in \text{conv}\{2y'_{\ell_2+1}, y'_{\ell_2+1} + y'_{\ell_2+2}\}$. To estimate Q_ℓ for $\ell \in \mathcal{C}\backslash\mathcal{I}$ we use the estimates in the proof of Theorem 2.2.

After some algebraic computations, we get the bound

$$
\begin{aligned}
|\mathcal{E}'_{\mathrm{qnl}}(y)[v] - \mathcal{E}'_{\mathrm{a}}(y)[v]| \leq{}& M_2(\mathcal{S}_1)\Big\{\varepsilon^2 |y''_{\ell_1-1}||v'_{\ell_1}| + \varepsilon^2 |y''_{\ell_2+1}||v'_{\ell_2+1}|\Big\} \\
&+ M_2(\mathcal{S}_2)\Big\{\varepsilon^3 \sum_{\ell=-N+1}^{\ell_1-1} |y'''_\ell||v'_\ell| + \varepsilon^3 \sum_{\ell=\ell_2+2}^{N} |y'''_\ell||v'_\ell|\Big\} \\
&+ M_3(\mathcal{S}_3)\Big\{\tfrac{1}{2}\varepsilon^3 \sum_{\ell=1}^{\ell_1-1} |y''_\ell|^2\big(|v'_\ell| + |v'_{\ell+1}|\big) \\
&\qquad + \tfrac{1}{2}\varepsilon^3 \sum_{\ell=\ell_2+1}^{N} |y''_\ell|^2\big(|v'_\ell| + |v'_{\ell+1}|\big)\Big\}.
\end{aligned}
$$

The estimate of the above bound is similar as that in the proof of Theorem 2 and finally we obtain

$$
\begin{aligned}
|\mathcal{E}'_{\mathrm{qnl}}(y)[v] - \mathcal{E}'_{\mathrm{a}}(y)[v]| \leq \Big\{&\varepsilon M_2(\mathcal{S}_3)\|y''\|_{\ell^p_\varepsilon(\mathcal{I}_q)} + \varepsilon^2 M_2(\mathcal{S}_1)\|y'''\|_{\ell^p_\varepsilon(\mathcal{C}_{\ell_1-1,\ell_2+2})} \\
&+ 2\varepsilon^2 M_3(\mathcal{S}_2)\|y''\|^2_{\ell^{2p}_\varepsilon(\mathcal{C}_{\ell_1-1,\ell_2+1})}\Big\}\|v'\|_{\ell^{p'}_\varepsilon}.
\end{aligned}
$$

In view of the definition of the negative norm $\|\cdot\|_{\mathcal{U}^{-1,p}}$, this estimate establishes the stated result. □

2.3.5 Discussion and comparison

In the analysis of this section we have estimated the consistency errors of three different QC methods in negative Sobolev norms. We see that the leading order terms in the upper bounds are $O(\varepsilon^2)$, $O(\varepsilon^{1/p})$ and $O(\varepsilon)$ for the QCL, QCE, and QNL methods, respectively. However, a much finer distinction can and should be made.

First of all, we note that since all three methods reduce to the Cauchy–Born approximation in the continuum region (in the case of the QCL method the entire

domain is understood as the continuum region), the corresponding contributions are all of second order.

Second, we see that the QCE method (and only the QCE method) has a zeroth-order term $2M_1\varepsilon^{1/p}$ in the interface region. The origin of this term is the occurrence of 'ghost forces', that is, the fact that homogeneous deformations are not equilibria of the QCE model:

$$E'_{\mathrm{qce}}(Fx) \neq 0,$$

which we have previously mentioned in Section 1.3.1.2. The origin and effect of the ghost forces are discussed in more detail in [66, 43, 15, 16, 45].

We call this term zeroth order for several reasons: (i) From any possible perspective, this term is of zeroth order if $p = \infty$, in which case the consistency error is related to the error in the $\mathcal{U}^{1,\infty}$-norm. (ii) The parameter ε is a constant of the problem and does *not* tend to zero. (iii) Indeed, our understanding of the order of consistency is related more closely to the dependence of the error on the smoothness of the solution, and the term $2M_1\varepsilon^{1/p}$ is independent of the magnitude of $\boldsymbol{y}''$ in the interface region. The scaling $\varepsilon^{1/p}$ in the QCE consistency error bound is related only to the *width* of the interface region.

Finally, we point out the first-order consistency term in the interface region for the QNL method. The origin of this term is, in essence, the loss of symmetry that is introduced by changing the interaction law at the interface between the atomistic and continuum regions. The analysis in [16], and our numerical experiments in the present paper, also show that this asymmetry creates effectively a higher order ghost force.

We also briefly compare our results to similar results in the literature. A detailed discussion of the consistency error estimate for the QNL method can be found in [51], hence we focus on our analysis of the QCE method. The first detailed analysis of the effect of the ghost force on the quasicontinuum error was given in [15]. In this paper, the authors formulated a linearized model problem, which allowed an explicit calculation of the effect of the ghost force on the quasicontinuum solution. While our analysis is more straightforward, is easily applied in the nonlinear setting, and possibly gives even sharper consistency error estimates, the analysis in [15] reveals much finer qualitative details such as the decay of the effect of the ghost force in the QCE solution.

2.4 Coarse-Graining

The transition from an atomistic to a continuum model is only the first step in the construction of a practical QC method. In the second step, one coarse-grains the continuum region using finite element methods in order to reduce the number of degrees of freedom. However, the effect of the coarse-graining has been neglected by previous analyzes of the QC methods. In this section, we construct the coarse-grained solution space of the QC models and introduce the mesh-dependent inner product as the approximation of the external energy, which corresponds to the finite element solution space S_h and the linear form $\langle \ell_h, v_h \rangle$ on the right hand side of (2.1.4) respectively. The full QC model with coarse-graining is then established.

The following construction of the coarse-grained spaces of displacements and deformations follows largely the convention in [40, 41].

We partition the domain by choosing a set of representative atoms (or, *repatoms*)

$$\mathcal{L}_{\text{rep}} = \{t_1, t_2, \ldots, t_{N_{\text{rep}}}\} \subseteq \{1, 2, \ldots, N\},$$

such that $N_{\text{rep}} \ll N$ and $t_1 < t_2 < \ldots < t_{N_{\text{rep}}}$. For simplicity of the implementation and analysis of the QCE and QNL methods we assume that

$$\begin{aligned} &\{\ell_1 - 2, \ldots, \ell_2 + 2\} \subset \mathcal{L}_{\text{rep}} \text{ for the QCE method, and} \\ &\{\ell_1 - 1, \ldots, \ell_2 + 1\} \subset \mathcal{L}_{\text{rep}} \text{ for the QNL method.} \end{aligned} \tag{2.4.1}$$

For the analysis of the QCL method, no restriction of this kind is required as all the atoms are considered to be in the continuum region.

Since the domain is periodic, the grid is also extended periodically, that is, we define $t_{i+N_{\text{rep}}} = t_i + N$. For simplicity, we also assume that $t_0 = -N$ and $t_{N_{\text{rep}}} = N$. The positions of the repatoms in the reference lattice are $x_{t_i} = \varepsilon t_i$. The mesh size functions for the elements and for the nodes are

$$h_i = \varepsilon(t_i - t_{i-1}) \quad \text{and} \quad H_i = \tfrac{1}{2}\varepsilon(t_{i+1} - t_{i-1}), \qquad \text{for } i \in \mathbb{Z}.$$

We then define the mesh-dependent inner product

$$\langle v, w \rangle_h = \sum_{i=1}^{N_{\text{rep}}} H_i v_{t_i} w_{t_i} \qquad \forall v, w \in \mathbb{R}^{\mathbb{Z}},$$

which is a trapezoidal rule approximation of $\langle \cdot, \cdot \rangle_\varepsilon$.

Finally, we define the coarse-grained displacement space as

$$\begin{aligned} \mathcal{U}_{\text{qc}} &= \big\{u \in \mathbb{R}^{\mathbb{Z}} : u \text{ is } N\text{-periodic, p.w. affine w.r.t. } \mathcal{L}_{\text{rep}}, \text{ and } \langle u, 1 \rangle_h = 0\big\}, \\ &= \big\{u \in \mathbb{R}^{\mathbb{Z}} : u_{t_i} = u_{t_i + N_{\text{rep}}}, u_\ell = \frac{t_{i+1} - \ell}{t_{i+1} - t_i} u_{t_i} + \frac{\ell - t_i}{t_{i+1} - t_i} u_{t_{i+1}}, \\ &\qquad \text{for } t_i < \ell \le t_{i+1} \text{ where } t_i \in \mathcal{L}_{\text{rep}}, \text{and } \sum_{i=1}^{N_{\text{rep}}} \tfrac{1}{2}\varepsilon(t_{i+1} - t_{i-1}) u_{t_i} = 0\big\}, \end{aligned} \tag{2.4.2}$$

and the corresponding space of admissible deformations as

$$\mathcal{Y}_{\rm qc} = \{y \in \mathbb{R}^{\mathbb{Z}} : y_\ell = \varepsilon F\ell + u_\ell,\ u \in \mathcal{U}_{\rm qc}\}. \tag{2.4.3}$$

We remark that, if u is a piecewise affine grid function then $\langle u, 1\rangle_h = \langle u, 1\rangle_\varepsilon$, and hence $\mathcal{U}_{\rm qc} \subset \mathcal{U}$ and $\mathcal{Y}_{\rm qc} \subset \mathcal{Y}$.

Next, we redefine the total QC energy, by approximating the external forces via the mesh-dependent inner product, as

$$E_{\rm qc}(y) = \mathcal{E}_{\rm qc}(y) - \langle f, u\rangle_h, \tag{2.4.4}$$

where qc $\in \{\text{qcl}, \text{qce}, \text{qnl}\}$ and $u = y - Fx$. We are now seeking a solution to

$$y_{\rm qc} \in \operatorname{argmin} E_{\rm qc}(\mathcal{Y}_{\rm qc}). \tag{2.4.5}$$

If $\min_\ell (y_{\rm qc})'_\ell > 0$, then $E_{\rm qc}$ is differentiable at $y_{\rm qc}$ and the first-order necessary optimality condition for (2.4.5), in variational form, reads

$$\mathcal{E}'_{\rm qc}(y_h)[v_h] = \langle f, v_h\rangle_h \qquad \forall v_h \in \mathcal{U}_{\rm qc}. \tag{2.4.6}$$

2.5 A Superconvergence Estimate

Having established the full QC model, as in a typical finite element error analysis,we may split the error $e = y_{\rm a} - y_{\rm qc}$ by the triangle inequality into

$$\begin{aligned}\|e\|_{\mathcal{U}^{1,p}} \le& \|I_h e\|_{\mathcal{U}^{1,p}} + \|e - I_h e\|_{\mathcal{U}^{1,p}} \\ =& \|I_h y_{\rm a} - y_{\rm qc}\|_{\mathcal{U}^{1,p}} + \|y_{\rm a} - I_h y_{\rm a}\|_{\mathcal{U}^{1,p}},\end{aligned}$$

where the interpolation operator I_h will be properly defined later so that $I_h u \in \mathcal{U}_{\rm qc}$ and $I_h y \in \mathcal{Y}_{\rm qc}$.

As we pointed out in Section 2.1, we need to estimate two error terms caused by the coarse-graining of the solution space. The first one is $\|y_{\mathrm{a}} - I_h y_{\mathrm{a}}\|_{\mathcal{U}^{1,p}}$ and the second one is $\|\{\mathcal{E}'_{\mathrm{qc}}(y_a) - \mathcal{E}'_{\mathrm{qc}}(I_h y_a)\}\|_{\mathcal{U}^{-1,2}}$ which corresponds to the error defined in (2.1.10) and will appear in the estimate of $\|I_h e\|_{\mathcal{U}^{1,2}} := \|I_h y_{\mathrm{a}} - y_{\mathrm{qc}}\|_{\mathcal{U}^{1,2}}$ in Section 2.8. The reason for restricting the estimate of $I_h e$ in the $\mathcal{U}^{1,2}$-norm rather than in general $\mathcal{U}^{1,p}$-norm is because we will only establish the $\mathcal{U}^{1,2}$-stability of the QC methods in Section 2.7.

We first define a modified nodal interpolation operator $I_h : \mathcal{U} \to \mathcal{U}_{\mathrm{qc}}$ by $(I_h u)_{t_i} = u_{t_i} + C$ where the constant $C = -\langle u, 1\rangle_h$ is chosen so that $\langle I_h u, 1\rangle_h = 0$. With slight abuse of notation, we also define the interpolation operator $I_h : \mathcal{Y} \to \mathcal{Y}_{\mathrm{qc}}$ by

$$(I_h y)_{t_i} = \varepsilon F t_i + (I_h u)_{t_i}. \tag{2.5.1}$$

We note that, for $y_1, y_2 \in \mathcal{Y}$, $y_1 - y_2 \in \mathcal{U}$, and as a result $e, I_h e, y_{\mathrm{a}} - I_h y_{\mathrm{a}} \in \mathcal{U}$.

To estimate the interpolation error $\|y^{\mathrm{a}} - I_h y^{\mathrm{a}}\|_{\mathcal{U}^{1,2}}$ we can use the following result.

Lemma 2.5. *Let $y \in \mathcal{Y}$, and $p \in [1, \infty)$, then*

$$\|y' - I_h y'\|_{\ell^p_\varepsilon} \leq \frac{1}{2}\Big(\sum_{i \in \mathcal{C}_c} h_i^p \|y''\|^p_{\ell^p_\varepsilon(\mathcal{K}_i^2)}\Big)^{\frac{1}{p}},$$

where

$$\mathcal{C}_c = \{i \in \mathbb{Z} : t_i - t_{i-1} \geq 2\}, \quad \textit{and} \quad \mathcal{K}_i^2 = \{t_{i-1} + 1, \ldots, t_i - 1\}.$$

Moreover, for $p = \infty$, we have

$$\|y' - I_h y'\|_{\ell^\infty_\varepsilon} \leq \frac{1}{2} \max_{i \in \mathcal{C}_c} \big(h_i \|y''\|_{\ell^\infty_\varepsilon(\mathcal{K}_i^2)}\big).$$

Proof. If the ℓ^p_ε-norm is replaced by the ℓ^q_ε-norm, $q \in \{1, \infty\}$, then the result follows immediately from Theorem A.4 of [55]. For $p \in (1, \infty)$ it is obtained using the Riesz-Thorin interpolation theorem. □

Having the interpolation error estimate in hand, we derive an estimate of the coarse graining error $\|\mathcal{E}'_{\mathrm{qc}}(y_a) - \mathcal{E}'_{\mathrm{qc}}(I_h y_a)\|_{\mathcal{U}^{-1,2}}$ in the remainder of the present section. The estimate turns out to be a superconvergence result because of the one dimensional feature of the problem.As we will see in Section 2.8, where a complete estimate for $\|I_h e\|_{\mathcal{U}^{1,2}}$ is given, this superconvergence result is a crucial ingredient for the error analysis.

Lemma 2.6. *Let $y \in \mathcal{Y}$ such that $\min_\ell y'_\ell > 0$, then*

$$\sup_{\substack{w \in \mathcal{U}_{\mathrm{qc}} \\ \|w'\|_{\ell^2_\varepsilon} = 1}} \big|\{\mathcal{E}'_{\mathrm{qc}}(y) - \mathcal{E}'_{\mathrm{qc}}(I_h y)\}[w]\big| \leq C_1 \Big(\sum_{i \in \mathcal{C}_c} h_i^4 \|y''\|^4_{\ell^4_\varepsilon(\mathcal{K}_i^2)} \Big)^{\frac{1}{2}} =: \mathscr{E}_{\mathrm{fem}}(y) \qquad (2.5.2)$$

for some constant

$$C_1 = \tfrac{1}{8} M_3(\mathcal{S}_1) + M_3(2\mathcal{S}_1),$$

where

$$\mathcal{S}_1 = \big[\min_{\ell \in \mathcal{C}_{\ell_1 - 1, \ell_2 + 2}} y'_\ell, \max_{\ell \in \mathcal{C}_{\ell_1 - 1, \ell_2 + 2}} y'_\ell \big]$$

and where $M_i(\mathcal{S}_1)$ is defined in (2.2.20)*. (For* qc = qcl *we set $\ell_1 = \ell_2 + 2$ in the definition of $\mathcal{S}_1$.)*

Proof. We begin by noting that the values of $I_h y'_\ell$ in the continuum region are convex combinations of the values of y'_ℓ in the continuum region, and hence $I_h y'_\ell \in \mathcal{S}_1$ for all occurrences below.

Whenever $t_i - t_{i-1} = 1$ (i.e., $h_i = \varepsilon$), we have $y'_{t_i} = I_h y'_{t_i}$, and hence it is easy to see, using assumption (2.4.1), that

$$\begin{aligned}\{\mathcal{E}'_{\mathrm{qc}}(y) - \mathcal{E}'_{\mathrm{qc}}(I_h y)\}[w] =& \varepsilon \sum_{\ell=-N+1}^{N} \Big\{ [\phi'(y'_\ell) - \phi'(I_h y'_\ell)] + 2[\phi'(2y'_\ell) - \phi'(2I_h y'_\ell)] \Big\} w'_\ell \\ =& \varepsilon \sum_{i \in \mathcal{C}_c} \sum_{\ell=t_{i-1}+1}^{t_i} \{W'(y'_\ell) - W'(I_h y'_\ell)\} w'_\ell,\end{aligned}$$

where we recall that $W'(r) = \phi'(r) + 2\phi'(2r)$. Note also that this formula is independent of the choice of QC method.

A Taylor expansion yields

$$W'(y'_\ell) - W'(I_h y'_\ell) = W''(I_h y'_\ell)(y'_\ell - I_h y'_\ell) + \tfrac{1}{2} W'''(\theta_\ell)(y'_\ell - I_h y'_\ell)^2,$$

for some $\theta_\ell \in \mathcal{S}_1$. Using the property that $\sum_{\ell=t_{i-1}+1}^{t_i} (y'_\ell - I_h y'_\ell) = 0$ and the values of w'_ℓ, $\phi''(I_h y'_\ell)$ and $\phi''(2I_h y'_\ell)$ do not change inside an element (i.e., they take the same value for $\ell = t_{i-1}+1, \ldots, t_i$), we arrive at

$$\big|\{E'_{\mathrm{qc}}(y) - E'_{\mathrm{qc}}(I_h y)\}[w]\big| \le \varepsilon \sum_{i \in \mathcal{C}_c} \sum_{\ell=t_{i-1}+1}^{t_i} \frac{1}{2} |W'''(\theta_\ell)| |y'_\ell - I_h y'_\ell|^2 |w'_\ell|.$$

Since $W'''(r) = \phi'''(r) + 8\phi'''(2r)$ and $\theta_\ell \in \mathcal{S}_1$, we have

$$\max_\ell |W'''(\theta_\ell)| \le M_3(\mathcal{S}_1) + 8M_3(2\mathcal{S}_1) =: 8C_1.$$

Therefore, we get the following estimate

$$\begin{aligned}\big|\{E'_{\mathrm{qc}}(y) - E'_{\mathrm{qc}}(I_h y)\}[w]\big| &\le 4C_1 \varepsilon \sum_{i \in \mathcal{C}_c} \sum_{\ell=t_{i-1}+1}^{t_i} |y'_\ell - I_h y'_\ell|^2 |w'_\ell| \\ &\le 4C_1 \sum_{i \in \mathcal{C}_c} \frac{1}{4} h_i^2 \, \varepsilon \sum_{\ell=t_{i-1}+1}^{t_i - 1} |y''_\ell|^2 |w'_\ell| \\ &\le C_1 \Big(\sum_{i \in \mathcal{C}_c} h_i^4 \|y''\|^4_{\ell^4_\varepsilon(\mathcal{K}_i^2)} \Big)^{\frac{1}{2}} \|w\|_{\mathcal{U}^{1,2}}.\end{aligned}$$

The last two steps follow from Lemma 2.5 as $|w'_\ell|$ is constant in each element and a weighted Hölder's inequality. □

2.6 Analysis of the External Force

In this section, we give the consistency error estimate of the linear functional corresponding to (2.1.11). In our problem, this is due to the approximation of external energy. The following estimate is a generalization of a similar result in [55].

Lemma 2.7. *For $f \in \mathcal{U}$, we have*

$$\sup_{\substack{v\in\mathcal{U}_{\mathrm{qc}}\\ \|v'\|_{\ell^2_\varepsilon}=1}} \left|\langle f, v\rangle_h - \langle f, v\rangle_\varepsilon\right| \le \left(\sum_{i\in\mathcal{C}_c} h_i^4 \left[\frac{1}{32}\|f''\|^2_{\ell^2_\varepsilon(\mathcal{K}_i^2)} + \frac{1}{2}\|f'\|^2_{\ell^2_\varepsilon(\mathcal{K}_i^1)'}\right]\right)^{1/2} =: \mathscr{E}_{\mathrm{ext}}(\boldsymbol{f}), \tag{2.6.1}$$

where $\mathcal{K}_i^1 = \{t_{i-1}+1, \dots, t_i\}$, and where $\mathcal{K}_i^2$ and $\mathcal{C}_c$ are defined in Lemma 2.5.

Proof. The proof of this lemma is a modification of the last part of the proof of [55, Thm 3.2]. For $v \in \mathcal{U}_{\mathrm{qc}}$, we apply [55, Thm A.4] with $p = 1$ to estimate

$$\left|\langle f, v\rangle_h - \langle f, v\rangle_\varepsilon\right| \le \sum_{i\in\mathcal{C}_c} \frac{1}{4} h_i^2 |(fv)''|_{\ell^1_\varepsilon(\mathcal{K}_i^2)}.$$

Using the fact that $v''_\ell = 0$ for $\ell \in \mathcal{K}_i^2$, we have

$$\begin{aligned}(fv)''_\ell &= \frac{f_{\ell+1}v_{\ell+1} - 2f_\ell v_\ell + f_{\ell-1}v_{\ell-1}}{\varepsilon^2} \\ &= \frac{f_{\ell+1} - 2f_\ell + f_{\ell-1}}{\varepsilon^2} v_\ell + \frac{f_{\ell+1} - f_\ell}{\varepsilon}\frac{v_{\ell+1} - v_\ell}{\varepsilon} + \frac{f_\ell - f_{\ell-1}}{\varepsilon}\frac{v_\ell - v_{\ell-1}}{\varepsilon}.\end{aligned}$$

We then obtain the following estimate:

$$\begin{aligned}\left|\langle f, v\rangle_h - \langle f, v\rangle_\varepsilon\right| &\le \frac{1}{4}\sum_{i\in\mathcal{C}_c} h_i^2 \left[\|f''\|_{\ell^2_\varepsilon(\mathcal{K}_i^2)}\|v\|_{\ell^2_\varepsilon(\mathcal{K}_i^2)} + 2\|f'\|_{\ell^2_\varepsilon(\mathcal{K}_i^1)}\|v'\|_{\ell^2_\varepsilon(\mathcal{K}_i^1)}\right] \\ &\le \frac{1}{4}\Big[\sum_{i\in\mathcal{C}_c} h_i^4 \|f''\|^2_{\ell^2_\varepsilon(\mathcal{K}_i^2)}\Big]^{\frac{1}{2}}\|v\|_{\ell^2_\varepsilon} + \frac{1}{2}\Big[\sum_{i\in\mathcal{C}_c} h_i^4\|f'\|^2_{\ell^2_\varepsilon(\mathcal{K}_i^1)}\Big]^{\frac{1}{2}}\|v'\|_{\ell^2_\varepsilon}.\end{aligned}$$

Application of a discrete Poincaré inequality (see [16, Remark 1]), $\|v\|_{\ell^2_\varepsilon} \leq \frac{1}{2}\|v'\|_{\ell^2_\varepsilon}$, and of the inequality $a^{1/2} + b^{1/2} \leq (2a + 2b)^{1/2}$, yield the bound

$$\begin{aligned}|\langle f, v\rangle_h - \langle f, v\rangle_\varepsilon| &\leq \Big([\frac{1}{64}\sum_{i\in\mathcal{C}_c} h_i^4 \|f''\|^2_{\ell^2_\varepsilon(\mathcal{K}_i^2)}]^{\frac{1}{2}} + [\frac{1}{4}\sum_{i\in\mathcal{C}_c} h_i^4 \|f'\|^2_{\ell^2_\varepsilon(\mathcal{K}_i^1)}]^{\frac{1}{2}} \Big) \|v'\|_{\ell^2_\varepsilon}, \\ &\leq \Big(\sum_{i\in\mathcal{C}_c} h_i^4 [\frac{1}{32}\|f''\|^2_{\ell^2_\varepsilon(\mathcal{K}_i^2)} + \tfrac{1}{2}\|f'\|^2_{\ell^2_\varepsilon(\mathcal{K}_i^1)}] \Big)^{\frac{1}{2}} \|v'\|_{\ell^2_\varepsilon}.\end{aligned}$$

This estimate establishes the stated result. □

2.7 Stability of QC methods

Aside from consistency error estimates for the QC approximations, which was analyzed in the previous section, their stability is the second key ingredient for deriving error bounds as we mentioned in Section 2.1. Since we are in a one-dimensional situation it would not be too difficult to derive stability results in the spaces $\mathcal{U}^{1,p}$, $p \in [1, \infty]$ (see, e.g., [55, 16, 45, 40]). However, such stability results would be difficult to obtain in more than one dimension, and therefore, we will only use stability in the space $\mathcal{U}^{1,2}$ in our subsequent error analysis.

According to (2.1.5), we need an estimate of the form

$$|E'_{\rm qc}(I_h y_{\rm a})[I_h e] - E'_{\rm qc}(y_{\rm qc})[I_h e]| \geq \alpha \|I_h e\|^2_{\mathcal{U}^{1,p}},$$

where $I_h e := I_h y_{\rm a} - y_{\rm qc}$ or even more general that

$$|E'_{\rm qc}(y_h^1)[e_h] - E'_{\rm qc}(y_h^2)[e_h]| \geq \alpha \|e_h\|^2_{\mathcal{U}^{1,p}} \quad \forall y_h^1, y_h^2 \in \mathcal{Y}_{\rm qc},$$

where $e_h := y_h^1 - y_h^2$. However, such estimate is hard to establish directly because of the formulation of $E'_{\rm qc}(\cdot)[\cdot]$. As a result, we give the stability analysis through another approach.

For an a priori error analysis, the natural notion of stability for energy minimization problems is coercivity (or, positivity) of the approximate Hessian at the atomistic solution y_a:

$$E''_{\rm qc}(y_a)[v,v] \geq c_{\rm qc}(y_a)\|v'\|^2_{\ell^2_\varepsilon} \qquad \forall v \in \mathcal{U}, \tag{2.7.1}$$

for some constant $c_{\rm qc}(y_a) > 0$. This notion of stability corresponds to an assumption on the atomistic solution that y_a is a 'deep minimum' of the atomistic problem such that a perturbation of the hessian from $E''_a(y_a)$ to $E''_{\rm qc}(y_a)$ does not change the positive definiteness. However, in this section we will not derive the positive definiteness of $E''_{\rm qc}(y_a)$ from $E''_a(y_a)$ but only give explicit conditions on the deformations y_a such that (2.7.1) holds. We refer to [51] for a further discussion on the 'deep minima' assumption.

The simplest of the three Hessian operators is the QCL Hessian, which is given by

$$E''_{\rm qcl}(y)[v,v] = \varepsilon \sum_{\ell=-N+1}^{N} A^{\rm qcl}_\ell |v'_\ell|^2,$$

where

$$A^{\rm qcl}_\ell = \phi''(y'_\ell) + 4\phi''(2y'_\ell), \qquad \text{for } \ell = \{-N+1,\dots,N\}. \tag{2.7.2}$$

Hence we immediately see that we can choose $c_{\rm qcl}(y) = \min_\ell A^{\rm qcl}_\ell$.

To obtain similar results for the QCE and QNL energies we need to overcome some difficulties due to the nonlocal interactions, following the ideas developed in [51, 17].

The Hessian of the QNL energy functional at y is given by,

$$\begin{aligned} E''_{\rm qnl}(y)[v,v] =& \varepsilon \sum_{\ell=-N+1}^{N} \phi''(y'_\ell)|v'_\ell|^2 \\ &+\varepsilon \sum_{\ell=-N+1}^{\ell_1} \left[\frac{1}{2}\phi''(2y'_\ell)|2v'_\ell|^2 + \frac{1}{2}\phi''(2y'_{\ell+1})|2v'_{\ell+1}|^2\right] \\ &+\varepsilon \sum_{\ell=\ell_1}^{\ell_2} \phi''(y'_\ell + y'_{\ell+1})|v'_\ell + v'_{\ell+1}|^2 \\ &+\varepsilon \sum_{\ell=\ell_2+1}^{N} \left[\frac{1}{2}\phi''(2y'_\ell)|2v'_\ell|^2 + \frac{1}{2}\phi''(2y'_{\ell+1})|2v'_{\ell+1}|^2\right]. \end{aligned}$$

We now note that the 'non-local' Hessian terms $|v'_\ell + v'_{\ell+1}|^2$ can be rewritten in terms of the 'local' terms $|v'_\ell|^2$ and $|v'_{\ell+1}|^2$ and a strain-gradient correction,

$$|v'_\ell + v'_{\ell+1}|^2 = 2|v'_\ell|^2 + 2|v'_{\ell+1}|^2 - \varepsilon^2|v''_\ell|^2.$$

Using this formula, we can rewrite the Hessian in the form

$$E''_{\rm qnl}(y)[v,v] = \varepsilon \sum_{\ell=-N+1}^{N} A_\ell^{\rm qnl}|v'_\ell|^2 + \varepsilon \sum_{\ell=\ell_1}^{\ell_2} \varepsilon^2 B_\ell^{\rm qnl}|v''_\ell|^2,$$

where

$$A_\ell^{\rm qnl} = \phi''(y'_\ell) + \begin{cases} 2\phi''(y'_{\ell-1} + y'_\ell) + 2\phi''(y'_\ell + y'_{\ell+1}), & \ell \in \{\ell_1+1, \dots, \ell_2\}, \\ 2\phi''(y'_\ell + y'_{\ell+1}) + 2\phi''(2y'_\ell), & \ell = \ell_1, \\ 2\phi''(y'_{\ell-1} + y'_\ell) + 2\phi''(2y'_\ell), & \ell = \ell_2 + 1, \\ 4\phi''(2y'_\ell), & \ell \in \mathcal{C}_{\ell_1-1,\ell_2+2}, \end{cases} \tag{2.7.3}$$

$$B_\ell^{\rm qnl} = -\phi''(y'_\ell + y'_{\ell+1}).$$

Using similar algebraic manipulations, we can write the QCE Hessian as (see also [17, Eq. (15)] for the case $y = Fx$)

$$E''_{\rm qce}(y)[v,v] = \varepsilon \sum_{\ell=-N+1}^{N} A_\ell^{\rm qce}|v'_\ell|^2 + \varepsilon \sum_{\ell=\ell_1-1}^{\ell_2+1} \varepsilon^2 B_\ell^{\rm qce}|v''_\ell|^2,$$

where

$$
\begin{aligned}
A_\ell^{\rm qce} =& \phi''(y'_\ell) \\
&+ \begin{cases}
2\phi''(y'_{\ell-1}+y'_\ell) + 2\phi''(y'_\ell+y'_{\ell+1}), & \ell \in \{\ell_1+2,\dots,\ell_2-1\}, \\
\phi''(y'_{\ell-1}+y'_\ell) + \phi''(y'_\ell+y'_{\ell+1}) + 2\phi''(2y'_\ell), & \ell \in \{\ell_1,\ell_2+1\} \\
\phi''(y'_\ell+y'_{\ell+1}) + 4\phi''(2y'_\ell), & \ell = \ell_1-1, \\
\phi''(y'_{\ell-1}+y'_\ell) + 2\phi''(y'_\ell+y'_{\ell+1}), & \ell = \ell_1+1, \\
\phi''(y'_\ell+y'_{\ell+1}) + 2\phi''(y'_{\ell-1}+y'_\ell), & \ell = \ell_2, \\
\phi''(y'_{\ell-1}+y'_\ell) + 4\phi''(2y'_\ell), & \ell = \ell_2+2, \\
4\phi''(2y'_\ell), & \ell \in \mathcal{C}_{\ell_1-2,\ell_2+3},
\end{cases}
\end{aligned}
\tag{2.7.4}
$$

and

$$
B_\ell^{\rm qce} = \begin{cases}
-\frac{1}{2}\phi''(y'_\ell+y'_{\ell+1}), & \ell \in \{\ell_1-1,\ell_1,\ell_2,\ell_2+1\}, \\
-\phi''(y'_\ell+y'_{\ell+1}), & \ell \in \{\ell_1+1,\dots,\ell_2-1\},
\end{cases}
\tag{2.7.5}
$$

Recall our assumption that ϕ is convex in $(0, r_*)$ and concave in $(r_*, +\infty)$. For typical pair interaction potentials, $y'_\ell < r_*/2$ can only be achieved under extreme compressive forces. Since, under such extreme conditions a pair potential may be an inappropriate model to employ anyhow, it is not too restrictive to assume that the atomistic solution $\boldsymbol{y}$ satisfies

$$
y'_\ell \geq r_*/2 \qquad \forall \ell \in \{1,\dots,N\}.
$$

As a result of this assumption, and the properties of ϕ, we have

$$
-\phi''(y'_\ell+y'_{\ell+1}) \geq 0,
$$

for all ℓ and thus

$$
-B_\ell^{\rm qc} \geq 0,
$$

for all ℓ and for $\mathrm{qc} \in \{\mathrm{qce}, \mathrm{qnl}\}$

As an immediate consequence we obtain the following lemma, which gives sufficient conditions under which stability of QC methods can be guaranteed.

Lemma 2.8. *Let $y \in \mathcal{Y}$ satisfy $\min_\ell y'_\ell \geq r_*/2$; then, for $\mathrm{qc} \in \{\mathrm{qcl}, \mathrm{qce}, \mathrm{qnl}\}$,*

$$E''_{\mathrm{qc}}(y)[v,v] \geq A^{\mathrm{qc}}_*(y)\|v'\|^2_{\ell^2_\varepsilon} \qquad \forall v \in \mathcal{U}, \quad \textit{where} \quad A^{\mathrm{qc}}_*(y) := \min_{\ell=1,\dots,N} A^{\mathrm{qc}}_\ell.$$

The coefficients A^{qc}_ℓ are defined, respectively, in (2.7.2), (2.7.5), *and* (2.7.3).

Proof. If $\min_\ell y_\ell \geq r_*/2$, then

$$E''_{\mathrm{qc}}(y)[v,v] \geq \varepsilon \sum_{\ell=-N+1}^{N} A^{\mathrm{qc}}_\ell |v'_\ell|^2 \geq A^{\mathrm{qc}}_*(y)\varepsilon \sum_{\ell=-N+1}^{N} |v'_\ell|^2 = A^{\mathrm{qc}}_*(y)\|v'\|^2_{\ell^2_\varepsilon}.$$

□

Remark 2.4. For the purpose of the a priori error estimates, only the coercivity of the QC Hessian at the the interpolated atomistic solution $I_h y_a$ is needed. However, to guarantee the existence of a corresponding QC solution, such coercivity at the original atomistic solution y_a [17, 51] is required and therefore, we give the stability analysis at y_a.

Our stability results are extensions of the sharp stability estimates in [17] to nonlinear deformations. It is explained in [51, Rem. 4.6], using results of [17], that the result for the QCL and QNL methods is "almost" sharp in the following sense: if y is a globally smooth deformation then, in the limit as $N \to \infty$, $E''_{\mathrm{qnl}}(y)$ is positive if and only if $E''_{\mathrm{a}}(y)$ is positive.

In the case of the QCE method, such a one-to-one correspondence between stability of the QC method and of the atomistic model is false. Even at a homogeneous

deformation $y = Fx$, we have (see [17, Sec. 5])

$$A_*^{\mathrm{a}} = \phi''(F) + 4\phi''(2F) > \phi''(F) + 4.5\phi''(2F) > \inf_{\|u\|_{\ell^2_\varepsilon}=1} E''_{\mathrm{qce}}(Fx)[u,u] \geq A_*^{\mathrm{qce}}.$$

An additional complication is the fact that homogeneous deformations are not, in the absence of external forces, equilibria of the QCE model. The interface ghost forces effect a further loss of stability, which is discussed in detail in [17, Sec. 5]. This means that there exist stable atomistic configurations near bifurcation points, which *cannot* be approximated by a QCE method.

Nevertheless, it is easy to check that in "deep" minima where next-nearest neighbour interactions are dominated by nearest-neighbour interactions, our stability constant A_*^{qce} is positive. For deformations of this type our error analysis will be valid.

To establish the full stability result in the proof of the main theorem, which essentially establish the a priori error estimate, a local Lipschitz bound on $\mathcal{E}''_{\mathrm{qc}}$ which will be used. We present the local Lipschitz bound in the following lemma. Since the proof of the following is straightforward, particularly if no explicit constant is required, it is put in Appendix A.

Lemma 2.9. *Let* $\mathrm{qc} \in \{\mathrm{qcl}, \mathrm{qce}, \mathrm{qnl}\}$*, and let* $y, z \in \mathcal{Y}$ *such that* $\min_\ell y'_\ell \geq \mu$ *and* $\min_\ell z'_\ell \geq \mu$ *for some constant* $\mu > 0$*, then*

$$\left|\{\mathcal{E}''_{\mathrm{qc}}(y) - \mathcal{E}''_{\mathrm{qc}}(z)\}[v,w]\right| \leq C_{\mathrm{Lip}} \|y' - z'\|_{\ell^\infty_\varepsilon} \|v'\|_{\ell^2_\varepsilon} \|w'\|_{\ell^2_\varepsilon} \qquad \forall v, w \in \mathcal{U},$$

where $C_{\mathrm{Lip}} = M_3([\mu, +\infty)) + 9M_3([2\mu, +\infty))$.

2.8 The A Priori Error Estimates

We finally arrive at the derivation of the error estimates for $\|e\|_{\mathcal{U}^{1,2}}$ for the QCL, QCE, and QNL methods. The following theorem is obtained as a natural combination of the consistency error estimates and the stability analysis of the previous sections. To avoid technicalities associated with the nonlinearity of our models, we make an a priori assumption: we assume the existence of the atomistic and the QC solutions and make a mild requirement on their smoothness and closeness (cf. (2.8.1)). We comment further on this assumption in Remark 2.5 below.

Theorem 2.10. *Fix* $\mathrm{qc} \in \{\mathrm{qcl}, \mathrm{qce}, \mathrm{qnl}\}$. *Let* y_{a} *be a solution of the atomistic problem* (2.2.5) *whose gradients are such that* $\min_\ell (y_{\mathrm{a}})'_\ell \geq r_*/2$ *and* $A_*^{\mathrm{qc}}(y_{\mathrm{a}}) > 0$, *where* A_*^{qc} *is defined in the statement of Lemma 2.8. Suppose, further, that* $\boldsymbol{y}^{\mathrm{qc}}$ *is a solution of the QC model* (2.4.5) *such that, for some* $\tau > 0$,

$$\|(y_{\mathrm{a}} - I_h y_{\mathrm{a}})'\|_{\ell^\infty_\varepsilon} \leq \tau \quad \textit{and} \quad \|(y_{\mathrm{a}} - y_{\mathrm{qc}})'\|_{\ell^\infty_\varepsilon} \leq \tau. \tag{2.8.1}$$

Then, if τ *is sufficiently small, we have the error estimate*

$$\|y_{\mathrm{a}} - y_{\mathrm{qc}}\|_{\mathcal{U}^{1,2}} \leq \frac{1}{2}\Big(\sum_{i \in \mathcal{C}_c} h_i^2 \|y''\|^2_{\ell^2_\varepsilon(\mathcal{K}_i^2)}\Big)^{\frac{1}{2}} + \tfrac{2}{A_*^{\mathrm{qc}}(y_{\mathrm{a}})}\big(\mathscr{E}^{\mathrm{qc}}_{\mathrm{model}} + \mathscr{E}_{\mathrm{fem}} + \mathscr{E}_{\mathrm{ext}}\big), \tag{2.8.2}$$

as well as the superconvergence result

$$\|I_h y_{\mathrm{a}} - y_{\mathrm{qc}}\|_{\mathcal{U}^{1,2}} \leq \tfrac{2}{A_*^{\mathrm{qc}}(y_{\mathrm{a}})}\big(\mathscr{E}^{\mathrm{qc}}_{\mathrm{model}} + \mathscr{E}_{\mathrm{fem}} + \mathscr{E}_{\mathrm{ext}}\big), \tag{2.8.3}$$

where the QC consistency error $\mathscr{E}^{\mathrm{qc}}_{\mathrm{model}} = \mathscr{E}^{\mathrm{qc}}_{\mathrm{model}}(y_{\mathrm{a}})$ *is defined in* (2.3.8), (2.3.16), *or* (2.3.20), *the superconvergent finite element coarse-graining error* $\mathscr{E}_{\mathrm{fem}} = \mathscr{E}_{\mathrm{fem}}(y_{\mathrm{a}})$ *is defined in* (2.5.2), *and the approximation error for the external forces* $\mathscr{E}_{\mathrm{ext}} = \mathscr{E}_{\mathrm{ext}}(f)$ *is defined in* (2.6.1).

Proof. From the mean value theorem we deduce that there exists $\theta \in \mathrm{conv}\{I_h y_{\mathrm{a}}, y_{\mathrm{qc}}\}$ such that

$$\mathcal{E}''_{\mathrm{qc}}(\theta)[I_h e, I_h e] = \mathcal{E}'_{\mathrm{qc}}(I_h y_{\mathrm{a}})[I_h e] - \mathcal{E}'_{\mathrm{qc}}(y_{\mathrm{qc}})[I_h e].$$

Using the first-order optimality conditions for y_{a} and y_{qc} we obtain

$$\begin{aligned}\mathcal{E}'_{\mathrm{qc}}(I_h y_{\mathrm{a}})[I_h e] - \mathcal{E}'_{\mathrm{qc}}(y_{\mathrm{qc}})[I_h e] =& \big\{\mathcal{E}'_{\mathrm{qc}}(y_{\mathrm{a}})[I_h e] - \mathcal{E}'_{\mathrm{a}}(y_{\mathrm{a}})[I_h e]\big\} \\ &+ \big\{\mathcal{E}'_{\mathrm{qc}}(I_h y_{\mathrm{a}})[I_h e] - \mathcal{E}'_{\mathrm{qc}}(y_{\mathrm{a}})[I_h e]\big\} \\ &+ \big\{\langle f, I_h e\rangle_{\varepsilon} - \langle f, I_h e\rangle_h\big\}.\end{aligned}$$

The three groups of the right hand side of the equation, in abstract sense, corresponds to the consistency error of the semilinear form in (2.1.9), the error of coarse-graining in (2.1.10) and the consistency error for the linear functional in (2.1.11) respectively. The first group is estimated in Lemma 2.6, the second group in Theorem 2.2 (QCL), Theorem 2.3 (QCE), or in Theorem 2.4 (QNL), and the last group in Lemma 2.7. Inserting these estimates we arrive at

$$\mathcal{E}''_{\mathrm{qc}}(\theta)[I_h \boldsymbol{e}, I_h \boldsymbol{e}] \leq \big(\mathscr{E}^{\mathrm{qc}}_{\mathrm{model}} + \mathscr{E}_{\mathrm{fem}} + \mathscr{E}_{\mathrm{ext}}\big)\|I_h \boldsymbol{e}'\|_{\ell^2_\varepsilon}. \tag{2.8.4}$$

It remains to prove a lower bound on $\mathcal{E}''_{\mathrm{qc}}(\theta)[I_h \boldsymbol{e}, I_h \boldsymbol{e}]$. From our assumption that $\min_\ell(\boldsymbol{y}^{\mathrm{a}})'_\ell \geq r_*/2$, and from (2.8.1) it follows that

$$\min_\ell \theta'_\ell \geq r_*/2 - \tau.$$

Assuming that τ is sufficiently small, e.g., $\tau \leq \tau_1 := \frac{1}{4}\min_\ell y'_\ell$, we can apply Lemma 2.9 to deduce that

$$\begin{aligned}\mathcal{E}''_{\mathrm{qc}}(\theta)[I_h \boldsymbol{e}, I_h \boldsymbol{e}] \geq\ & \mathcal{E}''_{\mathrm{qc}}(\boldsymbol{y}^{\mathrm{a}})[I_h \boldsymbol{e}, I_h \boldsymbol{e}] - C_{\mathrm{Lip}}\|(\theta - \boldsymbol{y}^{\mathrm{a}})'\|_{\ell^\infty_\varepsilon}\|I_h \boldsymbol{e}'\|^2_{\ell^2_\varepsilon} \\ \geq\ & \mathcal{E}''_{\mathrm{qc}}(\boldsymbol{y}^{\mathrm{a}})[I_h \boldsymbol{e}, I_h \boldsymbol{e}] - C_{\mathrm{Lip}}\tau\|I_h \boldsymbol{e}'\|^2_{\ell^2_\varepsilon}.\end{aligned} \tag{2.8.5}$$

where C_{Lip} may depend on τ_1.

We can now apply our stability analysis in Section 2.7. Since $(\boldsymbol{y}^{\mathrm{a}})'_\ell \geq r_*/2$ for all ℓ, Lemma 2.8 implies that

$$\mathcal{E}''_{\mathrm{qc}}(\boldsymbol{y}^{\mathrm{a}})[I_h\boldsymbol{e}, I_h\boldsymbol{e}] \geq A_*^{\mathrm{qc}}(\boldsymbol{y}^{\mathrm{a}})\|I_h\boldsymbol{e}'\|^2_{\ell^2_\varepsilon},$$

which, combined with (2.8.4) and (2.8.5), yields

$$\big(A_*^{\mathrm{qc}}(\boldsymbol{y}^{\mathrm{a}}) - C_{\mathrm{Lip}}\tau\big)\|I_h\boldsymbol{e}'\|^2_{\ell^2_\varepsilon} \leq \mathcal{E}''_{\mathrm{qc}}(\theta)[I_h\boldsymbol{e}, I_h\boldsymbol{e}] \leq \big(\mathscr{E}^{\mathrm{qc}}_{\mathrm{model}} + \mathscr{E}_{\mathrm{fem}} + \mathscr{E}_{\mathrm{ext}}\big)\|I_h\boldsymbol{e}'\|_{\ell^2_\varepsilon}.$$

Dividing through by $\|I_h\boldsymbol{e}'\|_{\ell^2_\varepsilon}$, and assuming that $\tau \leq \min(\tau_1, \tau_2)$ where $\tau_2 = A_*^{\mathrm{qc}}(\boldsymbol{y}^a)/(2C_{\mathrm{Lip}})$, we deduce that

$$\tfrac{A_*^{\mathrm{qc}}(\boldsymbol{y}^{\mathrm{a}})}{2}\|I_h\boldsymbol{e}'\|_{\ell^2_\varepsilon} \leq \mathscr{E}^{\mathrm{qc}}_{\mathrm{model}} + \mathscr{E}_{\mathrm{fem}} + \mathscr{E}_{\mathrm{ext}},$$

which concludes the proof of the superconvergence error estimate (2.8.3). The standard error estimate (2.8.2) follows from (2.8.3) and the interpolation error estimate given in Lemma 2.5. □

Remark 2.5. The assumption that τ be sufficiently small is fairly strong from an analytical point of view and deserves comments. A brief investigation of the proof of Theorem 2.10 shows that we have assumed $\tau \leq \min(\tau_1, \tau_2)$, with constants $\tau_1 = \frac{1}{4}\min_\ell(y_{\mathrm{a}})'_\ell$ and $\tau_2 = A_*^{\mathrm{qc}}(y_{\mathrm{a}})/(2C)$, where C is a local Lipschitz constant.

The first restriction, $\tau \leq \tau_1$ is only used to obtain some control on $(y_{\mathrm{qc}})'$ from below and could be easily replaced by appropriate a priori estimates on the solutions.

However, the second condition, $\tau \leq \tau_2$, is fundamental. It requires, essentially, that y_{a}, $I_h y_{\mathrm{a}}$, and y_{qc} all belong to a single convex subregion of $\mathcal{Y}$ in which $\mathcal{E}_{\mathrm{qc}}$

is convex. At first glance, this assumption may appear too strong to be satisfied in all situations. Indeed, given any two atomistic and QC solutions it would be difficult to justify it, as $\mathcal{E}_{\mathrm{qc}}$ is a highly non-convex functional. However, we are only assuming for the existence of *some* QC solution in a suitable neighbourhood of y_{a}. With some additional technical effort, this can be made rigorous using a quantitative inverse function theorem; we refer to [55, 51, 41, 45, 23] for examples of this technique applied in a similar context. .

2.9 Numerical Experiments

We conclude this chapter with a set of numerical experiments illustrating the results of our analysis. Throughout this section we fix $F = 1$, $N = 1000$, and let ϕ be the Morse potential

$$\phi(r) = \exp(-2\alpha(r-1)) - 2\exp(-\alpha(r-1)),$$

with the parameter $\alpha = 5$. We will solve three problems with different body forces.

Although our analysis was carried out in terms of deformations y, we will show the relative errors with respect to displacements $u = y - x$. While the absolute errors are of course identical, the relative errors are best measured in terms of the displacement from the undeformed state x. Moreover, we will show errors in the $\mathcal{U}^{1,2}$- as well as the $\mathcal{U}^{1,\infty}$-norm. While the former was the object of our analysis and is also closely related to errors in the energy, it does not always capture localised errors such as the interface oscillation caused by the ghost forces as well. Since we are primarily interested in the errors due to the coupling mechanisms, and in

order to avoid cluttered graphs, we do not show numerical experiments for the QCL method; however, see [40] for an interesting example.

For each numerical experiment we present four figures: 1. the displacement gradients of the exact atomistic solution; 2. the relative errors for the QCE and QNL methods in the displacement gradients $|e'_\ell| / \|u_{\mathrm{a}}\|_{\mathcal{U}^{1,\infty}}$ plotted against ℓ; 3. The relative errors for the QCE and QNL methods in the $\mathcal{U}^{1,2}$- and $\mathcal{U}^{1,\infty}$-norms, plotted against the size of the atomistic region; and 4. the same relative errors plotted against the mesh size.

2.9.1 Construction of $\mathcal{A}$ and $\mathcal{U}_{\mathrm{qc}}$

We choose the atomistic region symmetrically about the lattice point 500, that is, $\ell_1 = 500 - m$ and $\ell_2 = 500 + m$, $m \geq 0$, such that $\#\mathcal{A} = 2m + 1$.

To coarse-grain the continuum region we fix $K \geq 1$ and choose repatoms to create an exponentially graded mesh as follows:

- atom $\ell_2 + 1$ and N are repatoms.
- atom $\ell_2 + \sum_{i=1}^{k} 2^i$ is a repatom where $1 \leq k \leq K$.
- atom $\ell_2 + \sum_{i=0}^{K} 2^i + n2^K$ is a repatom for all $n \geq 1$ such that $\ell_2 + \sum_{i=0}^{K} 2^i + n2^K \leq N$ and atom N is a repatom.
- the repatoms in the left-hand half of the domain are chosen symmetrically.

In the figures where we plot errors against mesh size, we understand h to be the maximal mesh size, that is, $h = \varepsilon 2^K$.

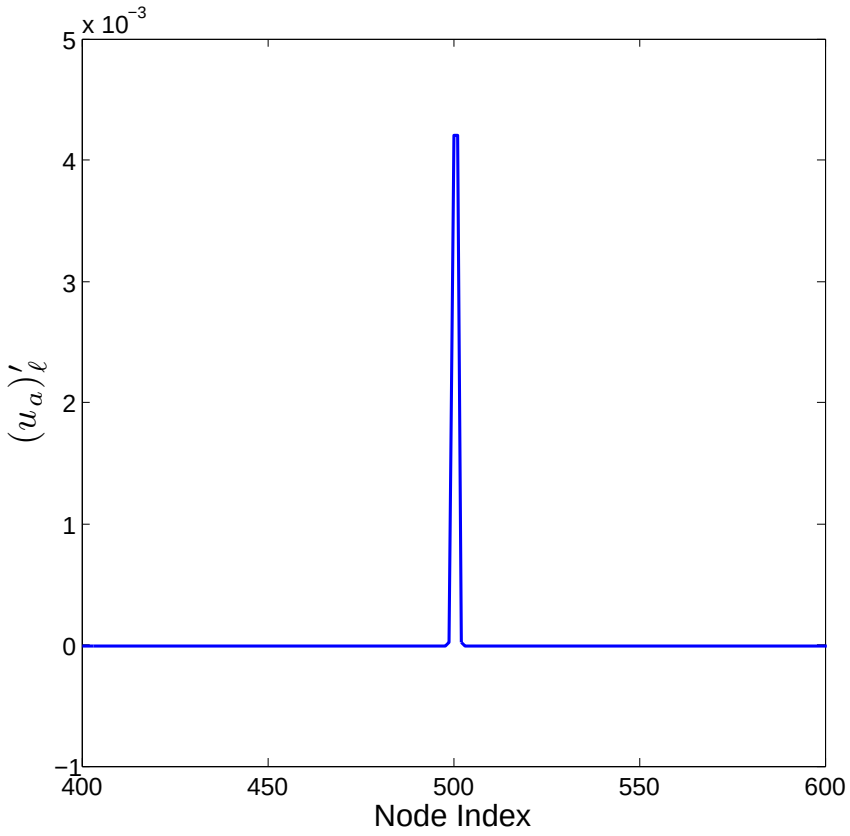

Figure 2.1: Plot of the displacement gradient of the atomistic solution

2.9.2 Numerical Experiment I

For our first numerical experiment, we define the body force f as

$$f_\ell = \begin{cases} -500, & \text{for } \ell = -1, \\ 500, & \text{for } \ell = 1, \\ 0, & \text{otherwise.} \end{cases}$$

This force pulls apart the atoms with indices $\ell = -1, 1$, creating a non-smooth disturbance in the displacement field. The effect on the displacement field is similar, to some extent, to a very localised defect in a 2D/3D lattice. We see from Figure 2.1 that the displacement gradient is large near $\ell = -1, 0, 1$ but decays rapidly to its preferred state.

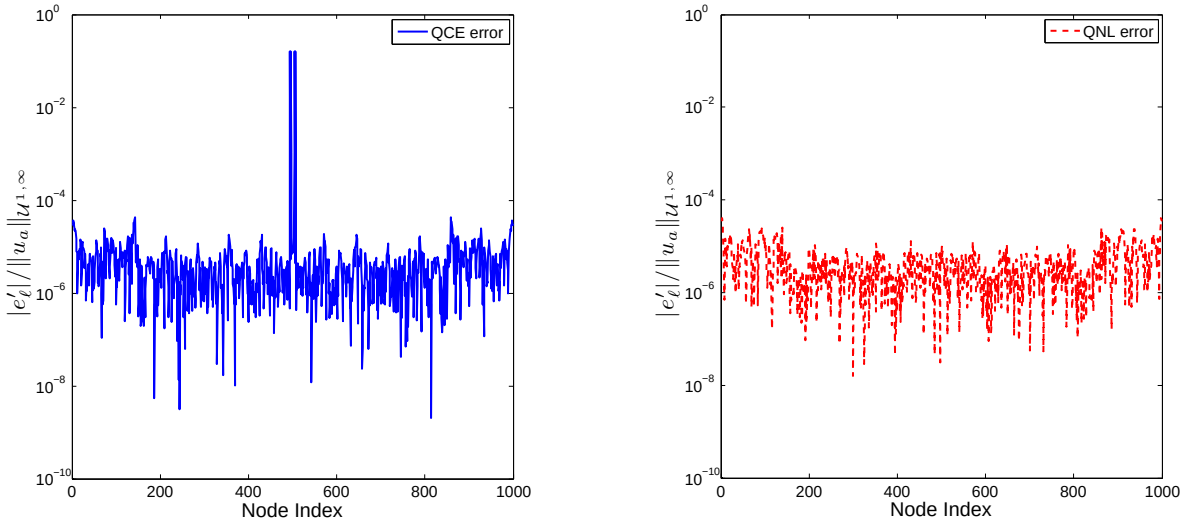

(a) QCE (b) QNL

Figure 2.2: Plots of the relative error $|e'_\ell| / \|(\boldsymbol{u}^{\mathrm{a}})'\|_{\mathcal{U}^{1,\infty}}$ for QCE and QNL.

In Figure 2.2 we plot the relative errors in the QCE and QNL displacement gradients as functions of ℓ. The size of the atomistic region is fixed to $\#\mathcal{A} = 10$. As previously observed and predicted theoretically, we see a large error of the QCE method in the atomistic to continuum interface, which is due to the presence of ghost forces. In our analysis these oscillations are captured by the zeroth order term $2\varepsilon^{1/p} M_1(\mathcal{S}_1)$ in (2.3.16). The error plot for the QNL method shows that it has in fact reached the precision of our nonlinear solver; indeed, from Figure 2.2 we see that the absolute error in the QNL displacement gradient is of the order $O(10^{-9})$.

In Figures 2.3 and 2.4 we plot the relative errors of the QCE and the QNL methods as we increase the size of the atomistic region, and as we increase the mesh size in the continuum region. We note that in both graphs, and for both methods, the relative errors remain essentially constant. This is explained by the rapid decay of $(u_{\mathrm{a}})'_\ell$ towards a homogeneous state, which implies that u_{a} is essentially constant

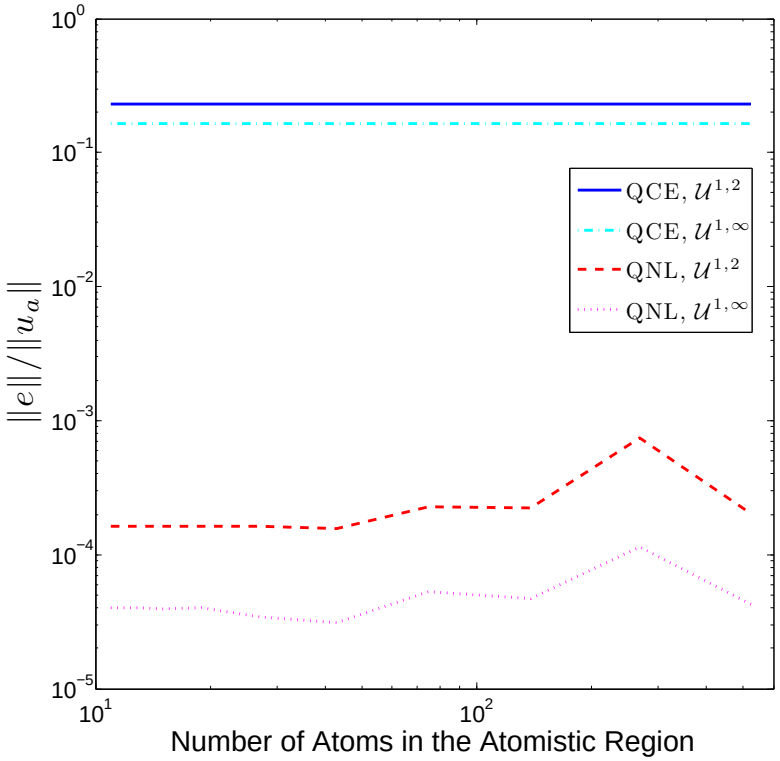

Figure 2.3: Plot of relative errors in different norms with respect to the size of the atomistic region $\sharp\mathcal{A}$

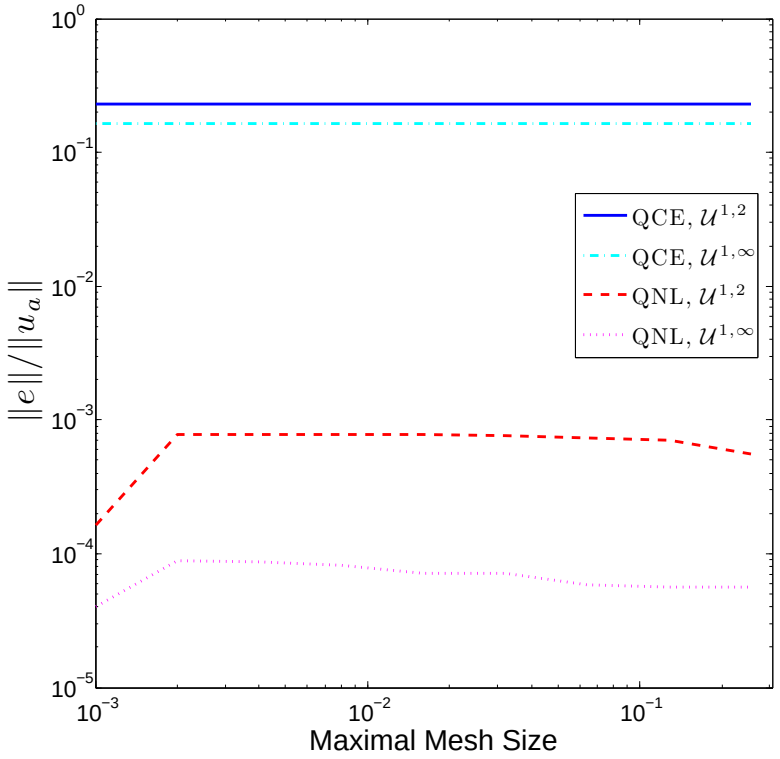

Figure 2.4: Plot of relative errors in different norms with respect to the maximal element size h

in continuum region. Thus, the location of the interface or the size of the mesh have only a marginal effect on the accuracy of either method. In the case of the QCE method, the ghost forces dominate all effects, while, in the case of the QNL method we obtain the accuracy of the nonlinear solver.

2.9.3 Numerical Experiment II

In the second problem, we assume

$$f_\ell = \begin{cases} (-1)^\ell 100\frac{10+\ell}{10}, & \text{for } -10 \leq \ell \leq -1, \\ (-1)^{\ell-1} 100\frac{10-\ell}{10}, & \text{for } 1 \leq \ell \leq 10, \\ 0, & \text{otherwise.} \end{cases}$$

This time, the area with irregular deformation is larger but it still behaves like the continuum in the bulk of the material. We can think of this physical process as tearing apart from the middle with some forces with changing directions around the dislocation core. Due to this force, the displacement gradient is also oscillating around the middle which is shown in Figure 2.5 but remain uniform in the rest of the system where the body force decays to 0.

Figure 2.6 shows the relative errors of the QCE solution and the QNL solution when the atomistic region is chosen to be from atom -12 to atom 12. Again two 'spikes' caused by the ghost force appear at the atomistic to continuum interface in the QCE solution is easily observed.

Figure 2.7 plots the relative errors of the QCE method and the QNL method in different norms as the number of atoms in the atomistic region increases. The QNL error was comparatively large at the beginning as the atomistic region does

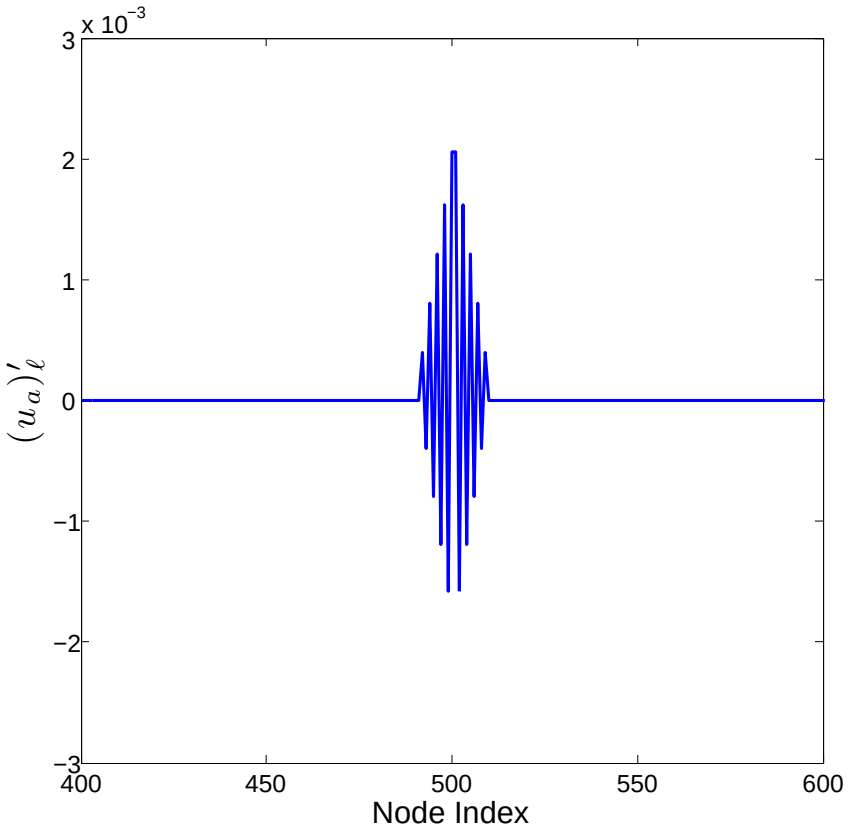

Figure 2.5: Plot of the displacement gradient of the atomistic solution

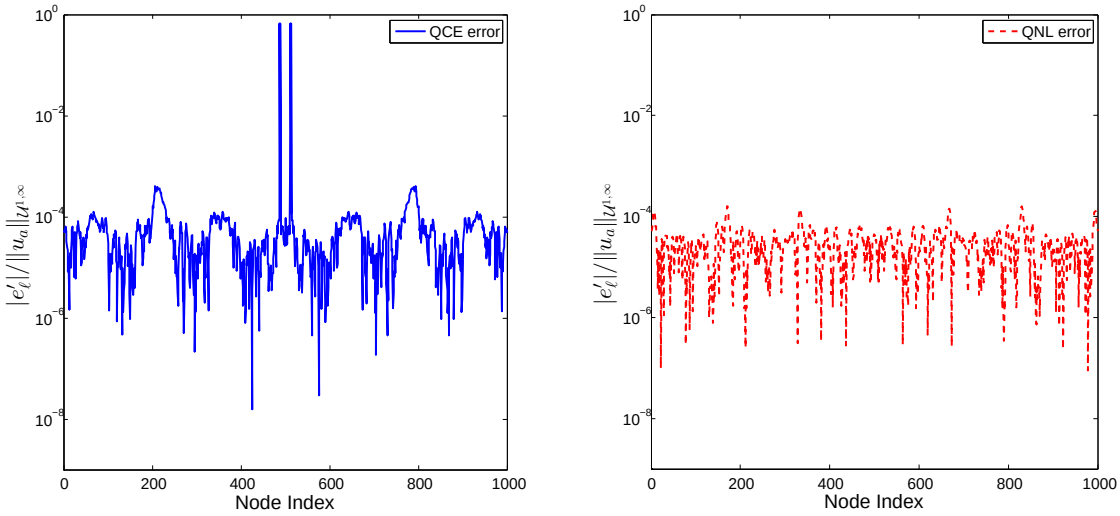

(a) QCE (b) QNL

Figure 2.6: Plots of the relative error $|e'_\ell| / \|(\boldsymbol{u}^{\mathrm{a}})'\|_{\mathcal{U}^{1,\infty}}$ for QCE and QNL.

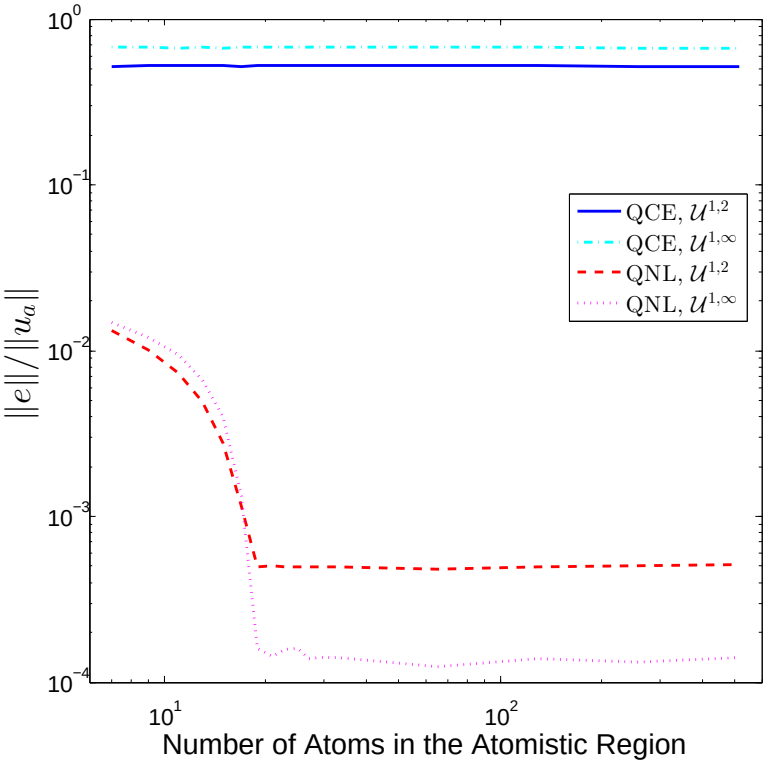

Figure 2.7: Plot of relative errors in different norms with respect to the size of the atomistic region $\sharp\mathcal{A}$

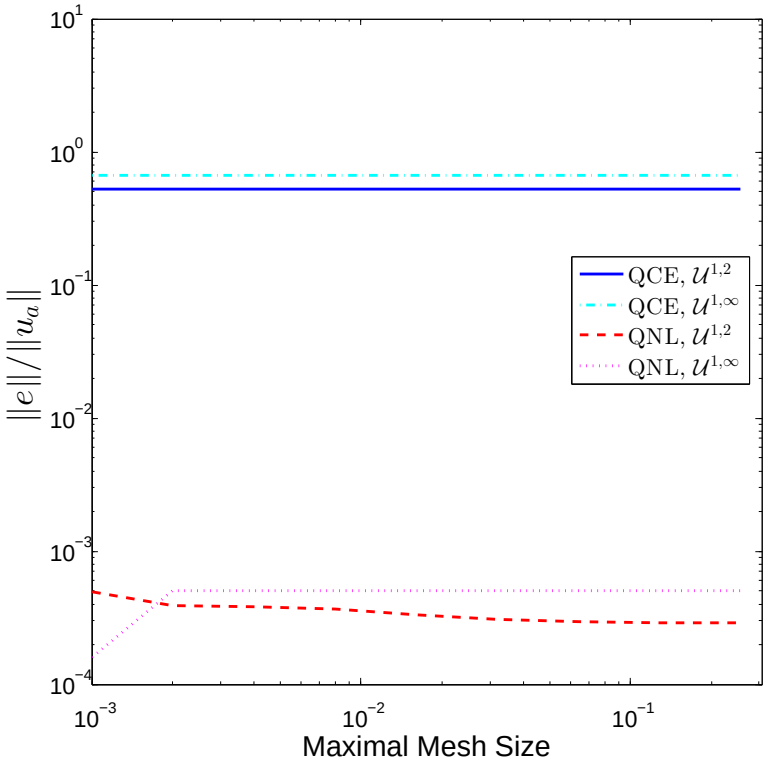

Figure 2.8: Plot of relative errors in different norms with respect to the maximal element size h

not entirely include the region with large deformation. As the atomistic region is enlarged, the error decays until it finally stays in the level of 10^{-3}. This shows the importance of the correct choice of the atomistic region for a QC method to be effective, which is related to the a posteriori error control of the method and will be discussed in detail in Chapter 3. However, the QCE error is of significantly lower order compared with the QNL error, which implies that the effect of the coupling interface still dominates error.

The relative errors of he QCE method and the QNL method as the finite element mesh size grows are shown in Figure 2.8. The atomistic region is chosen to be from atom -12 to atom 12 and again the errors remain in a certain level because of the almost uniform deformation in the continuum region.

2.9.4 Numerical Experiment III

In the third problem, we assume

$$f_\ell = \begin{cases} 8\frac{450+\ell}{450}, & \text{for } -450 \le \ell \le -1, \\ 0, & \text{for } \ell = 0, \\ 8\frac{450-\ell}{450}, & \text{for } 1 \le \ell \le 450. \end{cases}$$

For many real defects in 2D/3D materials, the decay of the displacement due to the presence of the defect is fairly slow, and this body force was chosen to mimic that situation. Indeed, we see from Figure 2.9 that the displacement gradient of the exact solution is nowhere (locally) uniform, and that the second difference of the atomistic solution decays only slowly away from the centre of the domain.

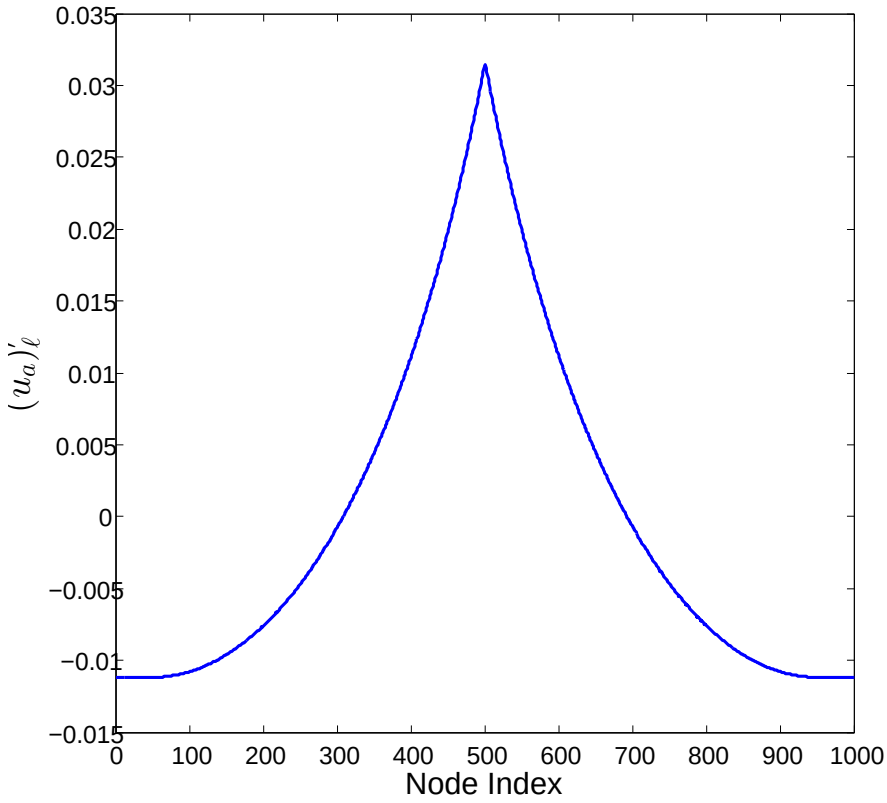

Figure 2.9: Plot of the displacement gradient of the atomistic solution

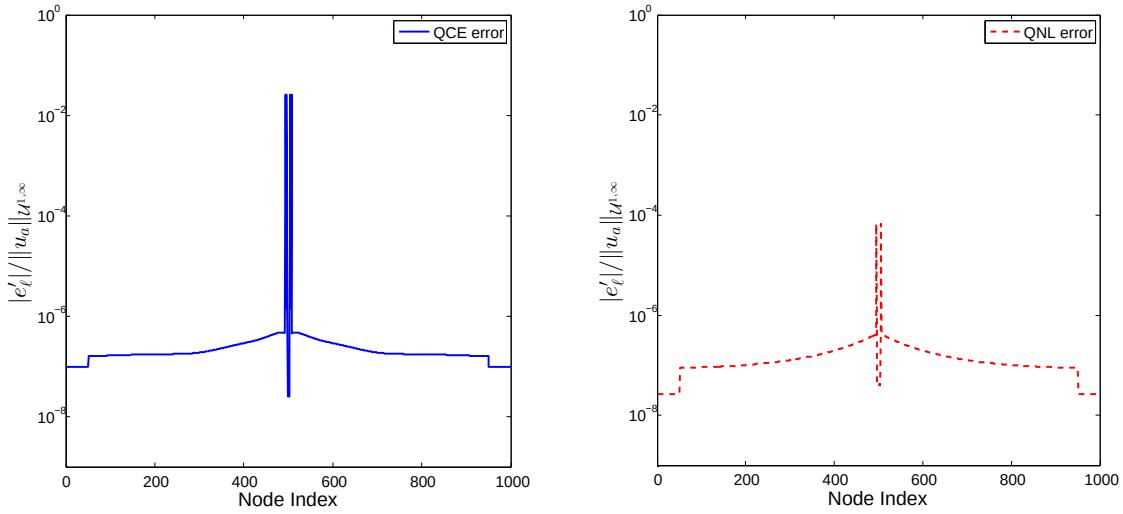

(a) QCE (b) QNL

Figure 2.10: Plots of the relative error $|e'_\ell|/\|(\boldsymbol{u}^{\mathrm{a}})'\|_{\mathcal{U}^{1,\infty}}$ for QCE and QNL.

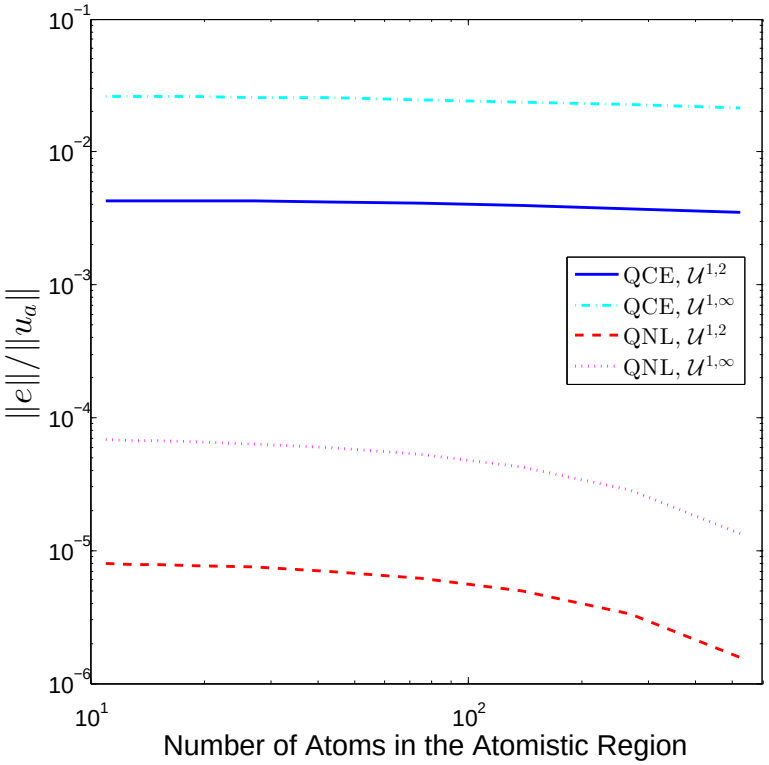

Figure 2.11: Plot of relative errors in different norms with respect to the size of the atomistic region $\sharp\mathcal{A}$

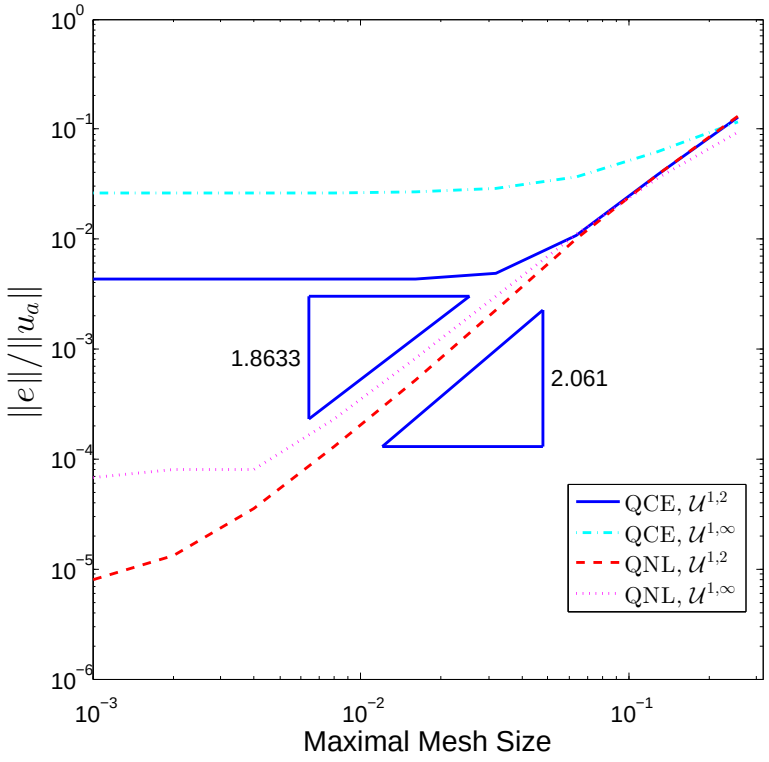

Figure 2.12: Plot of relative errors in different norms with respect to the maximal element size h

Figure 2.10 show the relative errors of the QCE and QNL solutions when the size of the atomistic region is fixed to $\#\mathcal{A} = 10$. We now observe a relatively large error in the QNL solution in the interface region, which is still several orders of magnitude smaller than the error in the QCE solution caused by the presence of ghost forces. This error in the QNL solution was predicted in our analysis in (2.3.20) by the term $\varepsilon M_2(\mathcal{S}_2)\|y''\|_{\ell^p_\varepsilon(\mathcal{I}_{\mathrm{qnl}})}$. This effect will not occur when y is locally homogeneous, as in our first and second experiments.

Figure 2.11 shows the relative errors of the QCE and the QNL methods in the $\mathcal{U}^{1,2}$- and $\mathcal{U}^{1,\infty}$-norms as the number of atoms in the atomistic region increases. We observe that the relative errors of the QCE method remain in a lower order in both norms while those of the QNL method decreases somewhat for very large atomistic regions when the curvature of y_{a} at the interface approaches zero. This demonstrates a fundamental difference between the QCE and QNL methods: the leading term of the QCE error bound has no dependance on the smoothness of the atomistic solution and cannot be controlled by adjusting the atomistic region or the mesh size, whereas that of the QNL error bound does have such a dependence and can therefore be controlled to some extent.

Figure 2.12 displays the relative errors of the QCE solution and the QNL solution with respect to the displacement gradient in the $\mathcal{U}^{1,2}$- and $\mathcal{U}^{1,\infty}$-norms against the finite element mesh size h. As the result of the non-uniform deformation gradient of the solution, the effect of the mesh size is noticeable for both methods. As the mesh size decreases, the error initially decays until it reaches a limit dictated by the modelling error. In the case of the QCE method, this happens very early due to the presence of the ghost forces. In the case of the QNL method, we obtain

a satisfactory relative accuracy of the order 10^{-5} to 10^{-6}.

We note that the slopes of the error curves are not precisely 2 as predicted by our analysis. This can be explained by the fact that neither our mesh, nor the second difference $(y_a)''$ are uniform.

We conclude this section by pointing out the issue we encountered in the third numerical examples which is the efficient mesh adaptivity in the continuum region. It is related to the a posteriori error control which will be the main problem we are dealing with in the next chapter.

Chapter 3

The A Posteriori Error Analysis For A Consistent Energy Based Quasicontinuum Approximation

In this chapter we present an a posteriori error analysis of a simplified variant of the energy-based QC approximation proposed in [64].

We use the residual-based approach [72, Chapter 2], which is well established in the finite element approximation of partial differential equations, to derive a posteriori error bounds for the energy-norm and for the energy itself. What distinguishes our setting from the classical one is one particular feature: the model approximation, which often corresponds to the change from the bilinear form $a(\cdot,\cdot)$ to $a_h(\cdot,\cdot)$ in the variational problems, is fundamentally different than quadrature approximations.

Our work extends [51], which considers a simplified setting. However, in the current work we do not tackle the question of model and mesh adaptivity for defect nucleation, but focus only on automatically choosing the *size* of the atomistic region and the finite element mesh in the continuum region. In many applications, a defect is inserted into the crystal before the computation, or it is known a priori

where a defect will nucleate. An extension of our work to include defect nucleation would be valuable, but cannot be pursued in the simplified 1D setting we are considering here.

As in Chapter 2, we briefly introduce the framework we follow to carry out the a posteriori error analysis and the outline of the content in the current chapter.

3.1 Framework and Outline of the Analysis

In classic finite element approximation of partial differential equations, one often deals the following problem:

$$a(u, v) = \langle \ell, v \rangle \quad \forall v \in V,$$
$$a(u_h, v_h) = \langle \ell, v_h \rangle \quad \forall v_h \in S_h,$$

where $S_h \subset V$. For the a posteriori error estimate, one usually employs

$$\gamma \|u - u_h\| \leq \sup_{w \in V} a(u - u_h, w) = \sup_{w \in V} \big[\langle l, w \rangle - a(u_h, w) \big]. \tag{3.1.1}$$

The inequality is often established by the coercivity of $a(\cdot, \cdot)$ on V (e.g., by Poincaré inequality for the variational formulation of the Poisson equation [72, Chapter 2, §1]) and to estimate the right hand side. Techniques like elementwise integrations by parts and properties like Galerkin orthogonality $a(u - u_h, v_h) = a(u, v_h) - \langle \ell, v_h \rangle = 0$, which are due to the specific formulation of $a(\cdot, \cdot)$ and S_h being a subspace of V, may be used.

Since our problem is in a nonlinear setting, we consider the problem

$$a(u; v) = \langle \ell, v \rangle \quad \forall v \in V,$$
$$a_h(u_h; v_h) = \langle \ell_h, v_h \rangle \quad \forall v_h \in S_h,$$

which is the same as the problem in Chapter 2 except that $S_h \nsubseteq V$ here. By defining the interpolation operators $I_h : V \to S_h$ and $I_\varepsilon : S_h \to V$, and $e := u - I_\varepsilon u_h$, we have

$$\begin{aligned} \gamma \|e\|^2 &\leq a(u; e) - a(I_\varepsilon u_h; e) \\ &= a_h(u_h; I_h e) - a(I_\varepsilon u_h; e) \qquad (3.1.2) \\ &\quad + \langle \ell, e \rangle - \langle \ell_h, I_h e \rangle. \qquad (3.1.3) \end{aligned}$$

(3.1.2) corresponds to the residual of the semilinear forms $a(\cdot;\cdot)$ and $a_h(\cdot;\cdot)$ at u_h and (3.1.3) corresponds to the residual of the linear forms $\langle \ell, \cdot \rangle - \langle \ell_h, \cdot \rangle$, which are both variational crimes.

In this chapter, we analyze the two parts of the residual and also prove an a posteriori stability result.

In Section 3.2 we introduce a 1D atomistic model problem, which mimics the behaviour of crystal defects in 2D/3D. Moreover, we review the construction of a QC method to efficiently approximate its solutions, and introduce the notation that will be used in this chapter.

In Section 3.3, we derive a residual estimates for the QC method in a discrete negative Sobolev norm, which correspond to the estimate of (3.1.2) and (3.1.3).

In Section 3.4, we present an a posteriori stability result.

In Section 3.5, we combine the residual estimate and the stability result to give a posteriori error estimates for the deformation gradient and for the energy.

In Section 3.6, we describe three mesh refinement algorithms based on our a posteriori error analysis and on previous a priori error estimates, and present a numerical example to illustrate the performance of these algorithms.

3.2 Model Problem and QC Approximation

3.2.1 Atomistic Model

Following previous works [16, 51] and the notation used in Chapter 2 we formulate a model problem in a discrete periodic domain containing $2N$ atoms, where $N \in \mathbb{N}$. Let $F > 0$ denote a macroscopic stretch and $\varepsilon = 1/(2N)$ the lattice spacing, both of which we fix throughout this chapter. We define the displacement and deformation spaces, respectively, by

$$\begin{aligned} \mathcal{U}^\varepsilon &:= \big\{u \in \mathbb{R}^{\mathbb{Z}} : u_{\ell+2N} = u_\ell, \text{ and } u_0 = 0\big\}, \quad \text{and} \\ \mathcal{Y}^\varepsilon &:= \big\{y \in \mathbb{R}^{\mathbb{Z}} : y_{\ell+2N} = F + y_\ell, \text{ and } y_0 = 0\big\}. \end{aligned}$$

Note that the spaces are almost the same as we have in Chapter 2 except for the boundary condition being changed from a periodic and zero mean condition to a periodic and Dirichlet condition. Again, we observe that $y \in \mathcal{Y}^\varepsilon$ if and only if $y = Fx + u$ for some $u \in \mathcal{U}^\varepsilon$.

The *stored energy* (per period) of an admissible deformation $y \in \mathcal{Y}^\varepsilon$ is given by

$$\mathcal{E}_{\mathrm{a}}(y) := \varepsilon \sum_{\ell=-N+1}^{N} \phi(y'_\ell) + \varepsilon \sum_{\ell=-N+1}^{N} \phi(y'_{\ell-1} + y'_\ell),$$

where $y'_\ell := \varepsilon^{-1}(y_\ell - y_{\ell-1})$ and $\phi \in C^3(0, +\infty)$ is a Lennard-Jones type interaction potential. The assumptions on ϕ is exactly the same as in Section 2.2.1.

Given a periodic dead load $f \in C^0(\mathbb{R}), f(x+1) = f(x)$, we define the *external energy* (per period) by

$$-\langle f, u\rangle_\varepsilon := -\varepsilon \sum_{\ell=-N+1}^{N} f_\ell u_\ell, \tag{3.2.1}$$

where $u = y - Fx$. Thus, the *total energy* (per period) under a deformation $y \in \mathcal{Y}^\varepsilon$ is given by

$$E_{\mathrm{a}}(y) := \mathcal{E}_{\mathrm{a}}(y) - \langle f, y - Fx \rangle_\varepsilon.$$

We wish to compute

$$y_{\mathrm{a}} \in \operatorname{argmin} E_{\mathrm{a}}(\mathcal{Y}^\varepsilon), \tag{3.2.2}$$

where argmin denotes the set of local minimizers.

Remark 3.1. 1. Since the internal energy is translation invariant, our choice $u_0 = 0$ (instead of the more common constraint $\sum_{\ell=-N+1}^{N} u_\ell = 0$) does not alter the problem but simplifies the treatment of external forces in Sections 3.3.2 and 3.3.4.

2. We adopt the notation for lattice functions defined in Remark 2.1 and Section 2.2.5 in last chapter and thus omit those definitions here.

3.2.2 Finite element notation

To construct the QC approximation in the next section, we first define some convenient notation. Let $\Omega := [-1/2, 1/2]$ denote the computational cell. We choose an atomistic region $\Omega_{\mathrm{a}} \subset \Omega$, where atomistic accuracy is required, and we define the continuum region by $\Omega_{\mathrm{c}} := \Omega \setminus \Omega_{\mathrm{a}}$. We will also use the periodic extension of Ω_{c}, denoted by $\Omega_{\mathrm{c}}^{\#} := (\Omega_{\mathrm{c}} + \mathbb{Z})$.

We assume throughout that Ω_{a} is an open interval $(L_{\mathrm{a}}, R_{\mathrm{a}})$ with $-1/2 < L_{\mathrm{a}} < R_{\mathrm{a}} < 1/2$. All our results (with the exception of Section 3.3.4) can be extended without difficulty to the case when Ω_{a} consists of a finite union of open intervals.

Let $\{T_k^h\}_{k\in\mathbb{Z}}$ be a partition of $\mathbb{R}$ into closed intervals with $T_k^h = [x_{k-1}^h, x_k^h]$, where $x_k^h > x_{k-1}^h$ are the nodes of the partition. We assume, without loss of generality, that x_1^h is the left-most node and x_K^h the right-most nodes in the interval $(-1/2, 1/2]$.

The length of an element is denoted by $h_k := |T_k^h| := x_k^h - x_{k-1}^h$. The space of continuous piecewise affine functions with respect to the partition $\mathcal{T}^h$ is denoted by $\mathcal{P}_1(\mathcal{T}^h)$.

We assume throughout that the partition $\mathcal{T}^h$ has the following properties:

(T1) $\mathcal{T}^h$ is periodic: there exists $K \in \mathbb{N}$ such that $x_{k+K}^h = 1 + x_k^h$ for all $k \in \mathbb{Z}$.

(T2) $\mathcal{T}^h$ has atomistic resolution in Ω_{a}: $\Omega_{\mathrm{a}} \cap \varepsilon\mathbb{Z} = \Omega_{\mathrm{a}} \cap \{x_k^h\}_{k\in\mathbb{Z}}$.

(T3) The a/c interface points are finite element nodes: $\partial\Omega_{\mathrm{a}} \subset \{x_k^h\}_{k\in\mathbb{Z}}$. In particular, each element belongs entirely to either the atomistic or continuum region.

(T4) If $T_k^h \subset \Omega_{\mathrm{c}}^{\#}$ then $|T_k^h| = h_k \geq 2\varepsilon$.

We define $\#\mathcal{T}^h$ to be the number of elements in one period of the mesh.

Property (T4) results from our two-neighbour interaction model and is not strictly required. However, it simplifies the analysis and is not a significant restriction.

Note also that we removed the restriction (except in the atomistic region) that finite element nodes must be positioned on atomic sites, which was previously required in Chapter 2. Although not necessary in 1D, it somewhat simplifies mesh generation, and to some extend mimics the fact that element edges or faces in 2D/3D cannot normally be aligned with the underlying crystal lattice.

The finite element displacement and deformation spaces are defined, respec-

tively, by

$$\mathcal{U}^h := \{u_h \in \mathcal{P}_1(\mathcal{T}^h) : u_h(x+1) = u_h(x) \text{ and } u_h(0) = 0\}, \quad \text{and} \tag{3.2.3}$$

$$\mathcal{Y}^h := \{y_h \in \mathcal{P}_1(\mathcal{T}^h) : y_h - Fx \in \mathcal{U}^h\}. \tag{3.2.4}$$

We comment on the relationship between $\mathcal{U}^\varepsilon$ and $\mathcal{U}^h$ here. As we mentioned in Remark 2.1, we identify a lattice function in $\mathcal{U}^\varepsilon$ with its piecewise affine interpolant. Since reference lattice points may not necessarily exist as nodes in $\mathcal{T}^h$, $u \in \mathcal{U}^\varepsilon$ and $u_h \in \mathcal{U}^h$ may be piecewise affine with different partitions and $\mathcal{U}^h$ is not necessary a subspace of $\mathcal{U}^\varepsilon$, which also imply that $\mathcal{Y}^h$ is not necessary a subset of $\mathcal{Y}^\varepsilon$.

For $g \in C^0(\mathbb{R})$, we define the interpolation operator $I_h : C^0(\mathbb{R}) \to \mathcal{P}_1(\mathcal{T}^h)$ by

$$(I_h g)(x_k^h) := g(x_k^h) \qquad \forall k \in \mathbb{Z}. \tag{3.2.5}$$

We note that $I_h : \mathcal{U}^\varepsilon \to \mathcal{U}^h$.

For future reference, we also define the micro-elements $T_\ell^\varepsilon := ((\ell-1)\varepsilon, \ell\varepsilon)$ for $\ell \in \mathbb{Z}$. Analogously, we define I_ε to be the nodal interpolant with respect to the atomistic grid. We will require this interpolant since the mesh nodes $\{x_k^h\}_{k\in\mathbb{Z}}$ do not necessarily coincide with lattice sites.

3.2.3 QC Approximation

The QC approximation we analyze in this chapter is the 1D variant of the ACC method described in [64] which was motivated by [34]. (An earlier variant of the idea was described in [51] and a similar construction in [31]. We focus on the formulation proposed in [64] since it can be readily generalised to 2D.)

The idea of the ACC method is based on the splitting of interaction bonds. A bond is an open interval $b = (\ell\varepsilon, (\ell + j)\varepsilon)$ for $\ell \in \mathbb{Z}$ and $j \in \{1, 2\}$ (since we consider only first and second neighbour interactions). Since our computational domain is $[-1/2, 1/2]$, the set of bonds over which the atomistic energy is defined is given by

$$\mathcal{B} := \big\{(\ell\varepsilon, (\ell + j)\varepsilon) : j = 1, 2; \ell = -N + 1, \dots, N\big\}. \tag{3.2.6}$$

For each bond $b = (\ell\varepsilon, (\ell + j)\varepsilon)$ we define $r_b := j$.

For any open interval $\omega = (L_\omega, R_\omega)$ (e.g., for a bond) with length $|\omega| := R_\omega - L_\omega > 0$ we define the finite difference operator

$$D_\omega v := \frac{v(R_\omega) - v(L_\omega)}{|\omega|} \qquad \text{for } v \in C^0(\mathbb{R}). \tag{3.2.7}$$

Note that, with this notation, we can rewrite $\mathcal{E}_{\mathrm{a}}(y) = \varepsilon \sum_{b\in\mathcal{B}} \phi\big(r_b D_b y\big)$.

For each bond b and deformation field $y \in W^{1,\infty}(\mathbb{R})$ we define its atomistic and continuum energy contributions to the stored energy, respectively, by

$$\begin{aligned} a_b(y) :=& \frac{|b \cap \Omega_{\mathrm{a}}|}{|b|} \phi\big(r_b D_{b\cap\Omega_{\mathrm{a}}} y\big) \quad \text{and} \\ c_b(y) :=& \frac{1}{|b|} \int_{b\cap\Omega_{\mathrm{c}}^{\#}} \phi\big(r_b y'(x)\big)\, \mathrm{d}x. \end{aligned}$$

If $|b \cap \Omega_{\mathrm{a}}| = 0$ then $D_{b\cap\Omega_{\mathrm{a}}} y$ is ill-defined; in that case we define $a_b \equiv 0$. The QC energy (which is essentially the ACC energy of [64]) of a deformation field $y \in W^{1,\infty}(\mathbb{R})$ is now defined by

$$\mathcal{E}_{\mathrm{qc}}(y) := \varepsilon \sum_{b\in\mathcal{B}} \big[a_b(y) + c_b(y)\big]. \tag{3.2.8}$$

The key property of this definition is that it satisfies the patch test [64, Section 3.3],

$$\mathcal{E}'_{\mathrm{a}}(Fx)[v_\varepsilon] = \mathcal{E}'_{\mathrm{qc}}(Fx)[v_h] = 0 \quad \text{for all } v_\varepsilon \in \mathcal{U}^\varepsilon \text{ and } v_h \in \mathcal{U}^h, \quad \forall F > 0. \tag{3.2.9}$$

The *external energy* (per period) is given by

$$-\langle f, u_h \rangle_h := -\int_\Omega I_h(f u_h)\,\mathrm{d}x. \tag{3.2.10}$$

Note that, in the atomistic region, this reduces to the same form as (3.2.1). The *total energy* (per period) of a deformation $y_h \in \mathcal{Y}^h$ is then given by

$$E_{\mathrm{qc}}(y_h) := \mathcal{E}_{\mathrm{qc}}(y_h) - \langle f, y_h - Fx \rangle_h.$$

In the QC approximation we seek

$$y_{\mathrm{qc}} \in \operatorname{argmin} E_{\mathrm{qc}}(\mathcal{Y}^h). \tag{3.2.11}$$

Remark 3.2. It is initially not obvious why the formulation (3.2.8) should reduce the complexity of the computation of y_{qc} over that of y_{a}, since $\mathcal{E}_{\mathrm{qc}}$ is still written as a summation over all bonds. However, one can readily check (see [64] for the details), that

$$\mathcal{E}_{\mathrm{qc}}(y_h) = \sum_{b \in \mathcal{B}} a_b(y_h) + \int_{\Omega_{\mathrm{c}}} W(y_h')\,\mathrm{d}x,$$

where $W(r) := \phi(r) + \phi(2r)$ is the Cauchy–Born stored energy function. This formulation requires only a sum over all bonds within the atomistic region, and a standard finite element assembly procedure to compute the energy contribution from the continuum region. Thus, the evaluation of $\mathcal{E}_{\mathrm{qc}}$ has only a computational complexity proportional to $\#\mathcal{T}^h$ (the number of elements in one period)..

Analogous results hold in 2D [64]; a more involved assembly procedure is required to make the ACC method efficient in 3D [63].

3.3 Residual Analysis

We give the residual estimate of the QC problem introduced in Section 3.2.3. To achieve this, we first derive the variational formulation of the atomistic problem and its QC approximation, then following the framework described in Section 3.1, we split the residual into two parts as in (3.1.2) and (3.1.3) and analyze them separately to give the total residual estimate. We again use the negative norm technique [51] as we did in the consistency error analysis in last chapter. We restrict our estimates in $\mathcal{U}^{-1,2}$-norm as we will only derive the $\mathcal{U}^{1,2}$-stability and several Poincaré inequalities we use in the analysis of the external residual may only hold in the L^2-norm.

3.3.1 The variational formulations and the residual

Let y_{a} be a solution of the atomistic problem (3.2.2). It is straightforward to see that, if $y_{\mathrm{a}}' > 0$, then $\mathcal{E}_{\mathrm{a}}$ is differentiable at y_{a} and hence the first order optimality condition for (3.2.2) is satisfied:

$$\mathcal{E}_{\mathrm{a}}'(y_{\mathrm{a}})[v] = \langle f, v\rangle_{\varepsilon} \qquad \forall v \in \mathcal{U}^{\varepsilon}, \tag{3.3.1}$$

where

$$\mathcal{E}_{\mathrm{a}}'(y_{\mathrm{a}})[v] = \varepsilon \sum_{b\in\mathcal{B}} \phi'(r_b D_b y_{\mathrm{a}}) r_b D_b v. \tag{3.3.2}$$

Similarly, if y_{qc} is a solution of the QC problem (3.2.11) with $y_{\mathrm{qc}}' > 0$ on $[-1/2, 1/2]$, then it satisfies the corresponding first order optimality condition

$$\mathcal{E}_{\mathrm{qc}}'(y_{\mathrm{qc}})[v_h] = \langle f, v_h\rangle_h \qquad \forall v_h \in \mathcal{U}^h, \tag{3.3.3}$$

where $\forall y_h \in \mathcal{Y}^h$,

$$\begin{aligned}\mathcal{E}'_{\mathrm{qc}}(y_h)[v_h] &= \varepsilon \sum_{b\in\mathcal{B}} \left(a'_b(y_h)[v_h] + c'_b(y_h)[v_h]\right) \\ &= \sum_{b\in\mathcal{B}} |b\cap\Omega_{\mathrm{a}}|\phi'(r_b D_{b\cap\Omega_{\mathrm{a}}} y_h) D_{b\cap\Omega_{\mathrm{a}}} v_h + \sum_{b\in\mathcal{B}} \int_{b\cap\Omega_{\mathrm{c}}^{\#}} \phi'(r_b y'_h(x)) v'_h \,\mathrm{d}x.\end{aligned} \tag{3.3.4}$$

These variational formulations of the problems essentially corresponds to the abstract forms $a(\cdot;\cdot) = \langle l, v\rangle$ and $a_h(\cdot;\cdot) = \langle l_h, v_h\rangle$ in Section 3.1.

Let $y_{\mathrm{qc}} \in \mathcal{Y}^h$ be a solution of (3.2.11), then we define its residual $R \in (\mathcal{U}^\varepsilon)^*$ by

$$R[v] := E'_{\mathrm{a}}(y_{\mathrm{qc}})[v], \tag{3.3.5}$$

Using (3.3.3) we can rewrite this as

$$\begin{aligned} R[v] =&\ E'_{\mathrm{a}}(y_{\mathrm{qc}})[v] - E'_{\mathrm{qc}}(y_{\mathrm{qc}})[I_h v] \\ =&\ \left\{\mathcal{E}'_{\mathrm{a}}(y_{\mathrm{qc}})[v] - \mathcal{E}'_{\mathrm{qc}}(y_{\mathrm{qc}})[I_h v]\right\} - \left\{\langle f, v\rangle_\varepsilon - \langle f, I_h v\rangle_h\right\} \\ =:&\ R_{\mathrm{int}}[v] + R_{\mathrm{ext}}[v], \end{aligned}$$

where we call R_{int} the internal residual and R_{ext} the external residual. The two residuals corresponding to (3.1.2) and (3.1.3) will be bounded separately in the next two sections.

3.3.2 Estimate for the internal residual

In this section, we analyze the internal residual R_{int}. To state the main theorem, we define the index set of all nodes in the continuum region and a/c interface (recall that Ω_{c} is closed),

$$\mathcal{K}_{\mathrm{c}} := \left\{k \in \{1,\dots,K\} : x_k^h \in \Omega_{\mathrm{c}}\right\}. \tag{3.3.6}$$

Theorem 3.1. *Let $y_h \in \mathcal{Y}^h$ such that $y_h' > 0$ and $R_{\text{int}}[v] = \mathcal{E}_{\text{a}}'(y_h)[v] - \mathcal{E}_{\text{qc}}'(y_h)[I_h v]$, then*

$$\left\|R_{\text{int}}\right\|_{\mathcal{U}^{-1,2}} \leq \Big(3 \sum_{k \in \mathcal{K}_{\text{c}}} \eta_k^2\Big)^{\frac{1}{2}} =: \eta(y_h), \tag{3.3.7}$$

where

$$\eta_k^2 := \sum_{\substack{b \in \mathcal{B} \\ x_k^h \in \text{int}(b)}} \Big(\left\|\phi'(r_b D_b y_h) - \phi'(r_b D_{b \cap \Omega_{\text{a}}} y_h)\right\|_{L^2(b \cap \Omega_{\text{a}})}^2 + \left\|\phi'(r_b D_b y_h) - \phi'(r_b y_h')\right\|_{L^2(b \cap \Omega_{\text{c}}^{\#})}^2 \Big). \tag{3.3.8}$$

Remark 3.3. 1. The expressions for η_k are reminiscent of the flux (or stress) jump terms that occur in the classical residual error analysis for partial differential equations. However, their origin in QC approximation is different: it results only from the model approximation. In the 1D case we analyze in this paper, the effect of the finite element coarsening does not show up as a result of the vanishing of $R_3[v]$ which is defined in the proof of the theorem. As is typical for 1D a posteriori error analysis, the finite element coarsening error component will only enter the external residual estimate.

2. With some additional work, the form of the estimates η_k can be turned into element contributions and further simplified by computing more explicit representations. A concrete example for this is given in Appendix B.1.

Proof. Let $v_h := I_h v$. From (3.3.2) and (3.3.4) we obtain

$$R_{\text{int}}[v] = \sum_{b\in\mathcal{B}} \Big\{ |b|\phi'(r_b D_b y_h) D_b v - |b\cap\Omega_{\text{a}}|\phi'(r_b D_{b\cap\Omega_{\text{a}}} y_h) D_{b\cap\Omega_{\text{a}}} v_h \\ - \int_{b\cap\Omega_{\text{c}}^{\#}} \phi'(r_b y_h') v_h' \,\mathrm{d}x \Big\}. \tag{3.3.9}$$

We subtract and add the terms

$$\sum_{b\in\mathcal{B}} |b\cap\Omega_{\text{a}}|\phi'(r_b D_{b\cap\Omega_{\text{a}}} y_h) D_{b\cap\Omega_{\text{a}}} v \quad \text{and} \quad \sum_{b\in\mathcal{B}} \int_{b\cap\Omega_{\text{c}}^{\#}} \phi'(r_b y_h'(x)) v' \,\mathrm{d}x$$

to split R_{int} into three components,

$$\begin{aligned} R_{\text{int}}[v] = \sum_{b\in\mathcal{B}} \Big\{ & |b|\phi'(r_b D_b y_h) D_b v - |b\cap\Omega_{\text{a}}|\phi'(r_b D_{b\cap\Omega_{\text{a}}} y_h) D_{b\cap\Omega_{\text{a}}} v \\ & - \int_{b\cap\Omega_{\text{c}}^{\#}} \phi'(r_b y_h'(x)) v' \,\mathrm{d}x \Big\} \\ & + \sum_{b\in\mathcal{B}} |b\cap\Omega_{\text{a}}|\phi'(r_b D_{b\cap\Omega_{\text{a}}} y_h) \big(D_{b\cap\Omega_{\text{a}}} v - D_{b\cap\Omega_{\text{a}}} v_h \big) \\ & + \sum_{b\in\mathcal{B}} \int_{b\cap\Omega_{\text{c}}^{\#}} \phi'(r_b y_h'(x)) \big(v' - v_h' \big) \,\mathrm{d}x \\ =: \; & R_1[v] + R_2[v] + R_3[v]. \end{aligned} \tag{3.3.10}$$

We will show that $R_2 \equiv R_3 \equiv 0$ and estimate R_1.

For R_2 this follows simply from the fact that $v_h = v$ in Ω_{a} and hence $D_{b\cap\Omega_{\text{a}}} v = D_{b\cap\Omega_{\text{a}}} v_h$ for all $b \in \mathcal{B}$ such that $|b\cap\Omega_{\text{a}}| > 0$.

For R_3, upon defining $\chi_{\mathcal{S}}$ to be the characteristic function of a set $\mathcal{S}$, we can

rewrite it as

$$
\begin{aligned}
&\sum_{b\in\mathcal{B}} \int_{b\cap\Omega_c^\sharp} \phi'(r_b y_h'(x))\left[r_b v' - v_h'\right] \mathrm{d}x \\
&= \sum_{b\in\mathcal{B}} \int_{\Omega_c^\sharp} \chi_b \phi'(r_b y_h'(x))\left[r_b v' - v_h'\right] \mathrm{d}x \\
&= \sum_{b\in\mathcal{B}} \sum_{k\in\mathcal{K}_c} \int_{T_k} \chi_b \phi'(r_b y_h'(x))\left[r_b v' - v_h'\right] \mathrm{d}x \\
&= \sum_{r=1}^{2} \sum_{b\in\mathcal{B},r_b=r} \sum_{k\in\mathcal{K}_c} \frac{1}{r} \int_{T_k} \chi_b \phi'(r y_h'(x))\left[r(v' - v_h')\right] \mathrm{d}x \\
&= \sum_{r=1}^{2} \sum_{k\in\mathcal{K}_c} \sum_{b\in\mathcal{B},r_b=r} \frac{1}{r} \int_{T_k} \chi_b \phi'(r y_h')\left[r(v' - v_h')\right] \mathrm{d}x \\
&= \sum_{r=1}^{2} \sum_{k\in\mathcal{K}_c} \phi'(r y_h'|_{T_k}) \int_{T_k} \Big[\sum_{b\in\mathcal{B},r_b=r} \frac{1}{r}\chi_b\Big]\left[r(v' - v_h')\right], \qquad (3.3.11)
\end{aligned}
$$

since $r y_h'|_{T_k}$ is a constant on each element. By the 1D bond density lemma[64, Lemma 3.4],

$$
\sum_{b\in\mathcal{B},r_b=r} \frac{1}{r}\chi_b(x) =_{a.e.} 1,
$$

we have

$$
\begin{aligned}
&\sum_{r=1}^{2} \sum_{k\in\mathcal{K}_c} \phi'(r y_h'|_{T_k}) \int_{T_k} \Big[\sum_{b\in\mathcal{B},r_b=r} \frac{1}{r_b}\chi_b\Big]\left[r(v' - v_h')\right] \\
&= \sum_{r=1}^{2} \sum_{k\in\mathcal{K}_c} \phi'(r_b y_h'(x)|_{T_k}) \Big[r\big(v(x_k) - v(x_{k-1})\big) - r\big(v_h(x_k) - v_h(x_{k-1})\big)\Big]. \qquad (3.3.12)
\end{aligned}
$$

Again by the definition of v_h,

$$
v_h(x_k^h) = v(x_k^h) \text{ and } v_h(x_{k-1}^h) = v(x_{k-1}^h),
$$

and thus (3.3.12) vanishes.

Finally, we turn to the analysis of $R_1 = \sum_{b\in\mathcal{B}} R_1^b$, where we define

$$
R_1^b[v] := |b|\phi'(r_b D_b y_h) D_b v - |b\cap\Omega_a|\phi'(r_b D_{b\cap\Omega_a} y_h) D_{b\cap\Omega_a} v - \int_{b\cap\Omega_c^\sharp} \phi'(r_b y_h'(x)) v' \,\mathrm{d}x.
$$

Using the fact that $|\omega| D_\omega v = \int_\omega v' \,\mathrm{d}x$ we obtain

$$\begin{aligned} R_1^b[v] = &\int_b \phi'(r_b D_b y_h) v' \,\mathrm{d}x - \int_{b\cap\Omega_\mathrm{a}} \phi'(r_b D_{b\cap\Omega_\mathrm{a}} y_h) v' \,\mathrm{d}x - \int_{b\cap\Omega_\mathrm{c}^\#} \phi'(r_b y_h'(x)) v' \,\mathrm{d}x \\ = &\int_{b\cap\Omega_\mathrm{a}} \left[\phi'(r_b D_b y_h) - \phi'(r_b D_{b\cap\Omega_\mathrm{a}} y_h)\right] v' \,\mathrm{d}x \\ &+ \int_{b\cap\Omega_\mathrm{c}^\#} \left[\phi'(r_b D_b y_h) - \phi'(r_b y_h')\right] v' \,\mathrm{d}x. \end{aligned}$$

If $b \subset \Omega_\mathrm{a}$, then $b \cap \Omega_\mathrm{a} = b$ and $|b \cap \Omega_\mathrm{c}| = 0$, and hence $R_1^b = 0$. Similarly, if $b \subset T_k^h \subset \Omega_\mathrm{c}^\#$, then $D_b y_h = y_h'|_{T_k^h}$ and $|b \cap \Omega_\mathrm{a}| = 0$ and hence $R_1^b = 0$. Thus, we observe that only bonds crossing continuum element boundaries, or the atomistic/continuum interface, contribute to the residual. These are precisely the points contained in $\mathcal{K}_\mathrm{c}$. In particular, we obtain

$$R_1[v] = \sum_{k\in\mathcal{K}_\mathrm{c}} \sum_{\substack{b\in\mathcal{B} \\ x_k^h \in \mathrm{int}(b)}} R_1^b[v], \tag{3.3.13}$$

where we used the fact that no bond can cross more than one point $x_k^h \in \mathcal{K}_\mathrm{c}$ due to our assumption that all elements have at least length 2ε.

From the definition of R_1^b, and applying two Cauchy–Schwarz inequalities, it is straightforward to estimate

$$\begin{aligned} \left|R_1^b[v]\right| \leq \Big(&\left\|\phi'(r_b D_b y_h) - \phi'(r_b D_{b\cap\Omega_\mathrm{a}} y_h)\right\|_{L^2(b\cap\Omega_\mathrm{a})}^2 \\ &+ \left\|\phi'(r_b D_b y_h) - \phi'(r_b y_h')\right\|_{L^2(b\cap\Omega_\mathrm{c}^\#)}^2 \Big)^{1/2} \|v'\|_{L^2(b)}, \end{aligned}$$

and after applying another Cauchy–Schwarz inequality,

$$\Big| \sum_{\substack{b\in\mathcal{B} \\ x_k^h \in \mathrm{int}(b)}} R_1^b[v] \Big| \leq \eta_k \Big(\sum_{\substack{b\in\mathcal{B} \\ x_k^h \in \mathrm{int}(b)}} \|v'\|_{L^2(b)}^2 \Big)^{1/2},$$

where η_k is defined in (3.3.7).

Combing our foregoing estimates, we arrive at

$$\begin{aligned} R_1[v] &\leq \sum_{k\in\mathcal{K}_c} \eta_k \Big(\sum_{\substack{b\in\mathcal{B} \\ x_k^h\in \mathrm{int}(b)}} \|v'\|^2_{L^2(b)} \Big)^{1/2} \\ &\leq \Big(\sum_{k\in\mathcal{K}_c} \eta_k^2 \Big)^{1/2} \Big(\sum_{k\in\mathcal{K}_c} \sum_{\substack{b\in\mathcal{B} \\ x_k^h\in \mathrm{int}(b)}} \|v'\|^2_{L^2(b)} \Big)^{1/2}, \end{aligned}$$

and we are only left to estimate the sums involving the test function.

To that end, we simply note that, due to (T4), for any fixed point $x \in (-1/2, 1/2]$, the maximal number of bonds appearing in the sum on the left-hand side below and crossing x is three; hence,

$$\sum_{k\in\mathcal{K}_c} \sum_{\substack{b\in\mathcal{B} \\ x_k^h\in \mathrm{int}(b)}} \|v'\|^2_{L^2(b)} \leq 3\|v'\|^2_{L^2}.$$

This concludes the proof. □

3.3.3 Estimate of the external residual

We now turn to the estimate of the residual of the external energy, which is defined as

$$R_{\mathrm{ext}}[v] = \langle f, v\rangle_\varepsilon - \langle f, I_h v\rangle_h = \int_\Omega \big[I_\varepsilon(fv) - I_h(fI_h v)\big]\,\mathrm{d}x, \tag{3.3.14}$$

and corresponds to the variational crime (3.1.3). We outline the key points of the argument for estimating R_{ext}, before stating the result.

We define a slightly extended continuum region,

$$\tilde{\Omega}_c := \bigcup \big\{ T_\ell^\varepsilon : |T_\ell^\varepsilon \cap \Omega_c| > 0 \big\};$$

then $I_\varepsilon(fv) = I_h(fI_hv)$ in $\Omega_{\mathrm{a}} \setminus \tilde{\Omega}_{\mathrm{c}}$, and therefore

$$\begin{aligned} R_{\mathrm{ext}}[v] &= \int_{\tilde{\Omega}_{\mathrm{c}}} \left[I_\varepsilon(fv) - I_h(fI_hv) \right] \mathrm{d}x \\ &= \int_{\tilde{\Omega}_{\mathrm{c}}} \left[I_\varepsilon(fv) - fv \right] \mathrm{d}x + \int_{\tilde{\Omega}_{\mathrm{c}}} \left[fv - fI_hv \right] \mathrm{d}x + \int_{\tilde{\Omega}_{\mathrm{c}}} \left[fI_hv - I_h(fI_hv) \right] \mathrm{d}x \\ &=: R_1[v] + R_2[v] + R_3[v]. \end{aligned} \tag{3.3.15}$$

The three terms can be estimated using standard interpolation error results, hence we only give a brief outline of the proof of the resulting bound.

Proposition 3.2. *Let $f \in C^2(\tilde{\Omega}_c)$, then*

$$\|R_{\mathrm{ext}}\|_{\mathcal{U}^{-1,2}} \leq \eta^f + \eta^q, \tag{3.3.16}$$

where the error due to external forces η^f and the "quadrature error" η^q are, respectively, defined as follows: for $* \in \{f, q\}$,

$$\begin{aligned} & (\eta^*)^2 := \sum_{\substack{k \in \{1,\dots,K\} \\ T_k^h \subset \tilde{\Omega}_{\mathrm{c}}}} (\eta_k^*)^2, \\ \textit{where} \qquad & (\eta_k^f)^2 := \tfrac{h_k^2}{\pi^2} \|f\|^2_{L^2(T_k^h)}, \\ \textit{and} \qquad & (\eta_k^q)^2 := (\varepsilon^4 + h_k^4) \|f'\|^2_{L^2(T_k^h)} + \tfrac{(\varepsilon^4 + h_k^4)}{4\pi^2} \|f''\|^2_{L^2(T_k^h)}. \end{aligned}$$

Remark 3.4. 1. Note that there is an error contribution from the atomistic region, due to the fact that in the elements touching the a/c interface, the "quadrature" approximation of the external forces is not exact. For the purpose of mesh refinement, we count this error towards the neighbouring elements in the continuum region.

2. An alternative residual estimate that does not use $f \in C^2(\tilde{\Omega}_c)$, but only in the discrete setting, is presented in Appendix C. This requires a much more involved argument.

Proof. From (3.3.15) we obtain

$$R_{\text{ext}}[v] = R_1[v] + R_2[v] + R_3[v].$$

Applying standard interpolation error estimates (see, e.g., [8, 7]) on elements T_ℓ^ε, T_k^h, we obtain

$$\begin{aligned}
\int_{T_\ell^\varepsilon} \big[I_\varepsilon(fv) - fv\big]\,\mathrm{d}x &\le \tfrac{1}{4}\|\varepsilon^2 f''\|_{L^2(T_\ell^\varepsilon)}\|v\|_{L^2(T_\ell^\varepsilon)} + \tfrac{1}{2}\|\varepsilon^2 f'\|_{L^2(T_\ell^\varepsilon)}\|v'\|_{L^2(T_\ell^\varepsilon)},\\
\int_{T_k^h} \big[fv - fI_h v\big]\,\mathrm{d}x &\le \tfrac{1}{\pi}\|h_k f\|_{L^2(T_k^h)}\|v'\|_{L^2(T_k^h)}, \quad \text{and}\\
\int_{T_k^h} \big[I_h(fI_h v) - fI_h v\big]\,\mathrm{d}x &\le \tfrac{1}{4}\|h_k^2 f''\|_{L^2(T_k^h)}\|I_h v\|_{L^2(T_k^h)} + \tfrac{1}{2}\|h_k^2 f'\|_{L^2(T_k^h)}\|(I_h v)'\|_{L^2(T_k^h)}.
\end{aligned}$$

Summing over all elements, applying the Cauchy–Schwarz inequality, and defining $h(x) := h_k$ for $x \in T_k^h$,

$$\begin{aligned}
R_1[v] &\le \tfrac{\varepsilon^2}{4}\|f''\|_{L^2(\tilde{\Omega}_c)}\,\|v\|_{L^2} + \tfrac{\varepsilon^2}{2}\|f'\|_{L^2(\tilde{\Omega}_c)}\,\|v'\|_{L^2},\\
R_2[v] &\le \tfrac{1}{\pi}\|hf\|_{L^2(\tilde{\Omega}_c)}\,\|v'\|_{L^2}, \qquad \text{and}\\
R_3[v] &\le \tfrac{1}{4}\|h^2 f''\|_{L^2(\tilde{\Omega}_c)}\,\|I_h v\|_{L^2} + \tfrac{1}{2}\|h^2 f'\|_{L^2(\tilde{\Omega}_c)}\,\|I_h v'\|_{L^2}.
\end{aligned}$$

We now use the estimates (which exploit the fact that $I_h v'$ is the L^2-orthogonal projection of v' onto piecewise constants)

$$\begin{aligned}
&\|v\|_{L^2} \le \tfrac{1}{\pi}\|v'\|_{L^2}, \quad \|I_h v'\|_{L^2} \le \|v'\|_{L^2},\\
\text{and} \quad &\|I_h v\|_{L^2} \le \tfrac{1}{\pi}\|I_h v'\|_{L^2} \le \tfrac{1}{\pi}\|v'\|_{L^2},
\end{aligned}$$

to deduce that

$$\begin{aligned} R_{\text{ext}}[v] &= R_1[v] + R_2[v] + R_3[v] \\ &\leq \tfrac{1}{\pi}\|hf\|_{L^2(\tilde{\Omega}_c)}\|v'\|_{L^2} \\ &\quad + \left(\tfrac{1}{4\pi^2}\|(\varepsilon^2+h^2)f''\|^2_{L^2(\tilde{\Omega}_c)} + \|(\varepsilon^2+h^2)f'\|^2_{L^2(\tilde{\Omega}_c)}\right)^{1/2}\|v'\|_{L^2}. \end{aligned}$$

The result follows by splitting the norms inside the brackets over elements. □

3.3.4 External residual estimate for singular forces

In our numerical experiments in Section 3.6 we shall employ an external force that behaves like $|f(x)| \sim |x|^{-1}$ near $x = 0$ (we use the "singularity" in the force to mimic a defect). Let us suppose that we also have $|f'(x)| \sim |x|^{-2}$ and $|f''(x)| \sim |x|^{-3}$ near the origin. We now give a formal motivation why the quadrature estimates employed in Proposition 3.2 are inadequate in this situation.

Applying the quadrature estimates to such a force field, we obtain

$$\eta_k^q \approx h_k^2\|f'\|_{L^2(T_k^h)} + h_k^2\|f''\|_{L^2(T_k^h)} \approx h_k^{5/2}|x_k^h|^{-3/2} + h_k^{5/2}|x_k^h|^{-5/2}.$$

We notice that, for T_k^h near the origin, $\|f''\|_{L^2(T_k^h)} \approx |x_k^h|^{-1}\|f'\|_{L^2(T_k^h)}$. Moreover, the quadrature estimate is $O(1)$ and cannot be controlled. By contrast,

$$\eta_k^f \approx h_k^{3/2}|x_k^h|^{-1},$$

from which we conclude that $h_k^2\|f'\|_{L^2(T_k^h)}$ is dominated by η_k^f, but that η_k^f is itself dominated by $h_k^2\|f''\|_{L^2(T_k^h)}$.

The origin of this undesirable effect is the (ab-)use of the Poincaré inequality in the proof of Proposition 3.2. In the remainder of this section, we shall remedy the

situation by replacing the standard Poincaré inequality with a weighted variant. This approach is inspired by [53].

Lemma 3.3. *Let $\tilde{\Omega}_c$ be defined as in Section 3.3.3, and let $w(x) := x\log(x)$, then*

$$\|w^{-1}v\|_{L^2(\tilde{\Omega}_c)} \leq \tfrac{1}{\log 2}\|v'\|_{L^2} \qquad \forall v \in H^1(\Omega), v(0) = 0,$$

Proof. We begin by noting that

$$|v(x)| \leq |x|^{1/2}\|v'\|_{L^2} \quad \text{for all } x \in \Omega.$$

Hence, we can estimate

$$\int_{\tilde{R}_a}^{1/2} |w^{-1}v(x)|^2 \,\mathrm{d}x \leq \|v'\|^2_{L^2(0,1/2)} \int_{\tilde{R}_a}^{1/2} \frac{1}{x\log^2(x)} \,\mathrm{d}x.$$

Since $(\log^{-1}(x))' = -(x\log^2(x))^{-1}$ we obtain

$$\int_{\tilde{R}_a}^{1/2} |w^{-1}v(x)|^2 \,\mathrm{d}x \leq \tfrac{1}{\log(2)}\|v'\|^2_{L^2(0,1/2)}.$$

Applying an analogous argument in the left half of the domain, we obtain the stated estimate. □

We now apply this estimate to obtain an alternative external residual estimate.

Proposition 3.4. *Let $f \in C^2(\tilde{\Omega}_c)$, then*

$$\|R_{\text{ext}}\|_{\mathcal{U}^{-1,2}} \leq \eta^f + \hat{\eta}^q, \tag{3.3.17}$$

where η^f is defined in (3.3.16) *and $\hat{\eta}^q$ is defined as follows:*

$$(\hat{\eta}^q)^2 := \sum_{\substack{k\in\{1,\dots,K\}\\ T_k^h\subset\tilde{\Omega}_c}} (\hat{\eta}_k^q)^2,$$

$$\text{where} \qquad (\hat{\eta}_k^q)^2 := (\varepsilon^4 + h_k^4)\|f'\|^2_{L^2(T_k^h)} + \tfrac{\varepsilon^4+h_k^4}{\log^2 2}\|wf''\|^2_{L^2(T_k^h)},$$

and where w is defined in Lemma 3.3.

Proof. We again use the splitting (3.3.15) to obtain

$$R_{\text{ext}}[v] = R_1[v] + R_2[v] + R_3[v].$$

The residual term $R_2[v]$ is estimated in the same way as in the proof of Proposition 3.2, and gives rise to the term η^f in the estimate.

We show only the modified estimate for $R_3[v]$, since the estimate for $R_1[v]$ is analogous. Applying again a standard interpolation error estimate, we obtain

$$\big|R_3[v]\big| \le \tfrac{1}{4}\|h^2(fI_hv)''\|_{L^1(\tilde{\Omega}_c)} \le \tfrac{1}{2}\|h^2f'I_hv'\|_{L^1(\tilde{\Omega}_c)} + \tfrac{1}{4}\|h^2f''I_hv\|_{L^1(\tilde{\Omega}_c)}. \quad (3.3.18)$$

The term $\frac{1}{2}\|h^2f'I_hv'\|_{L^1(\tilde{\Omega}_c)}$ can be treated in the same way as in the proof of Proposition 3.2.

To estimate the second term on the right-hand side of (3.3.18) we insert the weighting function w defined in Lemma 3.3 and then apply the weighted Poincaré inequality:

$$\begin{aligned}\tfrac{1}{4}\|h^2f''I_hv\|_{L^1(\tilde{\Omega}_c)} &= \tfrac{1}{4}\big\|(h^2wf'')(w^{-1}I_hv)\big\|_{L^1(\tilde{\Omega}_c)}\\ &\le \tfrac{1}{4}\|h^2wf''\|_{L^2(\tilde{\Omega}_c)}\,\|w^{-1}I_hv\|_{L^2(\tilde{\Omega}_c)}\\ &\le \tfrac{1}{4\log 2}\|h^2wf''\|_{L^2(\tilde{\Omega}_c)}\,\|I_hv'\|_{L^2}.\end{aligned}$$

By continuing to argue as in the proof of Proposition 3.2 we obtain the stated estimate. □

We can now revisit the issue of relative magnitude of the various contributions to the residual estimate for the case where $|f(x)| \sim |x|^{-1}$, $|f'(x)| \sim |x|^{-2}$ and $|f''(x)| \sim |x|^{-3}$. Note that the effect of the weighting function is that $|w(x)f''(x)| \sim |\log(x)||x|^{-2}$ which is now comparable to $|f'(x)|$ up to a log factor.

More precisely, suppose that T_k^h is near the origin, then we now obtain

$$\hat{\eta}_k^q \approx h_k^{5/2}|x_k^h|^{-3/2} + h_k^{5/2}|x_k^h|^{-3/2}\log(x_k^h).$$

In particular, we observe that in the new external residual estimate, the quadrature error is dominated by the main error term η^f, which is the same as in the standard estimate given in Proposition 3.2. Thus, in our numerical algorithms presented in Section 3.6 we will be justified in neglecting the effect of the quadrature errors.

3.4 Stability

We follow a similar approach as in Section 2.7 to establish the a posteriori stability of the QC approximation.

Our aim is to prove coercivity (or, positivity) of the atomistic Hessian at the QC solution $y_{\rm qc}$:

$$E_{\rm a}''(y_{\rm qc})[v,v] \geq c_{\rm a}(y_{\rm qc})\|v'\|_{L^2}^2 \qquad \forall v \in \mathcal{U}, \tag{3.4.1}$$

for some constant $c_{\rm a}(y_{\rm qc}) > 0$, where the Hessian operator of the atomistic model is given by

$$E_{\rm a}''(y)[v,v] = \varepsilon \sum_{\ell=-N+1}^{N} \phi''(y'_\ell)|v'_\ell|^2 + \varepsilon \sum_{\ell=-N+1}^{N} \phi''(y'_\ell + y'_{\ell+1})|v'_\ell + v'_{\ell+1}|^2.$$

Following [17, 51] and Section 2.7 we note that the 'non-local' Hessian Stability of the exact (i.e., the atomistic) model is the second key ingredient for deriving an a posteriori error bound. terms $|v'_\ell + v'_{\ell+1}|^2$ can be rewritten in terms of the 'local' terms $|v'_\ell|^2$ and $|v'_{\ell+1}|^2$ and a strain-gradient correction,

$$|v'_\ell + v'_{\ell+1}|^2 = 2|v'_\ell|^2 + 2|v'_{\ell+1}|^2 - \varepsilon^2 |v''_\ell|^2.$$

Using this formula, we can rewrite the Hessian in the form

$$E''_{\rm a}(y)[v,v] = \varepsilon \sum_{\ell=-N+1}^{N} A_\ell |v'_\ell|^2 + \varepsilon^3 \sum_{\ell=-N+1}^{N} B_\ell |v''_\ell|^2,$$

where

$$\begin{aligned} A_\ell(y) &:= \phi''(y'_\ell) + 2\phi''(y'_{\ell-1} + y'_\ell) + 2\phi''(y'_\ell + y'_{\ell+1}) \\ B_\ell(y) &:= -\phi''(y'_\ell + y'_{\ell+1}). \end{aligned} \tag{3.4.2}$$

Recall our assumption in §3.2.1 that ϕ is convex in $(0, r_*)$ and concave in $(r_*, +\infty)$. For typical interactions such as Lennard-Jones or Morse potentials one generally observes that $y'_\ell \geq r_*/2$, hence we shall assume this throughout. As a result of this assumption, and the properties of ϕ, we have $B_\ell \geq 0 \; \forall \ell \in \mathbb{Z}$.

As an immediate consequence we obtain the following lemma, which gives sufficient conditions for the stability of the atomistic Hessian evaluated at the QC solution.

Proposition 3.5. *Let $y_{\rm qc} \in \mathcal{Y}^\varepsilon$ satisfy $\min_\ell (y_{\rm qc})'_\ell \geq r_*/2$, then*

$$E''_{\rm a}(y_{\rm qc})[v,v] \geq A_*(y_{\rm qc}) \|v'\|^2_{\ell^2_\varepsilon} \qquad \forall v \in \mathcal{U}, \quad \textit{where} \quad A_*(y_{\rm qc}) := \min_{\ell=1,\dots,N} A_\ell(y_{\rm qc}),$$

and the coefficients $A_\ell(y_{\rm qc})$ are defined in (3.4.2).

Remark 3.5. Since the minimum in the definition of A_* is taken over $2N$ lattice sites, it appears at first glance that A_* is expensive to evaluate. However, for $y_h \in \mathcal{Y}^h$, we can exploit the fact that y_h is piecewise affine to evaluate $A_*(y_h)$ in $O(K)$ operations:

Case i: If $\operatorname{dist}(\varepsilon(\ell - 1/2), \{x_k^h\}) < \frac{3}{2}\varepsilon$ then we evaluate $A_\ell(y_{\rm qc})$ using (3.4.2). There are $O(K)$ lattice sites of this type.

Case ii: If $\operatorname{dist}(\varepsilon(\ell - 1/2), \{x_k^h\}) \geq \frac{3}{2}\varepsilon$ then

$$A_\ell(y_{\rm qc}) = \phi''(y_h'|_{T_k^h}) + 4\phi''(2y_h'|_{T_k^h}),$$

that is, we only need to evaluate this formula once for each element.

3.4.1 Estimates for the Hessian

Before we present our main theorems, we state two useful auxiliary results: a local bound and a local Lipschitz bound on $E_{\rm a}''$. The proofs are in Appendix A. The former one will be used in the estimate of error of the energy and the later one is an analogy of the Lipschitz bound on $E_{\rm qc}''$ in Section 3.4.

Lemma 3.6. *Let $y, z \in \mathcal{Y}^\varepsilon$ such that $\min_\ell y_\ell' \geq \mu$ and $\min_\ell z_\ell' \geq \mu$ for some constant $\mu > 0$, then*

$$\begin{aligned} \left|\mathcal{E}_{\rm a}''(y)[v,w]\right| &\leq C_{\rm H}\|v'\|_{\ell^2_\varepsilon}\|w'\|_{\ell^2_\varepsilon}, \qquad \text{and} \\ \left|\{\mathcal{E}_{\rm a}''(y) - \mathcal{E}_{\rm a}''(z)\}[v,w]\right| &\leq C_{\rm Lip}\|y' - z'\|_{\ell^\infty_\varepsilon}\|v'\|_{\ell^2_\varepsilon}\|w'\|_{\ell^2_\varepsilon} \qquad \forall v, w \in \mathcal{U}, \end{aligned}$$

where $C_{\rm H} := M_2(\mu) + 4M_2(2\mu)$ and $C_{\rm Lip} := M_3(\mu) + 8M_3(2\mu)$ and $M_j(t) := \max_{s \geq t} |\phi^{(j)}(s)|$.

3.5 A Posteriori Error Estimates

We combine the residual estimates and the stability analysis to give an a posteriori error estimate for the error of deformation gradient in the first half of this section. In the second half, we derive an a posteriori error bound for the total energy of the system being approximated which is another important quantity of interest in many applications of the QC methods.

3.5.1 A posteriori error estimate for the solution

As in the a priori error analysis in Section 2.8, we will *assume* the existence of an atomistic solution y_a in a neighbourhood of y_{qc} (cf. (3.5.1)), and estimate the error $y_a - I_\varepsilon y_{qc}$. It is in principle possible to rigorously prove the existence of such a solution y_a in a neighbourhood of y_{qc}, following for example [55, 51], however, this would require substantial additional technicalities.

Theorem 3.7. *Let y_{qc} be a solution of the QC problem* (3.2.11) *with $\min_\ell (y_{qc})'_\ell \geq r_*/2$ and $A_*(y_{qc}) > 0$, where A_* is defined in the statement of Lemma 3.5. Suppose, further, that y_a is a solution of the atomistic model* (3.2.2) *such that, for some $\tau > 0$,*

$$\|y'_a - (I_\varepsilon y_{qc})'\|_{L^\infty(\Omega)} \leq \tau. \tag{3.5.1}$$

If τ is sufficiently small, then we have the error estimate

$$\|y'_a - (I_\varepsilon y_{qc})'\|_{L^2(\Omega)} \leq \tfrac{2}{A_*(y_{qc})}\big(\eta(y_{qc}) + \eta^f + \eta^q\big), \tag{3.5.2}$$

where η is defined in (3.3.7) *and η^f and η^q are defined in* (3.3.16).

Proof. Let $e := y_{\mathrm{a}} - I_\varepsilon y_{\mathrm{qc}}$. We require that $\tau \leq \frac{1}{2}\min y'_{\mathrm{qc}}$, then by the mean value theorem we know that there exists $\theta \in \mathrm{conv}\{y_{\mathrm{a}}, I_\varepsilon y_{\mathrm{qc}}\}$, such that

$$\begin{aligned} E''_{\mathrm{a}}(\theta)[e,e] =& E'_{\mathrm{a}}(y_{\mathrm{a}})[e] - E'_{\mathrm{a}}(I_\varepsilon y_{\mathrm{qc}})[e] \\ =& E'_{\mathrm{qc}}(y_{\mathrm{qc}})[I_h e] - E'_{\mathrm{a}}(I_\varepsilon y_{\mathrm{qc}})[e] \\ =& \big(\mathcal{E}'_{\mathrm{qc}}(y_{\mathrm{qc}})[I_h e] - \mathcal{E}'_{\mathrm{a}}(I_\varepsilon y_{\mathrm{qc}})[e]\big) - \big(\langle f, I_h e\rangle_h - \langle f, e\rangle_\varepsilon\big). \end{aligned}$$

In this proof we write $\mathcal{E}_{\mathrm{a}}(I_\varepsilon y_{\mathrm{qc}})$ to emphasize that we are comparing y'_{a} with $(I_\varepsilon y_{\mathrm{qc}})'$.

Applying Theorem 3.1 and Proposition 3.2, the two groups are respectively bounded by

$$\begin{aligned} \big|\mathcal{E}'_{\mathrm{qc}}(y_{\mathrm{qc}})[I_h e] - \mathcal{E}'_{\mathrm{a}}(I_\varepsilon y_{\mathrm{qc}})[e]\big| \leq \eta(y_{\mathrm{qc}})\|e'\|_{L^2}, \quad \text{and} \\ \big|\langle f, I_h e\rangle_h - \langle f, e\rangle_\varepsilon\big| \leq (\eta^f + \eta^q)\|e'\|_{L^2}, \end{aligned}$$

and hence we obtain

$$\mathcal{E}''_{\mathrm{a}}(\theta)[e,e] \leq \big(\eta(y_{\mathrm{qc}}) + \eta^f + \eta^q\big)\|e'\|_{L^2}. \tag{3.5.3}$$

Next, we compute a lower bound on $\mathcal{E}''_{\mathrm{a}}(\theta)[e,e]$. Using the Lipschitz estimate given in Lemma 3.6, Proposition 3.5 together with our assumption that $y'_{\mathrm{qc}} \geq r_*/2$, and the a priori bound (3.5.1), we have

$$\begin{aligned} \mathcal{E}''_{\mathrm{a}}(\theta)[e,e] &\geq \mathcal{E}''_{\mathrm{a}}(y_{\mathrm{qc}})[e,e] - C_{\mathrm{Lip}}\|y'_{\mathrm{a}} - y'_{\mathrm{qc}}\|_{L^\infty}\|e'\|_{L^2}^2 \\ &\geq \big(A_*(y_{\mathrm{qc}}) - C_{\mathrm{Lip}}\tau\big)\|e'\|_{L^2}^2. \end{aligned}$$

Hence, we if require that $\tau \leq A_*(y_{\mathrm{qc}})/(2C_{\mathrm{Lip}})$ (since C_{Lip} is bounded as τ decreases this is satisfied for τ sufficiently small), then we arrive at

$$\tfrac{1}{2}A_*(y_{\mathrm{qc}})\|e'\|_{L^2}^2 \leq \big(\eta^e(y_{\mathrm{qc}}) + \eta^f + \eta^q\big)\|e'\|_{L^2}.$$

Dividing through by $\|e'\|_{L^2}$ yields the stated estimate. □

3.5.2 A posteriori error estimate for the energy

An important quantity of interest is the total energy of the system being approximated. In this section, we derive an a posteriori estimate for the energy difference $E_{\mathrm{a}}(y_{\mathrm{a}}) - E_{\mathrm{qc}}(y_{\mathrm{qc}})$. To that end we decompose the energy difference into

$$\begin{aligned}\big|E_{\mathrm{a}}(y_{\mathrm{a}}) - E_{\mathrm{qc}}(y_{\mathrm{qc}})\big| = \big|E_{\mathrm{a}}(y_{\mathrm{a}}) - E_{\mathrm{a}}(I_\varepsilon y_{\mathrm{qc}})\big| + \big|\mathcal{E}_{\mathrm{a}}(I_\varepsilon y_{\mathrm{qc}}) - \mathcal{E}_{\mathrm{qc}}(y_{\mathrm{qc}})\big| \\ + \big|\langle f, I_\varepsilon y_{\mathrm{qc}} - Fx\rangle_\varepsilon - \langle f, y_{\mathrm{qc}} - Fx\rangle_h\big|\end{aligned} \tag{3.5.4}$$

and analyze each component separately.

For the first group on the right-hand side of (3.5.4), the result is standard:

Lemma 3.8. *Let $y, z \in \mathcal{Y}^\varepsilon$ such that $\min_\ell y'_\ell \geq \mu$ and $\min_\ell z'_\ell \geq \mu$ for some constant $\mu > 0$, and $y \in \mathrm{argmin} E_{\mathrm{a}}(\mathcal{Y}^\varepsilon)$, then*

$$\big|E_{\mathrm{a}}(y) - E_{\mathrm{a}}(z)\big| \leq \tfrac{1}{2} C_{\mathrm{H}} \|y' - z'\|_{L^2}^2, \tag{3.5.5}$$

where $C_{\mathrm{H}} = C_{\mathrm{H}}(\mu)$ was defined in Lemma 3.6.

Proof. There exists $\theta \in \mathrm{conv}\{y, z\}$ such that

$$E_{\mathrm{a}}(z) = E_{\mathrm{a}}(y) + E'_{\mathrm{a}}(y)[z - y] + \tfrac{1}{2} E''_{\mathrm{a}}(\theta)[z - y, z - y].$$

Since $E'_{\mathrm{a}}(y)[z - y] = 0$ and $E''_{\mathrm{a}} = \mathcal{E}''_{\mathrm{a}}$ applying Lemma 3.6 yields the stated result. □

For the second group on the right-hand side of (3.5.4), the estimate is obtained from a straightforward computation, using only the fact that the energy of a bond lying entirely inside an element is exact in the QC energy. The proof is omitted. Although the form of the error contributions μ_k looks complex at first glance, they

are in fact straightforward to compute. A concrete example of this error is given in Appendix B.2.

Lemma 3.9. *For $y_h \in \mathcal{Y}^h$ and $y_h' > 0$, we have*

$$\left|\mathcal{E}_{\mathrm{a}}(y_h) - \mathcal{E}_{\mathrm{qc}}(y_h)\right| \leq \mu(y_h) := \sum_{k \in \mathcal{K}_{\mathrm{c}}} \mu_k, \qquad \text{where} \tag{3.5.6}$$

$$\mu_k := \Bigg| \sum_{\substack{b \in \mathcal{B} \\ x_k^h \in \mathrm{int}(b)}} \Bigg\{ \tfrac{|b \cap \Omega_{\mathrm{a}}|}{r_b} \Big[\phi(r_b D_b y_h) - \phi\big(r_b D_{b \cap \Omega_{\mathrm{a}}} y_h\big) \Big] + \frac{1}{r_b} \int_{b \cap \Omega_{\mathrm{c}}^{\#}} \left[\phi(r_b D_b y_h) - \phi(r_b y_h') \right] \mathrm{d}x \Bigg\} \Bigg|. \tag{3.5.7}$$

Finally, the third group on the right-hand side of (3.5.4) can be estimated similarly as the external residual, however since the "test function" $u_h = y_h - Fx$ is now known explicitly, some additional structure can be exploited. Note that the error due to quadrature is again of higher order.

Lemma 3.10. *Let $y_h \in \mathcal{Y}^h$ and $u_h := y_h - Fx$, then*

$$\left|\langle f, u_h \rangle_h - \langle f, I_\varepsilon u_h \rangle_\varepsilon\right| \leq \mu^f(y_h) + \mu^q(y_h), \tag{3.5.8}$$

where $\mu^f(y_h)$ is the error due to external forces, and $\mu^q(y_h)$ the error due to quadrature. They are, respectively, defined as follows:

$$\mu^f(y_h) := \sum_{k \in \mathcal{K}_{\mathrm{c}}} \mu_k^f, \quad \text{where} \quad \mu_k^f := \tfrac{\varepsilon}{2} \|f\|_{L^1(\omega_k)} \left|[u_h']_{x_k^h}\right|, \quad \text{and}$$

$$\mu^q(y_h) := \sum_{k : T_k^h \subset \tilde{\Omega}_{\mathrm{c}}} \mu_k^q, \quad \text{where} \quad \mu_k^q := \tfrac{\varepsilon^2}{4} \left\|(f I_\varepsilon u_h)''\right\|_{L^1(T_k^h)} + \tfrac{h_k^2}{4} \left\|(f u_h)''\right\|_{L^1(T_k^h)},$$

where the second derivative $(fI_\varepsilon u_h)''$ *is to be understood in the piecewise sense,* $\omega_k = T^\varepsilon_\ell$ *if* $(\ell-1)\varepsilon < x^h_k < \ell\varepsilon$ *and* $\omega_k = \emptyset$ *if no such* $(\ell-1) \in \mathbb{Z}$ *exists, and* $[u'_h]_{x^h_k} := u'_h(x^h_k+) - u'_h(x^h_k-)$.

Remark 3.6. 1. It is straightforward to evaluate (possibly upper bounds of) the error contributions η^f_k and η^q_k with $O(K)$ computational complexity. This is due to the fact that u_h is piecewise linear on T^h_k, and $I_\varepsilon u_h = u_h$ except in the neighbourhoods ω_k of the element interfaces.

2. For the purpose of mesh refinement, we will group the residual contribution of the elements touching the a/c interface, so that no error contributions are associated with the atomistic region, which cannot be further refined.

Proof. Similarly as in the external residual estimate we write the external energy difference as

$$\langle f, I_\varepsilon u_h\rangle_\varepsilon - \langle f, u_h\rangle_h = \int_\Omega \left[I_\varepsilon(fI_\varepsilon u_h) - I_h(fu_h)\right] \mathrm{d}x.$$

Using $I_\varepsilon(fv) = I_h(fI_h v)$ in $\Omega \setminus \tilde{\Omega}_\mathrm{c}$, we decompose this difference into

$$\begin{aligned}\int_\Omega \left[I_\varepsilon(fI_\varepsilon u_h) - I_h(fu_h)\right] \mathrm{d}x &= \int_{\tilde{\Omega}_\mathrm{c}} \left[I_\varepsilon(fI_\varepsilon u_h) - I_h(fu_h)\right] \mathrm{d}x \\ &= \int_{\tilde{\Omega}_\mathrm{c}} \left[I_\varepsilon(fI_\varepsilon u_h) - fI_\varepsilon u_h\right] \mathrm{d}x + \int_{\tilde{\Omega}_\mathrm{c}} \left[fI_\varepsilon u_h - fu_h\right] \mathrm{d}x \\ &\quad + \int_{\tilde{\Omega}_\mathrm{c}} \left[fu_h - I_h(fu_h)\right] \mathrm{d}x\end{aligned} \tag{3.5.9}$$

Unlike in the proof proof of Proposition 3.2, where v_h was unknown, we can use our explicit knowledge of u_h, to estimate the first and third groups on the

right-hand side of (3.5.9) as follows:

$$\begin{aligned} \left| \int_{\tilde{\Omega}_{\mathrm{c}}} \left[I_\varepsilon(f I_\varepsilon u_h) - f I_\varepsilon u_h \right] \mathrm{d}x \right| &\leq \left\| \tfrac{\varepsilon^2}{4} (f I_\varepsilon u_h)'' \right\|_{L^1}, \qquad \text{and} \\ \left| \int_{\tilde{\Omega}_{\mathrm{c}}} \left[I_h(f u_h) - f u_h \right] \mathrm{d}x \right| &\leq \left\| \tfrac{h^2}{4} (f u_h)'' \right\|_{L^1}, \end{aligned} \tag{3.5.10}$$

where the second derivatives are understood in a piecewise sense.

To estimate the second group on the right-hand side of (3.5.9), we note that $I_\varepsilon u_h = u_h$ except near element boundaries. Upon defining ω_k and $[u_h']_{x_k}$ as in the statement of the result, we have

$$\begin{aligned} \int_{\tilde{\Omega}_{\mathrm{c}}} \left[f I_\varepsilon u_h - f u_h \right] \mathrm{d}x &= \sum_{\substack{k=1,\dots,K \\ x_k^h \in \tilde{\Omega}_{\mathrm{c}}}} \int_{\omega_k} \left[f I_\varepsilon u_h - f u_h \right] \mathrm{d}x \\ &\leq \sum_{\substack{k=1,\dots,K \\ x_k^h \in \tilde{\Omega}_{\mathrm{c}}}} \tfrac{\varepsilon}{2} \|f\|_{L^1(\omega_k)} \left\| u_h' - I_\varepsilon u_h' \right\|_{L^\infty(\omega_k)} \qquad (3.5.11) \\ &\leq \sum_{\substack{k=1,\dots,K \\ x_k^h \in \tilde{\Omega}_{\mathrm{c}}}} \tfrac{\varepsilon}{2} \|f\|_{L^1(\omega_k)} \left| [u_h']_{x_k} \right|. \qquad (3.5.12) \end{aligned}$$

It is now straightforward to rearrange the various error contributions to obtain the stated result. □

Combining all the foregoing estimates yields an a posteriori error estimate for the energy.

Theorem 3.11. *Suppose that the conditions of Theorem 3.7 are satisfied, then*

$$\left| E_{\mathrm{a}}(y_{\mathrm{a}}) - E_{\mathrm{qc}}(y_{\mathrm{qc}}) \right| \leq \tfrac{4C_{\mathrm{H}}}{A_*(y_{\mathrm{qc}})^2} \left\{ \eta(y_{\mathrm{qc}})^2 + (\eta^f)^2 + (\eta^q)^2 \right\} + \mu(y_{\mathrm{qc}}) + \mu^f(y_{\mathrm{qc}}) + \mu^q(y_{\mathrm{qc}}), \tag{3.5.13}$$

where $\eta(y_{\mathrm{qc}})$ *is defined in* (3.3.7), η^f, η^q *in* (3.3.16), $\mu(y_{\mathrm{qc}})$ *in* (3.5.6) *and* $\mu^f(y_{\mathrm{qc}}), \mu^q(y_{\mathrm{qc}})$ *in* (3.5.8).

Proof. The second term on the right-hand side of (3.5.4) is estimated by $\mu(y_h)$, which gives rise to the second term on the right-hand side of (3.5.13) (cf. Lemma 3.9). The third term on the right-hand side of (3.5.4) is estimated by $\mu^f(y_h)$ and $\mu^q(y_h)$, which gives rise to the third and fourth terms on the right-hand side of (3.5.4) (cf. Lemma 3.10).

Finally, using Lemma 3.8, the first term on the right-hand side of (3.5.4) can be bounded above by

$$\left|E_{\mathrm{a}}(y_{\mathrm{a}}) - E_{\mathrm{a}}(I_\varepsilon y_{\mathrm{qc}})\right| \leq \tfrac{1}{2} C_{\mathrm{H}} \|y_{\mathrm{a}}' - (I_\varepsilon y_{\mathrm{qc}})'\|_{L^2}^2.$$

Employing Theorem 3.7 we obtain

$$\left|E_{\mathrm{a}}(y_{\mathrm{a}}) - E_{\mathrm{a}}(I_\varepsilon y_{\mathrm{qc}})\right| \leq \tfrac{4C_H}{A_*(y_{\mathrm{qc}})^2}\left(\eta(y_{\mathrm{qc}})^2 + (\eta^f)^2 + (\eta^q)^2\right). \qquad \square$$

3.6 Numerical Experiments

In this section, we present numerical experiments to illustrate the results of our analysis, and highlight further features of our a posteriori error estimates. In particular, we will propose an adaptive mesh refinement algorithm, and show numerically that it achieves an optimal "convergence rate" in terms of the number of degrees of freedom. (Strictly speaking, we cannot speak of convergence rates since the algorithm will eventually fully resolve the problem.)

Throughout this section we fix $F = 1$, $N = 25000$, and let ϕ be the Morse potential

$$\phi(r) = \exp(-2\alpha(r-1)) - 2\exp(-\alpha(r-1)),$$

with the parameter $\alpha = 5$. We defined the external force f to be

$$f(x) := \begin{cases} -0.4\frac{x+1/2}{x}, & \text{for } -1/2 \le x < 0, \\ 0 & \text{for } x = 0, \\ 0.4\frac{1/2-x}{x}, & \text{for } 0 < x \le 1/2. \end{cases}$$

Note that $f(x)$ behaves essentially like $|x|^{-1}$, which is a typical decay rate for elastic fields generated by long-ranged defects in 2D/3D. (By contrast local perturbations decay exponentially in our 1D model.) Thus, introducing this force allows us to study the performance of our adaptive algorithm in a setting that includes some of the features of 2D/3D problems. The constant 0.4 is fairly arbitrary. It was chosen sufficiently large to achieve a significant deformation, but sufficiently small to ensure that there exists an elastic stable equilibrium configuration.

We will analyze the relative errors of the deformation gradient and of the energy defined, respectively, by

$$\frac{\|(I_\varepsilon y_{\rm qc})' - y_{\rm a}'\|_{L^2(\Omega)}}{\|y_{\rm a}' - F\|_{L^2(\Omega)}} \qquad \text{and} \qquad \frac{|E_{\rm a}(y_{\rm a}) - E_{\rm qc}(y_{\rm qc})|}{|E_{\rm a}(y_{\rm a}) - E_{\rm a}(Fx)|}. \tag{3.6.1}$$

In all computations, we compare the QC solutions against the (computable) exact solutions.

3.6.1 A priori mesh refinement

We will compare the adaptive algorithm introduced in the next sub-section against a quasi-optimal a priori mesh refinement scheme, which exploits the known qualitative behaviour of the solution. For simplicity we keep the following discussions informal.

We expect that, away from the defect, the exact solution will essentially behave like $|u''| \lesssim |f|$. We choose the atomistic region to be of the form $(-M\varepsilon, M\varepsilon)$.

Closely following the analysis of [54, Sec. 7.1] to optimize the mesh $\mathcal{T}^h$ based on these assumptions, we obtain that the (quasi-)optimal mesh size in the continuum region is given, approximately, by

$$h^*(x) = 2\varepsilon \left| \frac{f(M\varepsilon)}{f(x)} \frac{|x|}{M\varepsilon} \right|^{\frac{2}{3}}.$$

The following algorithm generates a mesh with this quasi-optimal mesh size. We only state the construction for the right-hand half of the domain. By this we mean that the best approximation error committed on this mesh is within a constant of an optimal mesh with the same number of degrees of elements.

The mesh will be symmetric about the centre $x = 0$. The factor 2ε ensures that the restriction (T4) is observed.

Algorithm 3.1 (A priori mesh refinement).

1. Add the vertices $0, \varepsilon, \ldots, \varepsilon M$ to the mesh.
2. Let x_k^h be the right-most vertex already in the mesh. If $x_k^h + h^*(x_k^h) > N$, stop.
3. Otherwise, add the vertex $x_k^h + h^*(x_k^h)$ to the mesh. Continue at (2).

3.6.2 Adaptive algorithm

In our adaptive computations, we begin with a mesh that resolves the "defect" (i.e., has atomistic resolution near $x = 0$) but is coarse elsewhere. We then employ the algorithm stated below to locally refine the mesh where required and thus improve the quality of the solution.

Before we state the algorithm, we first define the error indicators according to which we drive the mesh refinement. Node-based error contributions are split

between neighbouring elements. Error contributions from the atomistic region are associated with the neighbouring continuum elements.

The element error indicators for the gradient-driven algorithm are given by (cf. (3.3.7) and (3.3.16))

$$(\rho_k^\nabla)^2 := \tfrac{4}{A_*(y_{\mathrm{qc}})} \cdot \begin{cases} 3\eta_{k-1}^2 + \tfrac{3}{2}\eta_k^2 + (\eta_k^f)^2 + (\eta_{k-1}^f)^2, & \text{if } x_{k-1}^h = R_{\mathrm{a}}, \\ \tfrac{3}{2}\eta_{k-1}^2 + 3\eta_k^2 + (\eta_k^f)^2 + (\eta_{k+1}^f)^2, & \text{if } x_k^h = L_{\mathrm{a}}, \\ \tfrac{3}{2}\eta_{k-1}^2 + \tfrac{3}{2}\eta_k^2 + (\eta_k^f)^2, & \text{otherwise.} \end{cases}$$

Note that we have ignored the quadrature contributions. We have carefully justified this omission in Section 3.3.4.

The element error indicators for the energy-driven algorithm are given by (cf. Theorem 3.11)

$$\rho_k^E := \tfrac{4C_{\mathrm{H}}}{A_*(y_{\mathrm{qc}})^2} (\rho_k')^2 + \begin{cases} \mu_{k-1} + \tfrac{1}{2}\mu_k + \mu_{k-1}^f + \tfrac{1}{2}\mu_k^f + \mu_{k-1}^q + \mu_k^q, & \text{if } x_k^h = R_{\mathrm{a}}, \\ \tfrac{1}{2}\mu_{k-1} + \mu_k + \tfrac{1}{2}\mu_{k-1}^f + \mu_k^f + \mu_k^q + \mu_{k+1}^q, & \text{if } x_k^h = L_{\mathrm{a}}, \\ \tfrac{1}{2}\mu_{k-1} + \tfrac{1}{2}\mu_k + \tfrac{1}{2}\mu_{k-1}^f + \tfrac{1}{2}\mu_k^f + \mu_k^q, & \text{otherwise.} \end{cases}$$

Since the energy error is formally second order, we did include the quadrature contribution μ^q in this case.

In the following algorithm, let $\rho_k \in \{\rho_k^\nabla, \rho_k^E\}$. Our algorithm is based on established ideas from the adaptive finite element literature [19, 46].

Algorithm 3.2 (A posteriori mesh refinement).

1. Add the nodes $0, \pm\varepsilon, \ldots, \pm 3\varepsilon$ to the mesh. Add the nodes $\{x_0^h = -1/2, x_K^h = 1/2\}$ to the mesh.

2. *Compute:* Compute the QC solution on the current mesh, compute the error indicators ρ_k. For $T_k^h \subset \Omega_{\mathrm{a}}$, set $\rho_k = 0$.

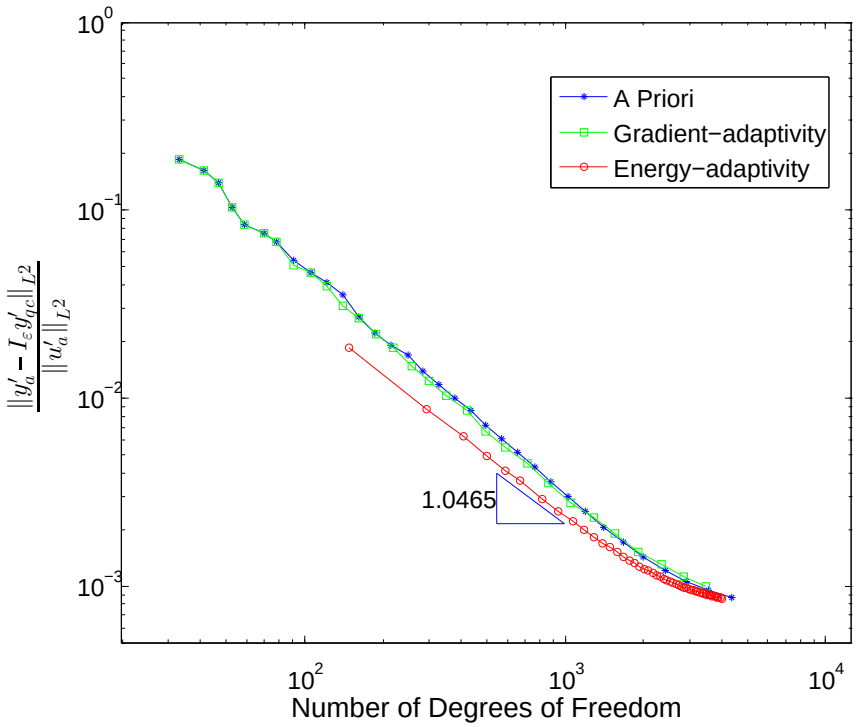

Figure 3.1: Relative errors in the deformation gradient (3.6.1) plotted against the number of degrees of freedom for three types of mesh refinements.

3. *Mark:* Choose a minimal subset $\mathcal{M} \subset \{1, \dots, K\}$ of indices such that

$$\sum_{k \in \mathcal{M}} \rho_k \geq \frac{1}{2} \sum_{k=1}^{K} \rho_k. \tag{3.6.2}$$

4. *Refine:* Bisect all elements T_k^h with indices belonging to $\mathcal{M}$.

   If an element that needs to be refined is adjacent to the atomistic region, merge this element into the atomistic region and create a new atomistic to continuum interface.

5. If the resulting mesh reaches a prescribed maximal number of degrees of freedom, stop algorithm; otherwise, go to Step (2).

3.6.3 Numerical Results

We summarize the results of the computations with meshes generated by the quasi-optimal refinement, and the adaptive algorithm with both gradient- and energy-

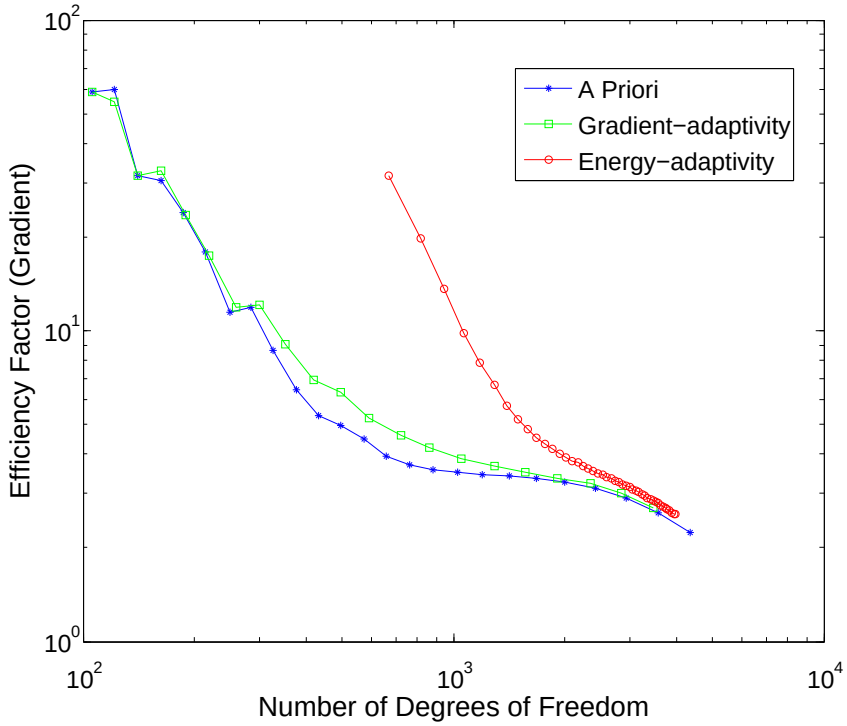

Figure 3.2: Efficiency factors (gradient a posteriori estimate divided by actual error) plotted against the number of degrees of freedom for three types of mesh refinements.

based error indicators.

1. In Figure 3.1 we display the gradient errors for the three types of mesh generation algorithms: quasi-optimal a priori refinement, gradient-driven a posteriori refinement and energy-driven a posteriori refinement. The differences among the three algorithms is negligible. We observe rates close to $(\#\text{DoF})^{-1}$ for all three algorithms. The efficiency indicators (estimate divided by actual error) are displayed in Figure 3.2 are moderate.

2. In Figure 3.3 we show the energy errors for the three types of mesh generation algorithms. Once again the differences between the three algorithms is negligible and the convergence rate is, as expected, twice the rate as compared with the gradient errors. However, the efficiency factors plotted in Figure 3.4 suggest that the constant prefactors in the estimators lead to a more substantial overestimation of the energy error.

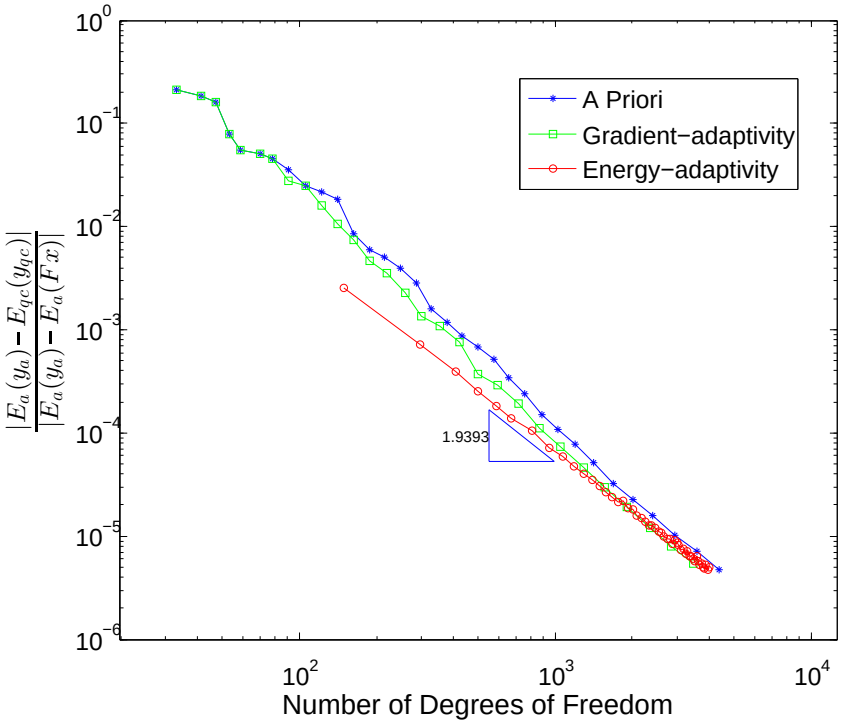

Figure 3.3: Relative Error of the total energy (3.6.1) plotted against the number of degrees of freedom for three types of mesh refinements.

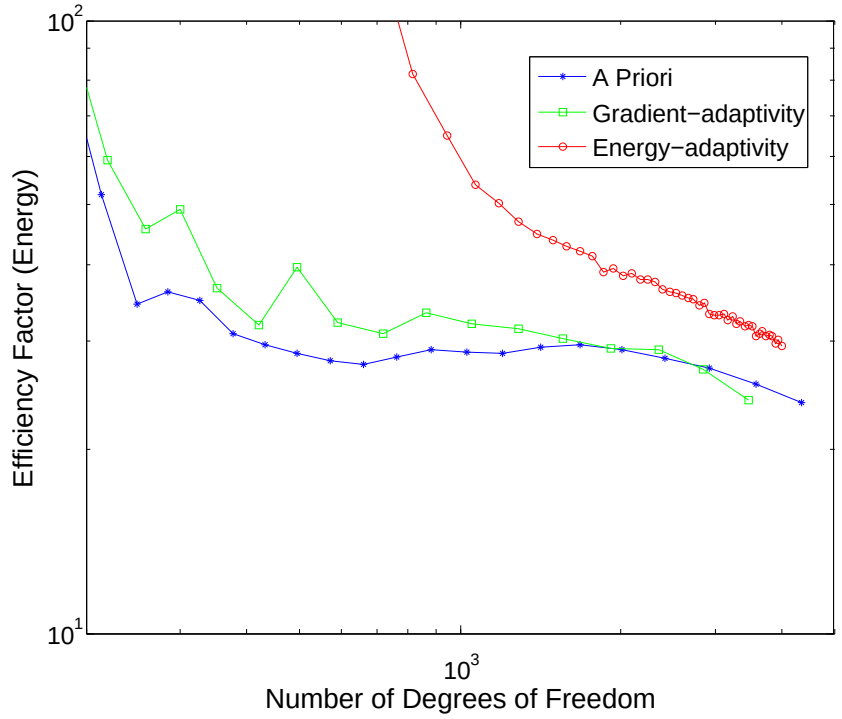

Figure 3.4: Efficiency Factor of the energy error estimator (energy a posteriori error estimate divided by actual energy error).

Thus we conclude that, at least in this model problem, both a posteriori error indicators can be used to select meshes that are quasi-optimal for both the deformation gradient and for the energy.

Chapter 4

Conclusion and Outlook

In this chapter, we first give a conclusion of this thesis and then an outlook of potential development of the QC methods.

In this thesis, we have established a priori error estimates and a posteriori error estimates for several different energy-based QC methods.

The a priori error estimates for three different energy-based quasicontinuum methods, which give a qualitative comparison of these methods, are given in Chapter 2. The error estimates followed the steps of the proof of a variation of the First Lemma of Strang. Using the techniques developed in [51], we gave optimal order consistency error estimates in the negative Soblev norms and showed the dependence of this error with respect to the smoothness of the solution to the original atomistic model. We also included coarse-graining in the error analysis, giving also a superconvergence result as a consequence of the one dimensional feature of our model problem. The stability results we obtained in this chapter are extensions of those in [17] to the nonlinear setting. Combining these results we derived quasi-optimal total error estimates. Several features of our analysis were further illuminated in the numerical experiments shown in Section 2.9. The message passed

by such analysis is that if an 'inappropriate' QC method is used in the computation, then the error caused by the method could be larger than the error caused by the coarse-graining of the computational domain.

Following the qualitative analysis of the QC methods, the a posteriori error estimates for an 'appropriate' QC method, which give the quantitative indicators of the mesh refinement for different quantity of interest, namely the deformation gradient and the energy, were given in Chapter 3. The residual-based a posteriori error estimates [72, Chapter2], was used with modifications to accommodate our model. Based on these estimators we proposed two adaptive mesh refinement algorithms, which we compared to quasi-optimal a priori mesh refinement. Our numerical experiments indicate that the resulting meshes are quasi-optimal. Though the theoretical importance of this analysis is less than the one we have achieved in Chapter 2, it is more useful in real computations.

We note that the framework we establish in Chapter 2 to the analysis of atomistic to continuum coupling methods in more complicated situations may be adopted and extended. A typical example is [54], where the a priori error estimate of a consistent energy based atomistic to continuum coupling method in 2D developed in [64] is given. We briefly give an introduction of the problem in an abstract formulation here.

The problem and its finite element variation can be abstractly (as the external force is absent in the problem) formulated as

$$a(u; v) = 0, \ \forall v \in \mathcal{U}, \text{ and} \tag{4.0.1}$$

$$a(u_h; v_h) = 0, \ \forall v_h \in \mathcal{U}_h, \tag{4.0.2}$$

where $\mathcal{U}_h \nsubseteq \mathcal{U}$. If we define interpolation operators $I_h : \mathcal{U} \to \mathcal{U}_h$ and $I_\varepsilon : \mathcal{U}_h \to \mathcal{U}$, and $e_h := I_h u - u_h$ then the error can be estimated by the following steps:

$$\begin{aligned}
\gamma \|e_h\| &\leq a_h(I_h u; e_h) - a_h(u_h; e_h) \\
&= a_h(I_h u; e_h) - a(u; I_\varepsilon e_h) \\
&= a_h(I_h u; e_h) - a(I_\varepsilon I_h u; I_\varepsilon e_h) \text{ (Consistency Error)} \\
&\quad + a(I_\varepsilon I_h u; I_\varepsilon e_h) - a(u; I_\varepsilon e_h) \text{ (Coarse-graining Error)} .
\end{aligned} \tag{4.0.3}$$

As we can see, (4.0.3) is a variation of (2.1.6) to (2.1.8) to give the consistency estimate which accommodate the features of the problem, namely the high dimensionality and the specific formulations of $a(\cdot;\cdot)$ and $a_h(\cdot;\cdot)$. However, the underlying principle of separating the generalized consistency error into the two different parts is essentially the same as we have in Chapter 3.

For the a posteriori error estimate of the above problem, the first step is to estimate (3.1.2), namely

$$\begin{aligned}
\gamma \|e\|^2 &\leq a(u; e) - a(I_\varepsilon u_h; e) \\
&= a_h(u_h; I_h e) - a(I_\varepsilon u_h; e),
\end{aligned}$$

where $e := u - I_\varepsilon u$. However, the estimate is much more involved as a result of the more difficult formulation and usage of the bond density lemma [64, Lemma 4.4] in higher dimensions, which makes the residual analysis less straight foward compared with (3.3.11) and (3.3.12). Though further work in the application relevant 2D/3D setting remains to be done, we conclude that adaptive mesh refinement driven by residual-based a posteriori error estimates can potentially lead to highly efficient atomistic/continuum mulitscale computations of atomistic material defects.

We conclude the thesis by pointing out an interesting issue arising for higher order and hp-finite element spaces. It would not be too difficult to extend our analysis to this setting. Note, however, that the Cauchy–Born modelling error is only of second order, while the coupling error is only of first order, which puts a severe lower bound on the accuracy that can be achieved. Thus, if one wants to take full advantage of the high accuracy of higher order finite element spaces, one would also need to construct higher order continuum models such as [1] and in particular higher order coupling mechanisms.

Appendix A

Lipschitz Constants for the Hessians of the Energy Functionals

In this appendix, we give a proof of Lemma 2.9 for three different QC methods and conclude C_{Lip} we defined in the lemma holds for all the three methods.

We begin with the QCL method.

Lemma A.1. *For $v, w \in \mathcal{U}$, and $y, z \in \mathcal{Y}$ such that $\min_\ell y'_\ell \geq \mu$ and $\min_\ell y'_\ell \geq \mu$, we have*

$$\left|\{\mathcal{E}''_{\mathrm{qcl}}(y) - \mathcal{E}''_{\mathrm{qcl}}(z)\}[v, w]\right| \leq C^{\mathrm{qcl}}_{\mathrm{Lip}} \|y' - z'\|_{\ell^\infty_\varepsilon} \|v'\|_{\ell^2_\varepsilon} \|w'\|_{\ell^2_\varepsilon} \qquad \forall v, w \in \mathcal{U},$$

where $C^{\mathrm{qcl}}_{\mathrm{Lip}} = M_3([\mu, +\infty)) + 8M_3([2\mu, +\infty))$.

Proof. By the definition of $\mathcal{E}_{\mathrm{qcl}}$, we have

$$\begin{aligned}
&\left|\{\mathcal{E}''_{\mathrm{qcl}}(y) - \mathcal{E}''_{\mathrm{qcl}}(z)\}[v, w]\right| \\
\leq &\varepsilon \sum_{\ell=-N+1}^{\ell=N} |\phi''(y'_\ell) - \phi''(z'_\ell)||v'_\ell||w'_\ell| + \varepsilon \sum_{\ell=-N+1}^{\ell=N} |\phi''(2y'_\ell) - \phi''(2z'_\ell)||2v'_\ell||2w'_\ell|
\end{aligned}$$

Using the estimates

$$|\phi''(y'_\ell) - \phi''(z'_\ell)| \leq M_3([\mu, +\infty)) \|y' - z'\|_{\ell^\infty_\varepsilon}, \tag{A.0.1}$$

and

$$|\phi''(2y'_\ell) - \phi''(2z'_\ell)| \le 2M_3([2\mu, +\infty))\|y' - z'\|_{\ell^\infty_\varepsilon}, \tag{A.0.2}$$

we obtain

$$\begin{aligned}\left|\{\mathcal{E}''_{\mathrm{qcl}}(y) - \mathcal{E}''_{\mathrm{qcl}}(z)\}[v,w]\right| \le & M_3([\mu, +\infty))\|y' - z'\|_{\ell^\infty_\varepsilon} \sum_{\ell=-N+1}^{\ell=N} |v'_\ell||w'_\ell| \\ & + 8M_3([2\mu, +\infty))\|y' - z'\|_{\ell^\infty_\varepsilon} \sum_{\ell=-N+1}^{\ell=N} |v'_\ell||w'_\ell| \\ \le & C^{\mathrm{qcl}}_{\mathrm{Lip}}\|y' - z'\|_{\ell^\infty_\varepsilon}\|v'\|_{\ell^2_\varepsilon}\|w'\|_{\ell^2_\varepsilon}.\end{aligned}$$

□

We then estimate for the QCE method.

Lemma A.2. *Suppose $v, w \in \mathcal{U}$ and $y, z \in \mathcal{Y}$ satisfy the same condition in Lemma A.1, and the atomistic region $\mathcal{A} := \{\ell_1, \dots, \ell_2\}$ and the continuum region $\mathcal{C} := \{-N+1, \dots, N\}\backslash\mathcal{A}$. Then*

$$\left|\{\mathcal{E}''_{\mathrm{qce}}(y) - \mathcal{E}''_{\mathrm{qce}}(z)\}[v,w]\right| \le C^{\mathrm{qce}}_{\mathrm{Lip}}\|y' - z'\|_{\ell^\infty_\varepsilon}\|v'\|_{\ell^2_\varepsilon}\|w'\|_{\ell^2_\varepsilon} \qquad \forall v, w \in \mathcal{U},$$

where $C^{\mathrm{qce}}_{\mathrm{Lip}} = M_3([\mu, +\infty)) + 9M_3([2\mu, +\infty))$.

Proof. Again by the definition of $\mathcal{E}_{\mathrm{qce}}$, we have

$$\begin{aligned}&\left|\{\mathcal{E}''_{\mathrm{qce}}(y) - \mathcal{E}''_{\mathrm{qce}}(z)\}[v,w]\right| \\ \le & \varepsilon \sum_{\ell=-N+1}^{\ell=N} |\phi''(y'_\ell) - \phi''(z'_\ell)||v'_\ell||w'_\ell| \\ & + \varepsilon \sum_{\ell\in\mathcal{C}} \frac{1}{2}\left[|\phi''(2y'_\ell) - \phi''(2z'_\ell)||2v'_\ell||2w'_\ell| + |\phi''(2y'_{\ell+1}) - \phi''(2z'_{\ell+1})||2v'_{\ell+1}||2w'_{\ell+1}|\right] \\ & + \varepsilon \sum_{\ell=\ell_1+1}^{\ell_2-1} |\phi''(y'_\ell + y'_{\ell+1}) - \phi''(z'_\ell + z'_{\ell+1})||v'_\ell + v'_{\ell+1}||w'_\ell + w'_{\ell+1}| \\ & + \varepsilon \sum_{\ell\in\{\ell_1-1,\ell_1,\ell_2,\ell_2+1\}} \frac{1}{2}|\phi''(y'_\ell + y'_{\ell+1}) - \phi''(z'_\ell + z'_{\ell+1})||v'_\ell + v'_{\ell+1}||w'_\ell + w'_{\ell+1}|.\end{aligned}$$

Using (A.0.1), (A.0.2) and

$$|\phi''(y'_\ell + y'_{\ell+1}) - \phi''(z'_\ell + z'_{\ell+1})| \le 2M_3([2\mu, +\infty))\|y' - z'\|_{\ell^\infty_\varepsilon}, \tag{A.0.3}$$

we obtain the following estimate

$$\begin{aligned}
&\left|\{\mathcal{E}''_{\mathrm{qce}}(y) - \mathcal{E}''_{\mathrm{qce}}(z)\}[v,w]\right| \\
\le&\varepsilon M_3([\mu,+\infty))\|y'-z'\|_{\ell^\infty_\varepsilon} \sum_{\ell=-N+1}^{\ell=N} |v'_\ell||w'_\ell| \\
&+ \varepsilon 2M_3([2\mu,+\infty))\|y'-z'\|_{\ell^\infty_\varepsilon}\Bigg[8\sum_{\ell=1}^{\ell_1-1}|v'_\ell||w'_\ell| + 4|v'_{\ell_1}||w'_{\ell_1}| \\
&\quad + 4|v'_{\ell_2+1}||w'_{\ell_2+1}| + 8\sum_{\ell=\ell_2+2}^{N}|v'_\ell||w'_\ell| \\
&\quad + \sum_{\ell\in\{\ell_1-1,\ell_1,\ell_2,\ell_2+1\}}\left\{|v'_\ell||w'_\ell| + |v'_\ell||w'_{\ell+1}| + |v'_{\ell+1}||w'_{\ell+1}| + |v'_{\ell+1}||w'_{\ell+1}|\right\} \\
&\quad + 2\sum_{\ell\in\{\ell_1+1,\ldots,\ell_2-1\}}\left\{|v'_\ell||w'_\ell| + |v'_\ell||w'_{\ell+1}| + |v'_{\ell+1}||w'_{\ell+1}| + |v'_{\ell+1}||w'_{\ell+1}|\right\}\Bigg]
\end{aligned}$$

After judiciously regrouping the terms and applying Chauchy-Schwarz inequalities, we obtain the stated result. □

Finally we present the case for QNL method.

Lemma A.3. *Suppose $v, w \in \mathcal{U}$ and $y, z \in \mathcal{Y}$ satisfy the same condition in Lemma A.1, and the atomistic region $\mathcal{A} := \{\ell_1, \ldots, \ell_2\}$ and the continuum region $\mathcal{C} := \{-N+1, \ldots, N\}\backslash\mathcal{A}$. Then*

$$\left|\{\mathcal{E}''_{\mathrm{qnl}}(y) - \mathcal{E}''_{\mathrm{qnl}}(z)\}[v,w]\right| \le C^{\mathrm{qnl}}_{\mathrm{Lip}}\|y'-z'\|_{\ell^\infty_\varepsilon}\|v'\|_{\ell^2_\varepsilon}\|w'\|_{\ell^2_\varepsilon} \qquad \forall v, w \in \mathcal{U},$$

where $C^{\mathrm{qnl}}_{\mathrm{Lip}} = M_3([\mu,+\infty)) + 9M_3([2\mu,+\infty))$.

Proof. Again by the definition of $\mathcal{E}_{\text{qnl}}$, we have

$$
\begin{aligned}
&\left|\{\mathcal{E}''_{\text{qnl}}(y) - \mathcal{E}''_{\text{qnl}}(z)\}[v,w]\right| \\
\leq &\varepsilon \sum_{\ell=-N+1}^{\ell=N} |\phi''(y'_\ell) - \phi''(z'_\ell)||v'_\ell||w'_\ell| \\
&+ \varepsilon \sum_{\ell\in\mathcal{C}} \frac{1}{2}\left[|\phi''(2y'_\ell) - \phi''(2z'_\ell)||2v'_\ell||2w'_\ell| + |\phi''(2y'_{\ell+1}) - \phi''(2z'_{\ell+1})||2v'_{\ell+1}||2w'_{\ell+1}|\right] \\
&+ \varepsilon \sum_{\ell=\ell_1+1}^{\ell_2-1} |\phi''(y'_\ell + y'_{\ell+1}) - \phi''(z'_\ell + z'_{\ell+1})||v'_\ell + v'_{\ell+1}||w'_\ell + w'_{\ell+1}|.
\end{aligned}
$$

Using (A.0.1), (A.0.2) and (A.0.3) we obtain the following estimate

$$
\begin{aligned}
&\left|\{\mathcal{E}''_{\text{qnl}}(y) - \mathcal{E}''_{\text{qnl}}(z)\}[v,w]\right| \\
\leq &\varepsilon M_3([\mu,+\infty))\|y' - z'\|_{\ell^\infty_\varepsilon} \sum_{\ell=-N+1}^{\ell=N} |v'_\ell||w'_\ell| \\
&+ \varepsilon 2M_3([2\mu,+\infty))\|y' - z'\|_{\ell^\infty_\varepsilon}\Bigg[8\sum_{\ell=1}^{\ell_1-1}|v'_\ell||w'_\ell| + 4|v'_{\ell_1}||w'_{\ell_1}| \\
&\quad + 4|v'_{\ell_2+1}||w'_{\ell_2+1}| + 8\sum_{\ell=\ell_2+2}^{N}|v'_\ell||w'_\ell| \\
&\quad + 2\sum_{\ell\in\mathcal{A}}\left\{|v'_\ell||w'_\ell| + |v'_\ell||w'_{\ell+1}| + |v'_{\ell+1}||w'_{\ell+1}| + |v'_{\ell+1}||w'_{\ell+1}|\right\}\Bigg]
\end{aligned}
$$

Again, the stated result is obtained by regrouping and applying Cauchy–Schwarz inequalities to each group. □

For a posteriori error estimates, we need the estimates for the hessian of the atomistic energy functional. The following is the proof of Lemma 3.6.

Proof. By the definition of $\mathcal{E}_{\mathrm{a}}$, we have

$$\begin{aligned}
&\left|\mathcal{E}_{\mathrm{a}}''(y)[v,w]\right| \\
\leq&\varepsilon \sum_{\ell=-N+1}^{\ell=N} |\phi''(y'_\ell)||v'_\ell||w'_\ell| \\
&+\varepsilon \sum_{\ell=-N+1}^{N} |\phi''(y'_\ell + y'_{\ell+1})||v'_\ell + v'_{\ell+1}||w'_\ell + w'_{\ell+1}|.
\end{aligned}$$

and

$$\begin{aligned}
&\left|\{\mathcal{E}_{\mathrm{a}}''(y) - \mathcal{E}_{\mathrm{a}}''(z)\}[v,w]\right| \\
\leq&\varepsilon \sum_{\ell=-N+1}^{\ell=N} |\phi''(y'_\ell) - \phi''(z'_\ell)||v'_\ell||w'_\ell| \\
&+\varepsilon \sum_{\ell=-N+1}^{N} |\phi''(y'_\ell + y'_{\ell+1}) - \phi''(z'_\ell + z'_{\ell+1})||v'_\ell + v'_{\ell+1}||w'_\ell + w'_{\ell+1}|.
\end{aligned}$$

We obtain the first estimate directly by the defintion of $M_j(t)$ and a Cauchy–Schwarz inequality. The second estimate is established by using (A.0.3) and Cauchy–Schwarz inequalities. □

Appendix B

Concrete Examples of the Internal Residuals

In this appendix, we give two concrete examples of the internal residuals in the analysis of the error in gradient and that in total energy.

B.1 Internal Residual of the Gradient

To illustrate the analysis of the internal residual in Theorem 3.1, we give explicit representations for (3.3.8) on each bond b that crosses a finite element node inside the continuum region or atomistic to continuum interface. We adopt the jump notation $[[\cdot]]$, which is frequently employed in the a posteriori error analysis for elliptic equations [7, 72]. To avoid the complication of the presentation, we assume $|T_k^h| \geq 2\varepsilon$.

We first list the three cases that correspond to the bonds crossing continuum elements' boundaries:

For $b = \big(\ell_k\varepsilon, (\ell_k+1)\varepsilon\big)$ and $x_k^h \in b$,

$$\begin{aligned}
[[\phi']]_b =& \|\phi'(r_b D_b y_h) - \phi'(r_b D_{b\cap\Omega_a} y_h)\|_{L^2(b)} \\
=& (1-\theta_k)\varepsilon\Big[\phi'\big((1-\theta_k)y_h'|_{T_{k+1}} + \theta_k y_h'|_{T_k}\big) - \phi'\big(y_h'|_{T_{k+1}}\big)\Big]^2 \\
&+ \theta_k\varepsilon\Big[\phi'\big((1-\theta_k)y_h'|_{T_{k+1}} + \theta_k y_h'|_{T_k}\big) - \phi'\big(y_h'|_{T_k}\big)\Big]^2.
\end{aligned}$$

For $b = \big(\ell_k\varepsilon, (\ell_k+2)\varepsilon\big)$ and $x_k^h \in b$,

$$\begin{aligned}
[[\phi']]_b =& (2-\theta_k)\varepsilon\Big[\phi'\big((2-\theta_k)y_h'|_{T_{k+1}} + \theta_k y_h'|_{T_k}\big) - \phi'\big(2y_h'|_{T_{k+1}}\big)\Big]^2 \\
&+ \theta_k\varepsilon\Big[\phi'\big((2-\theta_k)y_h'|_{T_{k+1}} + \theta_k y_h'|_{T_k}\big) - \phi'\big(2y_h'|_{T_k}\big)\Big]^2.
\end{aligned}$$

For $b = \big((\ell_k-1)\varepsilon, (\ell_k+1)\varepsilon\big)$ and $x_k^h \in b$,

$$\begin{aligned}
[[\phi']]_b =& (1-\theta_k)\varepsilon\Big[\phi'\big((1-\theta_k)y_h'|_{T_{k+1}} + (1+\theta_k)y_h'|_{T_k}\big) - \phi'\big(2y_h'|_{T_{k+1}}\big)\Big]^2 \\
&+ (1+\theta_k)\varepsilon\Big[\phi'\big((1-\theta_k)y_h'|_{T_{k+1}} + (1+\theta_k)y_h'|_{T_k}\big) - \phi'\big(2y_h'|_{T_k}\big)\Big]^2.
\end{aligned}$$

We then list the six cases that correspond to the bonds crossing the left and right (with respect to an atomistic region) atomistic to continuum interfaces.

One the left interface we have:

For $b = \big(\ell_k\varepsilon, (\ell_k+1)\varepsilon\big)$ and $x_k^h \in b$,

$$\begin{aligned}
[[\phi']]_b =& \|\phi'(r_b D_b y_h) - \phi'(r_b D_{b\cap\Omega_a} y_h)\|^2_{L^2(b\cap\Omega_a)} \\
&+ \|\phi'(r_b D_b y_h) - \phi'(r_b D_{b\cap\Omega_a} y_h)\|^2_{L^2(b\cap\Omega_c)} \\
=& (1-\theta_k)\varepsilon\Big[\phi'\big((1-\theta_k)y_h'|_{T_{k+1}} + \theta_k y_h'|_{T_k}\big) - \phi'\big(y_h'|_{T_{k+1}}\big)\Big]^2 \\
&+ \theta_k\varepsilon\Big[\phi'\big((1-\theta_k)y_h'|_{T_{k+1}} + \theta_k y_h'|_{T_k}\big) - \phi'\big(y_h'|_{T_k}\big)\Big]^2.
\end{aligned}$$

For $b = \big(\ell_k\varepsilon, (\ell_k+2)\varepsilon\big)$ and $x_k^h \in b$,

$$\begin{aligned}[[\phi']]_b =&(2-\theta_k)\varepsilon\Big[\phi'\big(y_h'|_{T_{k+2}} + (1-\theta_k)y_h'|_{T_{k+1}} + \theta_k y_h'|_{T_k}\big)\\ &\qquad - \phi'\big(\frac{2}{2-\theta_k}y_h'|_{T_{k+2}} + \frac{2(1-\theta_k)}{2-\theta_k}y_h'|_{T_k+1}\big)\Big]^2\\ &+\theta_k\varepsilon\Big[\phi'\big(y_h'|_{T_{k+2}} + (1-\theta_k)y_h'|_{T_{k+1}} + \theta_k y_h'|_{T_k}\big) - \phi'\big(2y_h'|_{T_k}\big)\Big]^2.\end{aligned}$$

For $b = \big((\ell_k-1)\varepsilon, (\ell_k+1)\varepsilon\big)$ and $x_k^h \in b$,

$$\begin{aligned}[[\phi']]_b =&(1-\theta_k)\varepsilon\Big[\phi'\big(y_h'|_{T_{k+2}} + (1-\theta_k)y_h'|_{T_{k+1}} + \theta_k y_h'|_{T_k}\big) - \phi'\big(2y_h'|_{T_{k+1}}\big)\Big]^2\\ &+(1+\theta_k)\varepsilon\Big[\phi'\big(y_h'|_{T_{k+2}} + (1-\theta_k)y_h'|_{T_{k+1}} + \theta_k y_h'|_{T_k}\big) - \phi'\big(2y_h'|_{T_k}\big)\Big]^2.\end{aligned}$$

One the right interface we have:
For $b = \big(\ell_k\varepsilon, (\ell_k+1)\varepsilon\big)$ and $x_k^h \in b$,

$$\begin{aligned}[[\phi']]_b =&(1-\theta_k)\varepsilon\Big[\phi'\big((1-\theta_k)y_h'|_{T_{k+1}} + \theta_k y_h'|_{T_k}\big) - \phi'\big(y_h'|_{T_{k+1}}\big)\Big]^2\\ &+\theta_k\varepsilon\Big[\phi'\big((1-\theta_k)y_h'|_{T_{k+1}} + \theta_k y_h'|_{T_k}\big) - \phi'\big(y_h'|_{T_k}\big)\Big]^2.\end{aligned}$$

For $b = \big(\ell_k\varepsilon, (\ell_k+2)\varepsilon\big)$ and $x_k^h \in b$,

$$\begin{aligned}[[\phi']]_b =&(2-\theta_k)\varepsilon\Big[\phi'\big((2-\theta_k)y_h'|_{T_{k+1}} + \theta_k y_h'|_{T_k}\big) - \phi'\big(2y_h'|_{T_{k+1}}\big)\Big]^2\\ &+\theta_k\varepsilon\Big[\phi'\big((2-\theta_k)y_h'|_{T_{k+1}} + \theta_k y_h'|_{T_k}\big) - \phi'\big(2y_h'|_{T_k}\big)\Big]^2.\end{aligned}$$

For $b = \big((\ell_k-1)\varepsilon, (\ell_k+1)\varepsilon\big)$, $x_k^h \in b$ and $k = R_a^i$, we have

$$\begin{aligned}[[\phi']]_b =&(1-\theta_k)\varepsilon\Big[\phi'\big((1-\theta_k)y_h'|_{T_{k+1}} + \theta_k y_h'|_{T_k} + y_h'|_{T_{k-1}}\big) - \phi'\big(2y_h'|_{T_{k+1}}\big)\Big]^2\\ &+(1+\theta_k)\varepsilon\Big[\phi'\big((1-\theta_k)y_h'|_{T_{k+1}} + \theta_k y_h'|_{T_k} + y_h'|_{T_{k-1}}\big)\\ &\qquad - \phi'\big(\frac{2\theta_k}{(1+\theta_k)}y_h'|_{T_k} + \frac{2}{1+\theta_k}y_h'|_{T_{k-1}}\big)\Big]^2.\end{aligned}$$

Remark B.1. As we mentioned, $[[\phi']]_b$ essentially behaves like the flux(or stress) jumps between adjacent elements. An alternative analysis of the internal residual could be found in [74].

B.2 Internal Residual of the Energy

In this section, we give explicit representations for (3.5.6). Our assumption is the same as in Appendix B.1. An alternative presentation but essentially the same approach can be found in [74].

We first list the three cases that correspond to the bonds crossing continuum elements' boundaries:

For $b = \big(\ell_k\varepsilon, (\ell_k+1)\varepsilon\big)$ and $x_k^h \in b$,

$$\bar{R}_e^b := \frac{|b\cap\Omega_{\mathrm{a}}|}{r_b}\Big[\phi(r_b D_b y_h) - \phi\big(r_b D_{b\cap\Omega_{\mathrm{a}}} y_h\big)\Big] + \frac{1}{r_b}\int_{b\cap\Omega_{\mathrm{c}}^\sharp}\big[\phi(r_b D_b y_h) - \phi(r_b y_h')\big]\,\mathrm{d}x$$
$$\varepsilon\big[\phi((1-\theta_k)y_h'|_{T_{k+1}} + \theta_k y_h'|_{T_k}) - \theta_k\phi(y_h'|_{T_k}) - (1-\theta_k)\phi(y_h'|_{T_{k+1}})\big].$$

For $b = \big(\ell_k\varepsilon, (\ell_k+2)\varepsilon\big)$ and $x_k^h \in b$,

$$\bar{R}_e^b = \frac{1}{2}\varepsilon\big[2\phi((1-\theta_k)y_h'|_{T_{k+1}} + (1+\theta_k)y_h'|_{T_k}) - (1+\theta_k)\phi(2y_h'|_{T_k}) - (1-\theta_k)\phi(2y_h'|_{T_{k+1}})\big].$$

For $b = \big((\ell_k-1)\varepsilon, (\ell_k+1)\varepsilon\big)$ and $x_k^h \in b$,

$$\bar{R}_e^b = \frac{1}{2}\varepsilon\big[2\phi((2-\theta_k)y_h'|_{T_{k+1}} + \theta_k y_h'|_{T_k}) - \theta_k\phi(2y_h'|_{T_{k+1}}) - (2-\theta_k)\phi(2y_h'|_{T_k})\big].$$

We then list the six cases that correspond to the bonds crossing the left and right atomistic to continuum interfaces.

One the left interface we have:

For $b = \big(\ell_k\varepsilon, (\ell_k+1)\varepsilon\big)$ and $x_k^h \in b$,

$$\bar{R}_e^b = \varepsilon\big[\phi((1-\theta_k)y_h'|_{T_{k+1}} + \theta_k y_h'|_{T_k}) - \theta_k\phi(y_h'|_{T_k}) - (1-\theta_k)\phi(y_h'|_{T_{k+1}})\big]$$

For $b = \big(\ell_k\varepsilon, (\ell_k+2)\varepsilon\big)$ and $x_k^h \in b$,

$$\begin{aligned}\bar{R}_e^b =& 2\varepsilon\big[\phi(y_h'|_{T_{k+2}} + \theta_k y_h'|_{T_k} + (1-\theta_k)y_h'|_{T_{k+1}}) \\ &- (2-\theta_k)\phi\big(\frac{2}{2-\theta_k}y_h'|_{T_{k+2}} + \frac{2(1-\theta_k)}{2-\theta_k}y_h'|_{T_{k+1}}\big) - \theta_k\phi(2y_h'|_{T_k})\big].\end{aligned}$$

For $b = \big((\ell_k-1)\varepsilon, (\ell_k+1)\varepsilon\big)$ and $x_k^h \in b$,

$$\bar{R}_e^b = 2\varepsilon\big[\phi((1-\theta_k)y_h'|_{T_{k+1}} + (1+\theta_k)\theta_k y_h'|_{T_k}) - (1-\theta_k)\phi(2y_h'|_{T_{k+1}}) - (1+\theta_k)\phi(2y_h'|_{T_k})\big].$$

One the right interface we have:

For $b = \big(\ell_k\varepsilon, (\ell_k+1)\varepsilon\big)$ and $x_k^h \in b$,

$$\bar{R}_e^b = \varepsilon\big[\phi((1-\theta_k)y_h'|_{T_{k+1}} + \theta_k y_h'|_{T_k}) - \theta_k\phi(y_h'|_{T_k}) - (1-\theta_k)\phi(y_h'|_{T_{k+1}})\big].$$

For $b = \big(\ell_k\varepsilon, (\ell_k+2)\varepsilon\big)$ and $x_k^h \in b$,

$$\bar{R}_e^b = 2\varepsilon\big[\phi((2-\theta_k)y_h'|_{T_{k+1}} + \theta_k y_h'|_{T_k}) - (2-\theta_k)\phi(2y_h'|_{T_{k+1}}) - \theta_k\phi\big(2y_h'|_{T_k}\big)\big].$$

For $b = \big((\ell_k-1)\varepsilon, (\ell_k+1)\varepsilon\big)$ and $x_k^h \in b$,

$$\begin{aligned}\bar{R}_e^b =& 2\varepsilon\big(\phi((1-\theta_k)y_h'|_{T_{k+1}} + \theta_k y_h'|_{T_k} + y_h'|_{T_{k-1}}) \\ &- (1+\theta_k)\phi\big(\frac{2\theta_k}{1+\theta_k}y_h'|_{T_k} + \frac{2}{1+\theta_k}y_h'|_{T_{k-1}}\big) - (1-\theta_k)\phi(2y_h'|_{T_{k+1}})\big).\end{aligned}$$

Appendix C

Alternative Estimate of the Residual of the External Force

In this appendix, we give an alternative estimate of the external residual as defined in Section 3.3.3. This alternate circumvent the continuity condition on the external force $f \in C^2(\bar{\Omega})$.

Upon defining $v_h := I_h v$, the residual of the external force is given by

$$\langle f, v_h \rangle_h - \langle f, v \rangle_\varepsilon, \tag{C.0.1}$$

where $f, v \in \mathcal{U}$.

To further analyze (C.0.1), we introduce a new partition $\mathcal{T}^r = \{T_j^r\}_{j=-\infty}^{+\infty}$ of the domain $\mathbb{R}$, such that all the nodes in partition $\mathcal{T}^\varepsilon$ and partition $\mathcal{T}^h$ are included in this partition. The indexing of the nodes in $\mathcal{T}^r$ follow the rule that the node x_k^h in $\mathcal{T}^h$ is labeled as $x_{j_k}^r$ in $\mathcal{T}^r$. We also assume there are n nodes in $\mathcal{T}^r$ in $[-1/2, 1/2]$, i.e.,

$$n = \big|\{\varepsilon, 2\varepsilon, \ldots, N\varepsilon\} \cup \{x_1, x_2, \ldots, x_K\}\big|,$$

where $|\mathcal{A}|$ denote the cardinality of a finite set $\mathcal{A}$ and are indexed from 1 to n. For the sake of presentation, we also index the nodes in T^ε, i.e., the nodes on the

reference lattice, from 1 to N in $(-1/2, 1/2]$ as opposed to from $-N+1$ to N in the main body of the thesis.

The inner product associated with $\mathcal{T}^r$ partition is then defined by

$$\langle f, g\rangle_r := \int_{-\frac{1}{2}}^{\frac{1}{2}} I_r(fg)\,\mathrm{d}x = \sum_{j=1}^{n} \frac{1}{2}(x_{j+1}^r - x_{j-1}^r) f_j^r g_j^r =: \langle f^r, g^r\rangle_r \quad \forall f, g \in C^0(\mathbb{R}), \tag{C.0.2}$$

where I_r is the linear nodal interpolation operator with respect to $\mathcal{T}^r$, and f^r and g^r are the vectorizations of f and g with respect to $\mathcal{T}^r$.

Now we decompose the residual of the external force into three parts by adding and subtracting the same terms,

$$\langle f, v_h\rangle_h - \langle f, v\rangle_\varepsilon = \big[\langle f, v\rangle_r - \langle f, v\rangle_\varepsilon\big] + \big[\langle f, v_h\rangle_r - \langle f, v\rangle_r\big] + \big[\langle f, v_h\rangle_h - \langle f, v_h\rangle_r\big]. \tag{C.0.3}$$

The following three lemma are derived to give the estimates of the three parts.

Lemma C.1. *Let f, v, f^r, v^r be the vectorizations of $f, v \in C^0(\mathbb{R})$ according to $\mathcal{T}^\varepsilon$ and $\mathcal{T}^r$. Then the following inequality holds*

$$\big|\langle f, v\rangle_r - \langle f, v\rangle_\varepsilon\big| = \big|\langle f^r, v^r\rangle_r - \langle f, v\rangle_\varepsilon\big| \leq \frac{1}{8}\varepsilon^2 \|f'\|_{\ell^2_\varepsilon(\mathcal{K}_U)} \|v'\|_{\ell^2_\varepsilon}, \tag{C.0.4}$$

where $\mathcal{K}_U = \big\{k \in \{1, \ldots, K\} : x_k \neq \ell_k \varepsilon\big\}$, in other words, $\mathcal{K}_U$ is the set of indices of the nodes x_k^h in $\mathcal{T}^h$ such that x_k^h does not coincide with any of the nodes in $\mathcal{T}^\varepsilon$.

Proof. We first write out the two inner products and eliminate the terms that are

the same

$$\begin{aligned}\langle f^r, v^r\rangle_r - \langle f, v\rangle_\varepsilon &= \sum_{\ell=1}^{n} \varepsilon^r_\ell \frac{1}{2}(f^r_\ell v^r_\ell + f^r_{\ell+1} v^r_{\ell+1}) - \sum_{\ell=1}^{N} \varepsilon \frac{1}{2}(f_\ell v_\ell + f_{\ell+1} v_{\ell+1}) \\ &= \sum_{k\in\mathcal{K}_U} \big(\varepsilon_{j_k} \frac{1}{2}(f^r_{j_k-1} v^r_{j_k-1} + f^r_{j_k} v^r_{j_k}) + \varepsilon_{j_k+1} \frac{1}{2}(f^r_{j_k} v^r_{j_k} + f^r_{j_k+1} v^r_{j_k+1})\big) \\ &\quad - \sum_{k\in\mathcal{K}_U} \varepsilon\big(f_{\ell_k} v_{\ell_k} + f_{\ell_k+1} v_{\ell_k+1}\big), \end{aligned} \tag{C.0.5}$$

as $\varepsilon_{j_k+2} = \varepsilon_{j_k+3} = \ldots = \varepsilon_{j_{k+1}-1} = \varepsilon$ and $f_{\ell_k+i} v_{\ell_k+i} = f^r_{j_k+i} v^r_{j_k+i}$, $\quad i = 1, 2, \ldots, \ell_{k+1} - \ell_k$, if $\ell_k \varepsilon \neq x_k$ and $\ell_{k+1}\varepsilon \neq x_{k+1}$.

For k such that $\ell_k \varepsilon \neq x_k$, by the definition of f, v, f^r and v^r, we have $f_{\ell_k} = f^r_{j_k-1}$, $v_{\ell_k} = v^r_{j_k-1}$, $f_{\ell_k+1} = f^r_{j_k+1}$ and $v_{\ell_k+1} = v^r_{j_k+1}$. We also have $f^r_{j_k} = (1-\theta_k) f_{\ell_k} + \theta_k f_{\ell_k+1}$ and $v^r_{j_k} = (1-\theta_k) v_{\ell_k} + \theta_k v_{\ell_k+1}$. Inserting these equalities, (C.0.5) can be estimated as

$$\begin{aligned}&\big|\langle f^r, v^r\rangle_r - \langle f, v\rangle_\varepsilon\big| \\ =&\Big| \sum_{k\in\mathcal{K}_U} \Big\{ \frac{1}{2}\theta_k \varepsilon f_{\ell_k} v_{\ell_k} + \frac{1}{2}\theta_k \varepsilon \big[(1-\theta_k) f_{\ell_k} + \theta_k f_{\ell_{k+1}}\big]\big[(1-\theta_k) v_{\ell_k} + \theta_k v_{\ell_k+1}\big] \\ &+ \frac{1}{2}(1-\theta_k)\varepsilon f_{\ell_k+1} v_{\ell_k+1} + \frac{1}{2}(1-\theta_k)\varepsilon \big[(1-\theta_k) f_{\ell_k} + \theta_k f_{\ell_k+1}\big]\big[(1-\theta_k) v_{\ell_k} + \theta_k v_{\ell_k+1}\big] \\ &- \frac{1}{2}\varepsilon f_{\ell_k} v_{\ell_k} - \frac{1}{2}\varepsilon f_{\ell_k+1} v_{\ell_k+1} \Big\}\Big| \\ =&\Big| \sum_{k\in\mathcal{K}_U} \frac{1}{2}\varepsilon \Big\{ \big[\theta_k(\theta_k-1)(f_{\ell_k+1} - f_{\ell_k}) v_{\ell_k+1}\big] - \big[\theta_k(\theta_k-1)(f_{\ell_k+1} - f_{\ell_k}) v_{\ell_k}\big] \Big\}\Big| \\ =& \sum_{k\in\mathcal{K}_U} \frac{1}{2}\varepsilon^3 \big|\theta_k(1-\theta_k) f'_{\ell_k+1} v'_{\ell_k+1}\big| \\ &\leq \frac{1}{8}\varepsilon^2 \Big(\sum_{k\in\mathcal{K}_U} \varepsilon |f'_{\ell_k+1}|^2 \Big)^{\frac{1}{2}} \Big(\sum_{k\in\mathcal{K}_U} \varepsilon |v'_{\ell_k+1}|^2 \Big)^{\frac{1}{2}} \leq \frac{1}{8}\varepsilon^2 \|f'\|_{\ell^2_\varepsilon(\mathcal{K}_U)} \|v'\|_{\ell^2_\varepsilon}, \end{aligned} \tag{C.0.6}$$

which concludes the proof. □

Remark C.1. If $\mathcal{K}_U = \emptyset$, i.e., every node in T^h is also in T^ε, which corresponds to the coarse-grained mesh in Chapter 2, then this part of the residual is 0.

Lemma C.2. *Let $f, v \in C^0(\mathbb{R}) \cap \mathcal{P}_1(\mathcal{T}^\varepsilon)$ and $v_h := I_h v \in C^0(\mathbb{R}) \cap \mathcal{P}_1(\mathcal{T}^h)$ be the $\mathcal{P}_1$ interpolation of v according to $\mathcal{T}^h$ partition. Let f^r, v^r and v_h^r be the $\mathcal{P}_1$ interpolation of f, v, v_h respectively according to $\mathcal{T}^r$, and $\mathcal{K}_c$ is defined in* (3.3.6)*. Then we have the following estimate*

$$\langle f, v_h\rangle_r - \langle f, v\rangle_r = \langle f^r, v_h^r\rangle_r - \langle f^r, v^r\rangle_r \leq \left[\sum_{k=\mathcal{K}_c} \tilde{h}_k^2 \|f^r\|^2_{\ell^2_{\bar{\varepsilon}^r}(\mathcal{D}_k^2)}\right]^{\frac{1}{2}} \|v'\|_{\ell^2_\varepsilon}, \tag{C.0.7}$$

$\bar{\varepsilon}_j^r = \frac{1}{2}(\varepsilon_j^r + \varepsilon_{j+1}^r)$, $\tilde{h}_k = \frac{1}{2}(j_{k+1} - j_k)\varepsilon$ *and* $\mathcal{D}_k^2 = \{j_k + 1, \ldots, j_{k+1} - 1\}$.

Proof. Using the fact that $(v_h^r)_{j_k} = v_{j_k}^r$ and by Cauchy-Schwarz inequality, we have

$$\begin{aligned}
\langle f^r, v_h^r\rangle_r - \langle f^r, v^r\rangle_r &= \sum_{j=1}^{n} \frac{1}{2}(\varepsilon_j^r + \varepsilon_{j+1}^r)(f_j^r (v_h^r)_j - f_j^r v_j^r) \\
&= \sum_{k\in\mathcal{K}_c} \sum_{j=j_{k-1}}^{j_k-1} \bar{\varepsilon}_j^r f_j^r \left[(v_h^r)_j - v_j^r\right] \\
&\leq \sum_{k\in\mathcal{K}_c} \left[\sum_{j=j_{k-1}+1}^{j_k-1} \bar{\varepsilon}_j^r (f_j^r)^2\right]^{\frac{1}{2}} \left\{\sum_{j=j_{k-1}+1}^{j_k-1} \bar{\varepsilon}_j^r \left[(v_h^r)_j - v_j^r\right]^2\right\}^{\frac{1}{2}},
\end{aligned} \tag{C.0.8}$$

where $\bar{\varepsilon}_j^r = \frac{1}{2}(\varepsilon_j^r + \varepsilon_{j+1}^r)$. Upon defining g such that $g_j = (v_h^r)_j - v_j^r$ (note $g_{j_k} = g_{j_{k+1}} = 0$) and by Lemma D.3 in Appendix D (Discrete Friedrich's Inequality) and Rieze-Thorin Theorem,

$$\left\{\sum_{j=j_{k-1}+1}^{j_k-1} \bar{\varepsilon}_j^r \left[(v_h^r)_j - v_j^r\right]^2\right\}^{\frac{1}{2}} = \left\{\sum_{j=j_{k-1}}^{j_k} \bar{\varepsilon}_j^r g_j^2\right\}^{\frac{1}{2}} \leq \frac{1}{2}(j_k - j_{k-1})\varepsilon \left\{\sum_{j=j_{k-1}+1}^{j_k} \varepsilon_j^r g_j'^2\right\}^{\frac{1}{2}}, \tag{C.0.9}$$

where $g_j' = \frac{g_j - g_{j-1}}{\varepsilon_j^r} = (v^r)_j' - (v_h^r)_j'$. ε appears in the last inequality since $\max_j \bar{\varepsilon}_j^r \leq \varepsilon$. Since v_h^r and v^r are both piecewise linear on $\mathcal{T}^r$, we have $(v_h^r)_j' - (v^r)_j' = (v' -$

$v_h')(x)\ \forall x \in (x^r_{j-1}, x^r_j)$, and as a result,

$$\Big\{ \sum_{j=j_{k-1}+1}^{j_k} \varepsilon^r_j \big[(v^r_h)'_j - (v^r)'_j\big]^2 \Big\}^{\frac{1}{2}} = \int_{x^r_{j_{k-1}}}^{x^r_{j_k}} |(v' - v'_h)(x)|^2 \,\mathrm{d}x = \|v' - v'_h\|_{L^2[x^r_{j_{k-1}}, x^r_{j_k}]}.$$

Since v'_h is the L^2 projection of v',

$$\|v' - v'_h\|_{L^2[x^r_{j_{k-1}}, x^r_{j_k}]} \le \|v'\|_{L^2[x^r_{j_{k-1}}, x^r_{j_k}]}.$$

Put all the results above together and apply Cauchy-Schwarz inequality, we obtain

$$\begin{aligned}
&\sum_{k\in\mathcal{K}_c} \Big[\sum_{j=j_{k-1}+1}^{j_k-1} \bar{\varepsilon}^r_j (f^r_j)^2 \Big]^{\frac{1}{2}} \Big\{ \sum_{j=j_{k-1}+1}^{j_k-1} \bar{\varepsilon}^r_j \big[(v^r_h)_j - v^r_j\big]^2 \Big\}^{\frac{1}{2}} \\
\le &\sum_{k\in\mathcal{K}_c} \Big\{ \tilde{h}_k \Big(\sum_{j=j_{k-1}+1}^{j_k-1} \bar{\varepsilon}^r_j f^{r2}_j \Big)^{\frac{1}{2}} \|v'\|_{L^2(x^r_{j_{k-1}}, x^r_{j_k})} \Big\} \\
\le &\Big[\sum_{k=\mathcal{K}_c} \tilde{h}^2_k \Big(\sum_{j=j_{k-1}+1}^{j_k-1} \bar{\varepsilon}^r_j f^{r2}_j \Big) \Big]^{\frac{1}{2}} \|v'\|_{L^2[-1/2,1/2]}. \qquad \text{(C.0.10)}
\end{aligned}$$

The eatimate in the theorem holds as $\|v'\|_{L^2[-1/2,1/2]} = \|v'\|_{\ell^2_\varepsilon}$ for $v \in C^0(\mathbb{R}) \cap \mathcal{P}_1(\mathcal{T}^\varepsilon)$. □

Lemma C.3. *Suppose f, v, v_h and f^r, v^r, v^r_h be the same as in Lemma C.2. We have the following estimate*

$$\begin{aligned}
&\langle f, v_h\rangle_h - \langle f, v_h\rangle_r \\
\le &\Big\{ \frac{1}{8} \Big[(n\varepsilon)^4 \sum_{k=\mathcal{K}_c} \hat{h}^4_{k+1} \|f^{r\prime\prime}\|^2_{\ell^2_{\bar{\varepsilon}^r}(\mathcal{D}^2_k)} \Big]^{\frac{1}{2}} + \Big[\sum_{k=\mathcal{K}_c} \hat{h}^4_{k+1} \|f^{r\prime}\|^2_{\ell^2_{\varepsilon^r}(\mathcal{D}^1_k)} \Big]^{\frac{1}{2}} \Big\} \|v'\|_{\ell^2_\varepsilon}. \qquad \text{(C.0.11)}
\end{aligned}$$

where $\mathcal{K}_c$ is defined in (3.3.6), *$\mathcal{D}^1_k = \{j_k + 1, \ldots, j_{k+1}\}$ and $\hat{h}_k$ will be defined in the proof.*

Proof. Since $I_h(fv_h)$ is also piecewise linear with respect to the $\mathcal{T}^r$ partition, we apply the trapezoidal rule here to evaluate $\langle f, v_h\rangle_h = \int_0^1 I_h(fv_h)\,\mathrm{d}x$ to obtain

$$\begin{aligned}
&\langle f, v_h\rangle_h - \langle f, v_h\rangle_r \\
&= \sum_{k\in\mathcal{K}_c}\Bigg\{\left[\frac{1}{2}\varepsilon^r_{j_{k-1}+1} I_h(fv_h)(x^r_k) + \sum_{j=j_{k-1}+1}^{j_k-1}\frac{1}{2}(\varepsilon^r_j+\varepsilon^r_{j+1}) I_h(fv_h)(x^r_j) + \frac{1}{2}\varepsilon^r_{j_k} I_h(fv_h)(x^r_{j_k})\right] \\
&\quad - \left[\frac{1}{2}\varepsilon^r_{j_{k-1}+1}(fv_h)(x^r_{j_{k-1}+1}) + \sum_{j=j_{k-1}+1}^{j_k-1}\frac{1}{2}(\varepsilon^r_j+\varepsilon^r_{j+1})(fv_h)(x^r_j) + \frac{1}{2}\varepsilon^r_{j_k}(fv_h)(x^r_{j_k})\right]\Bigg\}.
\end{aligned} \tag{C.0.12}$$

We define g and $\boldsymbol{G}$ such that $g_j = (fv_h)(x^r_j)$ and $G_j = (I_h(fv_h))(x^r_j)$. It is easy to check that $g_{j_k} = G_{j_k}$ and

$$G_{j_{k-1}+i} = g_{j_{k-1}} + \frac{\sum_{\ell=1}^{i}\varepsilon^r_{j_{k-1}+\ell}}{\varepsilon^h_k}(g_{j_k} - g_{j_{k-1}}) \quad \forall k\in\mathcal{K}_c \quad \textit{and} \quad i = 1,\dots,j_k - j_{k-1}, \tag{C.0.13}$$

where $\varepsilon^h_k = \sum_{j=j_{k-1}+1}^{j_k}\varepsilon^r_j = x_k - x_{k-1}$. Therefore, by Theorem D.4, we obatin the following estimate

$$\begin{aligned}
&|\langle f, v_h\rangle_h - \langle f^r, I_r v^h\rangle_r| \\
&= \left|\sum_{k\in\mathcal{K}_c}\left[\frac{1}{2}\varepsilon^r_{j_{k-1}}(g_{j_{k-1}} - G_{j_{k-1}}) + \sum_{j=j_{k-1}+1}^{j_k-1}\frac{1}{2}(\varepsilon^r_j+\varepsilon^r_{j+1})(g_j - G_j) + \frac{1}{2}\varepsilon^r_{j_k}(g_{j_k} - G_{j_k})\right]\right| \\
&\le \sum_{k\in\mathcal{K}_c}\frac{1}{4}\frac{\big((j_k - j_{k-1})\varepsilon\big)\big((j_k - j_{k-1}+1)\varepsilon\big)^2}{\varepsilon^h_k}\|g''\|_{\ell^1_{\bar{\varepsilon}^r}(\mathcal{D}^2_k)},
\end{aligned} \tag{C.0.14}$$

where g'' is the second finite difference derivative with respect to the $\mathcal{T}^r$.

By the definition of f^r and v^r_h, $g_j = (fv_h)(x^r_j) = f^r_j(v^r_h)_j$. Using $(v^r_h)''_j = 0\ \forall j \in \mathcal{D}^2_k$, g''_j can be written as

$$g''_j = (fv^r_h)''_j = (f^r)''_j(v^r_h)_j + \frac{\varepsilon^r_j}{\bar{\varepsilon}^r_j}(f^r)'_j(v^r_h)'_j + \frac{\varepsilon^r_{j+1}}{\bar{\varepsilon}^r_j}(f^r)'_{j+1}(v^r_h)'_{j+1}. \tag{C.0.15}$$

Noting that $\frac{\varepsilon^r}{\bar{\varepsilon}_j} \leq 2$ and $\frac{\varepsilon^r_{j+1}}{\bar{\varepsilon}_j} \leq 2$ and defining $\hat{h}_k := \left[\frac{((j_k - j_{k-1})\varepsilon)(j_k - j_{k-1}+1)\varepsilon)}{\varepsilon^h_k}\right]^{\frac{1}{2}}$, we have the following estimate

$$
\begin{aligned}
&\langle f, v_h\rangle_h - \langle f, v_h\rangle_r \\
\leq &\sum_{k\in\mathcal{K}_c} \frac{1}{4}\hat{h}_k^2\Big[\sum_{j=j_{k-1}+1}^{j_k-1} \bar{\varepsilon}^r_j \big|(f v_h^r)''_j\big|\Big] \\
\leq &\sum_{k\in\mathcal{K}_c} \frac{1}{4}\hat{h}_k^2\Big[\sum_{j=j_{k-1}+1}^{j_k-1} \bar{\varepsilon}^r_j \big|(f^r)''_j\big|\big|(v_h^r)_j\big| + 4\sum_{j=j_{k-1}+1}^{j_k} \varepsilon^r_j \big|(f^r)'_j\big|\big|(v_h^r)'_j\big|\Big] \\
\leq &\sum_{k\in\mathcal{K}_c} \frac{1}{4}\hat{h}_k^2\Big[\|f^{r\prime\prime}\|_{\ell^2_{\bar{\varepsilon}^r}(\mathcal{D}_k^2)}\|v_h^r\|_{\ell^2_{\bar{\varepsilon}^r}(\mathcal{D}_k^2)} + 4\|f^{r\prime}\|_{\ell^2_{\varepsilon^r(\mathcal{D}_k^1)}}\|(v_h^r)'\|_{\ell^2_{\varepsilon^r(\mathcal{D}_k^1)}}\Big] \\
\leq &\frac{1}{4}\Big[\sum_{k\in\mathcal{K}_c} \hat{h}_k^4\|f^{r\prime\prime}\|^2_{\ell^2_{\bar{\varepsilon}^r}(\mathcal{D}_k^2)}\Big]^{\frac{1}{2}}\|v_h^r\|_{\ell^2_{\bar{\varepsilon}^r}} + \Big[\sum_{k\in\mathcal{K}_c} \hat{h}_k^4\|f^{r\prime}\|^2_{\ell^2_{\varepsilon^r(\mathcal{D}_k^1)}}\Big]^{\frac{1}{2}}\|(v_h^r)'\|_{\ell^2_{\varepsilon^r}}.
\end{aligned}
\tag{C.0.16}
$$

For further estimate, we first bound $\|v_h^r\|_{\ell^2_{\bar{\varepsilon}^r}}$ by $\|(v_h^r)'\|_{\ell^2_{\varepsilon^r}}$. Since $v_h(x)$ is piecewise linear with respect to $\mathcal{T}^r$ partition, we can apply the trapezoidal rule to the integration on each element to get

$$
\sum_{j=1}^n \bar{\varepsilon}^r_j (v_h^r)_j = \sum_{j=1}^n \frac{1}{2}(\varepsilon^r_j + \varepsilon^r_{j-1})(v_h^r)_j = \sum_{j=1}^n \varepsilon^r_j \frac{1}{2}\big[(v_h^r)_j + (v_h^r)_{j+1}\big] = \int_{-\frac{1}{2}}^{\frac{1}{2}} v_h(x)\,\mathrm{d}x = 0.
\tag{C.0.17}
$$

The last equality holds by the periodic condition on v_h. Thus, we can apply Lemma D.2 in Appendix D and Riez-Thorin Theorem to obtain

$$
\|v_h^r\|_{\ell^2_{\bar{\varepsilon}^r}} \leq \frac{1}{2}n\varepsilon\Big(\sum_{j=1}^n \varepsilon^r_j (v_h^r)'^2_j\Big)^{\frac{1}{2}}.
\tag{C.0.18}
$$

Since $v_h'(x) = (v_h^r)'_j$ on (x^r_{j-1}, x^r_j),

$$
\sum_{j=1}^n \varepsilon^r_j (v_h^r)'^2_j = \int_0^1 (v_h')^2\,\mathrm{d}x = \|v_h'\|_{L^2[-1/2,1/2]}.
\tag{C.0.19}
$$

Again since v_h' is the L^2 projection of v', ,

$$\|v_h'\|_{L^2[0,1]} \leq \|v'\|_{L^2[0,1]} = \|v'\|_{\ell_\varepsilon^2}. \tag{C.0.20}$$

Combine these results, the estimate stated in the theorem is easy to establish. □

We present the theorem which essentially gives the estimate of the residual due to the pointwise defined external force, whose proof is a combination of the three lemma with the distribution to each element and thus omitted.

Theorem C.4. *For $f, v \in \mathcal{U}$ and $v_h := I_h v$, we have*

$$|\langle f, v_h\rangle_h - \langle f, v\rangle_\varepsilon| \leq \Big\{ \sum_{k\in\mathcal{K}_c} \eta_k^{f^2} \Big\}^{\frac{1}{2}} \|v'\|_{L^2[-1/2,1/2]}, \tag{C.0.21}$$

where

$$\begin{aligned}\eta_k^f =& \Big\{ \frac{1}{128}\big[\varepsilon^3 (f'_{\ell_{k-1}+1})^2 + \varepsilon^3 (f'_{\ell_k+1})^2\big]^2 + \tilde{h}_k^2 \|f^r\|^2_{\ell^2_{\tilde{\varepsilon}^r}(\mathcal{D}_k^2)} \\ &+ \frac{1}{64}(n\varepsilon)^4 \hat{h}_{k+1}^4 \|f^{r\prime\prime}\|^2_{\ell^2_{\tilde{\varepsilon}^r}(\mathcal{D}_k^2)} + \hat{h}_{k+1}^4 \|f^{r\prime}\|^2_{\ell^2_{\varepsilon^r}(\mathcal{D}_k^1)} \Big\}^{\frac{1}{2}},\end{aligned} \tag{C.0.22}$$

and $\mathcal{K}_c$ is defined in (3.3.6)*, $\mathcal{D}_k^2$ is defined in Lemma C.1, $\tilde{h}_k$, $\mathcal{D}_k^1$ is defined in Lemma C.2, and $\hat{h}_{k+1}$ is defined in Lemma C.3.*

Appendix D

Discrete Sobolev Inequalities on Non-uniform mesh

In this section, we prove some discrete Soblev inequalities on non-uniform mesh that are used in the estimate of the residual of pointwise defined external force in Appendix C. These results are extensions to the inequalities proved in [55, Lemma A.1, Lemma A.2, Theorem A.4] on non uniform mesh.

Lemma D.1. *Let* $g \in \mathbb{R}^L$, $\boldsymbol{\varepsilon}^0, \boldsymbol{\varepsilon}^1 \in \mathbb{R}^L$ *and* $\varepsilon_i^0, \varepsilon_i^1 > 0 \; \forall i = 1, \ldots, L$, $g' = (g_i')_{i=2}^L \in \mathbb{R}^{L-1}$, $g_i' := \frac{g_i - g_{i-1}}{\varepsilon^1}$ $i = 2, \ldots, L$. *If* $\sum_{i=1}^L \varepsilon_i^0 g_i = 0$, *then*

$$|g_i| \leq \frac{1}{h} \sum_{i=2}^{L} \bar{\varepsilon}_k^1 |g_k'| \phi_{i,k}, \tag{D.0.1}$$

where, $h = \sum_{i=1}^L \varepsilon_i^0$, $\phi_{i,k} = \sum_{\ell=1}^{k-1} \varepsilon_\ell^0$ *for* $k = 2, \ldots, i$ *and* $\phi_{i,k} = \sum_{\ell=k}^{L} \varepsilon_\ell^0$ *for* $k = i+1, \ldots, L$.

Proof. Let $i \in \{1, \ldots, L\}$, then

$$\begin{aligned} h|g_i| &= |hg_i - \sum_{j=1}^{L} \varepsilon_j^0 g_j| \\ &= |\sum_{j=1}^{L} \varepsilon_j^0 g_i - \sum_{j=1}^{L} \varepsilon_j^0 g_j| \\ &\leq \sum_{j=1}^{i-1} \varepsilon_j^0 |g_i - g_j| + \sum_{j=i+1}^{L} \varepsilon_j^0 |g_i - g_j|. \end{aligned}$$

Since

$$|g_i - g_j| = |\sum_{k=j+1}^{i} \varepsilon_k^1 g_k'|,$$

we have

$$\begin{aligned} h|g_i| &\leq \sum_{j=1}^{i-1} \varepsilon_j^0 \sum_{k=j+1}^{i} \varepsilon_k^1 |g_k'| + \sum_{j=i+1}^{L} \varepsilon_j^0 \sum_{k=i+1}^{j} \varepsilon_k^1 |g_k'| \\ &= \sum_{k=2}^{i} \varepsilon_k^1 |g_k'| (\sum_{j=1}^{k-1} \varepsilon_j^0) + \sum_{k=i+1}^{L} \varepsilon_k^1 |g_k'| (\sum_{j=k}^{L} \varepsilon_j^0) \\ &= \sum_{k=2}^{L} \varepsilon_k^1 |g_k'| \phi_{i,k}. \end{aligned}$$

Divide both sides by h, we obtain the stated result. □

Lemma D.2. *(Discrete Poincare's Inequality) Suppose that $L \geq 1$, $\boldsymbol{\varepsilon}^0, \boldsymbol{\varepsilon}^1 \in \mathbb{R}^L$ with $\varepsilon_i^0, \varepsilon_i^1 > 0$, $\forall i = 1, \ldots, L$. Let $g \in \mathbb{R}^L$ such that $\sum_{i=1}^{L} \varepsilon_i^0 g_i = 0$ and $g' = (g_i')_{i=2}^{L} \in \mathbb{R}^{L-1}$ such that $g_i' = \frac{g_i - g_{i-1}}{\varepsilon_i^1}$. Define $\mathcal{D}_0$ to be the set $\{1, \ldots, L\}$ and $\mathcal{D}_1$ to be the set $\{2, \ldots, L\}$, then*

$$\|g\|_{\ell^p_{\boldsymbol{\varepsilon}^0(\mathcal{D}_0)}} \leq \frac{1}{2} \frac{L^2 \max\{\max_{1 \leq i \leq L} \varepsilon_i^0, \max_{2 \leq k \leq L} \varepsilon_k^1\}^2}{h} \|g'\|_{\ell^p_{\boldsymbol{\varepsilon}^1(\mathcal{D}_1)}}, \tag{D.0.2}$$

for $p \in \{1, \infty\}$, where $h = \sum_{i=1}^{L} \varepsilon_i^0$.

Proof. Using the result of Lemma D.1, we have

$$\begin{aligned}\sum_{i=1}^{L} \varepsilon_i^0 |g_i| &\le \sum_{i=1}^{L} \frac{\varepsilon_i^0}{h} \sum_{k=2}^{i} \varepsilon_k^1 |g_k'| \phi_{i,k} + \sum_{i=1}^{L} \frac{\varepsilon_i^0}{h} \sum_{k=i+1}^{L} \varepsilon_k^1 |g_k'| \phi_{i,k} \\ &= \frac{1}{h} \Bigg[\sum_{k=2}^{L} \Big(\sum_{i=1}^{L} \varepsilon_i^0 \phi_{i,k} \Big) \varepsilon_k^1 |g_k'| \Bigg].\end{aligned}$$

Since

$$\sum_{i=1}^{L} \varepsilon_i^0 \phi_{i,k} \le \max_{1 \le i \le L} \varepsilon_i^0 \sum_{i=1}^{L} \phi_{i,k} = \max_{1 \le i \le L} \varepsilon_i^0 \Bigg[\sum_{i=1}^{k-1} \phi_{i,k} + \sum_{i=k}^{L} \phi_{i,k} \Bigg],$$

and

$$\begin{aligned}\sum_{i=1}^{k-1} \phi_{i,k} + \sum_{i=k}^{L} \phi_{i,k} &\le (k-1) \sum_{\ell=k}^{L} \varepsilon_\ell^0 + \big(L - (k-1)\big) \sum_{\ell=1}^{k-1} \varepsilon_\ell^0 \\ &\le \big[(k-1)\big(L-(k-1)\big) + \big(L-(k-1)\big)(k-1) \big] \max_{1 \le i \le L} \varepsilon_i^0 \\ &\le \frac{1}{2} \max_{1 \le i \le L} \varepsilon_i^0 L^2.\end{aligned}$$

Put these results together, we obtain the stated result for $p = 1$. For $p = \infty$,

$$\begin{aligned}|g_i| &\le \frac{1}{h} \sum_{k=2}^{L} \varepsilon_k^1 |g_k'| \phi_{i,k} \\ &\le \frac{1}{h} \Bigg[\sum_{k=2}^{i} \varepsilon_k^1 |g_k'| \phi_{i,k} + \sum_{k=i+1}^{L} \varepsilon_k^1 |g_k'| \phi_{i,k} \Bigg] \\ &\le \frac{1}{h} \sum_{k=2}^{L} \phi_{i,k} \max_{2 \le k \le L} \varepsilon_k^1 |g_k'| \\ &\le \frac{1}{2} \frac{L^2 \max_{1 \le i \le L} \varepsilon_i^0}{h} \max_{2 \le k \le L} \varepsilon_k^1 |g_k'|.\end{aligned}$$

The stated result is obtained by taking the maximum of ε_i^0 and ε_k^1 over $\mathcal{D}_0$ and $\mathcal{D}_1$. □

Lemma D.3. *(Discrete Friedrichs' Inequality) Suppose that $L \ge 1$, $\boldsymbol{\varepsilon}^0$, $\boldsymbol{\varepsilon}^1$, $\mathcal{D}_0$, $\mathcal{D}_2$ are the same as in Lemma D.2. Let $f \in \mathbb{R}^L$ such that $f_1 = f_L = 0$, and $f' = (f_i')_{i=2}^{L} \in \mathbb{R}^{L-1}$*

such that $f_i' = \frac{f_i - f_{i-1}}{\varepsilon_i^1}$, *then*

$$\|f\|_{\ell^p_{\varepsilon^0(\mathcal{D}_0)}} \leq \frac{1}{2}(L-1) \max_{2\leq i\leq L-1} \max\{\varepsilon_i^0, \varepsilon_i^1\} \|f'\|_{\ell^p_{\varepsilon^1(\mathcal{D}_1)}}, \tag{D.0.3}$$

for $p \in \{1, \infty\}$.

Proof. For $p = 1$,

$$\begin{aligned}
\sum_{i=1}^{L} \varepsilon_i^0 |f_i| &= \sum_{i=2}^{L-1} \varepsilon_i^0 |f_i| \\
&= \frac{1}{2} \sum_{i=2}^{L-1} \varepsilon_i^0 [|\sum_{j=2}^{i} (f_j - f_{j-1})| + |\sum_{j=i+1}^{L} (f_j - f_{j-1})|] \\
&\leq \frac{1}{2} \sum_{i=2}^{L-1} \varepsilon_i^0 [\sum_{j=2}^{i} \varepsilon_j^1 |f_j'| + \sum_{j=i+1}^{L} \varepsilon_j^1 |f_j'|] \\
&= \frac{1}{2} \sum_{i=2}^{L-1} \varepsilon_i^0 \sum_{j=1}^{L} \varepsilon_j^1 |f_j'| \\
&\leq \frac{1}{2}(L-1) \max_{2\leq i\leq L-1} \varepsilon_i^0 \sum_{j=1}^{L} \varepsilon_j^1 |f_j'|.
\end{aligned}$$

For $p = \infty$,

$$|f_i| \leq \sum_{j=2}^{i} \varepsilon_j^1 |f_j'| = (i-1) \max_{2\leq j\leq L} \varepsilon_j^1 \max_{2\leq j\leq L} |f_j'|,$$

and

$$|f_i| \leq \sum_{j=i+1}^{L} \varepsilon_j^1 |f_j'| = (L-i) \max_{2\leq j\leq L} \varepsilon_j^1 \max_{2\leq j\leq L} |f_j'|.$$

Thus we have

$$\begin{aligned}
\max_{i\in\mathcal{D}_0} |f_i| &\leq \min(i-1, L-i) \max_{2\leq j\leq L} \varepsilon_j^1 \max_{2\leq j\leq L} |f_j'| \\
&\leq \frac{1}{2}(L-1) \max_{2\leq j\leq L} \varepsilon_j^1 \max_{2\leq j\leq L} |f_j'|.
\end{aligned}$$

□

Remark D.1. The bounds we have got here are not optimal as if ε_i's and $\bar{\varepsilon}_j$'s vary too much, taking the maximum of them in the inequalities could significantly reduce the sharpness of the estimate. However, for the analysis of this paper, such a bound is optimal enough to produce efficient error estimators and we leave the work of looking for optimal bounds to future work.

Theorem D.4. *(bounds on the interpolation error) Let $L \geq 1$, $\boldsymbol{\varepsilon}^0, \boldsymbol{\varepsilon}^1, \boldsymbol{\varepsilon}^2 \in \mathbb{R}^L$, with $\varepsilon_i^0, \varepsilon_i^1, \varepsilon_i^2 > 0 \; \forall i = 1, \ldots, L$. Let $f \in \mathbb{R}^L$ and $\boldsymbol{F} = \in \mathbb{R}^L$ such that $F_1 = f_1$ and*

$$F_i = f_1 + \frac{\sum_{j=2}^{i} \varepsilon_i^0}{h}(f_L - f_1) \quad i = 2, \ldots, L, \tag{D.0.4}$$

where $h = \sum_{i=2}^{L} \varepsilon_i^0$. Define $f' = (f_i')_{i=2}^{L} \in \mathbb{R}^{L-1}$ such that $f_i' = \frac{f_i - f_{i-1}}{\varepsilon_i^1}$ and $f'' = (f_i'')_{i=2}^{L-1} \in \mathbb{R}^{L-2}$ such that $f_i'' = \frac{f_{i+1}' - f_i'}{\varepsilon_i^2}$, and $\boldsymbol{F}'$ and $\boldsymbol{F}''$ are defined in the same way. Let $\mathcal{D}_0$, $\mathcal{D}_1$ be the same sets defined in Lellmma D.2 and $\mathcal{D}_2$ be the set $\{2, \ldots, L-1\}$. Then, for $p \in \{1, \infty\}$,

$$\|f - \boldsymbol{F}\|_{\ell^p_{\boldsymbol{\varepsilon}^0}(\mathcal{D}_0)} \leq \frac{1}{4} \frac{L^3 \max_{2 \leq i \leq L-1} \varepsilon_i^0 \max_{2 \leq j \leq L-1} \varepsilon_j^1 \max_{2 \leq k \leq L-1} \varepsilon_j^2}{h} \|f''\|_{\ell^p_{\boldsymbol{\varepsilon}^2}(\mathcal{D}_2)}. \tag{D.0.5}$$

Proof. Let $g = f - \boldsymbol{F}$, by the definition of $\boldsymbol{F}$, we have $g_1 = g_L = 0$ and

$$\sum_{i=2}^{L} \varepsilon_i g_i' = \sum_{i=2}^{L} (f_i - f_{i-1}) - \sum_{i=2}^{L} (F_i - F_{i-1}) = 0.$$

By Lemma D.3,

$$\|g\|_{\ell^p_{\boldsymbol{\varepsilon}^1}(\mathcal{D}_0)} \leq \frac{1}{2}(L-1) \max_{2 \leq i \leq L-1} \max\{\varepsilon_i^0, \varepsilon_i^1\} \|g'\|_{\ell^p_{\boldsymbol{\varepsilon}}(\mathcal{D}_1)},$$

as $g_1 = g_L = 0$, and by Lemma D.2,

$$\|g'\|_{\ell^p_{\boldsymbol{\varepsilon}}(\mathcal{D}_1)} \leq \frac{1}{2} \frac{L^2 \max\{\max_{1 \leq i \leq L} \varepsilon_i^1, \max_{2 \leq k \leq L-1} \varepsilon_k^2\}^2}{h} \|g''\|_{\ell^p_{\bar{\boldsymbol{\varepsilon}}}(\mathcal{D}_2)},$$

as $\sum_{i=2}^{L} \varepsilon_i g_i' = 0$. Since $\boldsymbol{F}'' = 0$, from which we know $g'' = f''$, the stated estimate holds. □

Bibliography

[1] M. Arndt and M. Griebel. Derivation of higher order gradient continuum models from atomistic models for crystalline solids. *Multiscale Model. Simul.*, 4(2):531–562 (electronic), 2005.

[2] Marcel Arndt and Mitchell Luskin. Goal-oriented atomistic-continuum adaptivity for the quasicontinuum approximation. *Int. J. Multiscale Comput. Engrg.*, 5(49-50):407–415, 2007.

[3] Marcel Arndt and Mitchell Luskin. Error estimation and atomistic-continuum adaptivity for the quasicontinuum approximation of a Frenkel-Kontorova model. *Multiscale Model. Simul.*, 7(1):147–170, 2008.

[4] Marcel Arndt and Mitchell Luskin. Goal-oriented adaptive mesh refinement for the quasicontinuum approximation of a Frenkel-Kontorova model. *Comput. Methods Appl. Mech. Engrg.*, 197(49-50):4298–4306, 2008.

[5] Ted Belytschko, Wing Kam Liu, and Brian Moran. Nonlinear finite elements for continua and structures. 2000.

[6] X. Blanc, C. Le Bris, and P.-L. Lions. From molecular models to continuum mechanics. *Arch. Ration. Mech. Anal.*, 164(4):341–381, 2002.

[7] D Braess. *Finite Elements, Theory, Fast Solvers, and Applications in Solid Mechanics, 3rd Edition*. Cambridge University Press, Cambridge, 2007.

[8] S. Brenner and R. Scott. *The Mathematical Theory of Finite Element Methods, 3rd Edition*. Springer, New York, 2008.

[9] Jeremy Q. Broughton, Farid F. Abraham, Noam Bernstein, and Efthimios Kaxiras. Concurrent coupling of length scales: Methodology and application. *Phys. Rev. B*, 60:2391–2403, Jul 1999.

[10] P. G. Ciarlet. *The finite element method for elliptic problems*, volume 40 of *Classics in Applied Mathematics*. Society for Industrial and Applied Mathematics (SIAM), Philadelphia, PA, 2002. Reprint of the 1978 original.

[11] M. S. Daw and M. I. Baskes. Embedded-atom method: Derivation and application to impurities, surfaces, and other defects in metals. *Physical Review B*, 20, 1984.

[12] Murray S. Daw and M. I. Baskes. Embedded-atom method: Derivation and application to impurities, surfaces, and other defects in metals. *Phys. Rev. B*, 29:6443–6453, Jun 1984.

[13] M. Dobson and M. Luskin. Analysis of a force-based quasicontinuum approximation. *M2AN Math. Model. Numer. Anal.*, 42(1):113–139, 2008.

[14] M. Dobson and M. Luskin. Iterative solution of the quasicontinuum equilibrium equations with continuation. *J. Sci. Comput.*, 37(1):19–41, 2008.

[15] M. Dobson and M. Luskin. An analysis of the effect of ghost force oscillation on the quasicontinuum error. *M2AN Math. Model. Numer. Anal.*, 43(3):591–604, 2009.

[16] M. Dobson and M. Luskin. An optimal order error analysis of the one-dimensional quasicontinuum approximation. *SIAM J. Numer. Anal.*, 47(4):2455–2475, 2009.

[17] M. Dobson, M. Luskin, and C. Ortner. Accuracy of quasicontinuum approximations near instabilities. *J. Mech. Phys. Solids*, 58:1741–1757, 2010.

[18] M. Dobson, M. Luskin, and C. Ortner. Stability, instability, and error of the force-based quasicontinuum approximation. *Arch. Ration. Mech. Anal.*, 197(1):179–202, 07 2010.

[19] W. Dörfler. A convergent adaptive algorithm for poissons equation. *SIAM J. Numer. Anal.*, 33:1106–1124, 1996.

[20] W. E, J. Lu, and J.Z. Yang. Uniform accuracy of the quasicontinuum method. *Phys. Rev. B*, 74(21):214115, 2006.

[21] W. E and P. Ming. Analysis of the local quasicontinuum method. In *Frontiers and prospects of contemporary applied mathematics*, volume 6 of *Ser. Contemp. Appl. Math. CAM*, pages 18–32. Higher Ed. Press, Beijing, 2005.

[22] W. E and P. Ming. Cauchy-Born rule and the stability of crystalline solids: dynamic problems. *Acta Math. Appl. Sin. Engl. Ser.*, 23(4):529–550, 2007.

[23] W. E and P. Ming. Cauchy-Born rule and the stability of crystalline solids: static problems. *Arch. Ration. Mech. Anal.*, 183(2):241–297, 2007.

[24] Bernhard Eidel and Alexander Stukowski. A variational formulation of the quasicontinuum method based on energy sampling in clusters. *Journal of the Mechanics and Physics of Solids*, 57(1):87 – 108, 2009.

[25] J. L. Ericksen. On the Cauchy-Born rule. *Math. Mech. Solids*, 13(3-4):199–220, 2008.

[26] F. C. Frank and J. H. van der Merwe. One-dimensional dislocations. i. static theory. *Proceedings of the Royal Society of London. Series A. Mathematical and Physical Sciences*, 198(1053):205–216, 1949.

[27] M. Gunzburger and Y. Zhang. A quadrature-rule type approximation to the quasi-continuum method. *Multiscale Model. Simul.*, 8(2):571–590, 2010.

[28] J.E. Jones. On the determination of molecular fields. iii. from crystal measurements and kinetic theory data. *Proc. Roy. Soc. London A.*, 106:709–718, 1924.

[29] J. Knap and M. Ortiz. An analysis of the quasicontinuum method. *J. Mech. Phys. Solids*, 49:1899–1923, 2001.

[30] X. Li, M. Luskin, and C. Ortner. Positive-definiteness of the blended force-based quasicontinuum method. *ArXiv e-prints*, 1112.2528, 2011.

[31] X.H. Li and M. Luskin. A generalized quasi-nonlocal atomistic-to-continuum coupling method with finite range interaction. *ArXiv e-prints*, 1007.2336v2, 2011.

[32] P. Lin. Theoretical and numerical analysis for the quasi-continuum approximation of a material particle model. *Math. Comp.*, 72(242):657–675, 2003.

[33] P. Lin. Convergence analysis of a quasi-continuum approximation for a two-dimensional material without defects. *SIAM J. Numer. Anal.*, 45(1):313–332, 2007.

[34] P. Lin and A. Shapeev. Energy-based ghost force removing techniques for the quasicontinuum method. *ArXiv e-prints*, 0909.5437v1, 2009.

[35] J. Lu and P. Ming. Convergence of a force-based hybrid method for atomistic and continuum models in three dimension. *ArXiv e-prints*, 1102.2523v2, 2011.

[36] M. Luskin and C. Ortner. Atomistic-to-continuum coupling. *to appear in Springer Encyclopedia for Applied and Computational Methods*.

[37] M. Luskin and C. Ortner. An analysis of node-based cluster summation rules in the quasicontinuum method. *SIAM J. Numer. Anal.*, 47(4):3070–3086, 2009.

[38] M. Luskin, C. Ortner, and B. Van Koten. Formulation and optimization of the energy-based blended quasicontinuum method. *ArXiv e-prints*, 1112.2377, 2011.

[39] Mitchell Luskin and Christoph Ortner. An analysis of node-based cluster summation rules in the quasicontinuum method. *SIAM J. Numer. Anal.*, 47(4):3070–3086, 2009.

[40] C. Makridakis, C. Ortner, and E. Süli. Stress-based atomistic/continuum coupling: a new variant of the quasicontinuum approximation. *International Journal for Multiscale Computational Engineering*, 2010.

[41] C. Makridakis, C. Ortner, and E. Süli. A priori error analysis of two force-based atomistic/continuum models of a periodic chain. *Numerische Mathematik*, pages 1–39, 2011. 10.1007/s00211-011-0380-5.

[42] S Martin. *Principle of Functional Analysis*. American Mathematical Society, Providence, Rhode Island, 2002.

[43] R. E. Miller and E. B. Tadmor. The quasicontinuum method: Overview, applications and current directions. *Journal of Computer-Aided Materials Design*, 9:203–239, 2003.

[44] Ronald E Miller and E B Tadmor. A unified framework and performance benchmark of fourteen multiscale atomistic/continuum coupling methods. *Modelling Simul. Mater. Sci. Eng.*, 17(5):053001, 2009.

[45] P. Ming and J. Yang. Analysis of a one-dimensional nonlocal quasi-continuum method. *Multiscale Model. Simul.*, 7(4):1838–1875, 2009.

[46] P. Morin, R. H. Nochetto, and K. G. Siebert. Data oscillation and convergence of adaptive fem. *SIAM J. Numer. Anal.*, 38:466–488, 2000.

[47] P.M. Morse. Diatomic molecules according to the wave mechanics. ii. vibrational levels. *Phys.Rev.*, 34:57–64, 1929.

[48] M. Ortiz, R. Phillips, and E. B. Tadmor. Quasicontinuum analysis of defects in solids. *Philosophical Magazine A*, 73(6):1529–1563, 1996.

[49] C. Ortner. Gradient flows as a selection procedure for equilibria of nonconvex energies. *SIAM J. Math. Anal.*, 38(4):1214–1234, 2006.

[50] C. Ortner. A posteriori existence in numerical computations. *SIAM J. Numer. Anal.*, 47(4):2550–2577, 2009.

[51] C. Ortner. A priori and a posteriori analysis of the quasinonlocal quasicontinuum method in 1D. *Math. Comp.*, 80(275):1265–1285, 2011.

[52] C. Ortner. The role of the patch test in 2D atomistic-to-continuum coupling methods. *ESAIM Math. Model. Numer. Anal.*, 46, 2012.

[53] C. Ortner and M. Luskin. Atomistic-to-continuum coupling. In preparation.

[54] C. Ortner and A. Shapeev. Analysis of an Energy-based Atomistic/Continuum Coupling Approximation of a Vacancy in the 2D Triangular Lattice, forthcoming.

[55] C. Ortner and E. Süli. Analysis of a quasicontinuum method in one dimension. *M2AN Math. Model. Numer. Anal.*, 42(1):57–91, 2008.

[56] C. Ortner and F. Theil. Nonlinear elasticity from atomistic mechanics. *ArXiv e-prints*, 1202.3858v3, 2012.

[57] C. Ortner and H. Wang. A priori error estimates for energy-based quasicontinuum approximations of a periodic chain. *Math. Models Methods Appl. Sc.*, 21:2491–2521, 2011.

[58] C. Ortner and L. Zhang. Construction and sharp consistency estimates for atomistic/continuum coupling methods with general interfaces: a 2d model problem, 2011. arXiv:1110.0168v1.

[59] Serge. Prudhomme, Paul. Bauman, and Tinsley Oden. Error control for molecular statics problems. *Int. J. Multiscale Comput. Engrg.*, 4:647–662, 2007.

[60] Serge Prudhomme, Ludovic Chamoin, Hachmi Ben Dhia, and Paul T. Bauman. An adaptive strategy for the control of modeling error in two-dimensional atomic-to-continuum coupling simulations. *Computer Methods in Applied Mechanics and Engineering*, 198(21-26):1887 – 1901, 2009.

[61] Dong Qian, Gregory J. Wagner, and Wing Kam Liu. A multiscale projection method for the analysis of carbon nanotubes. *Computer Methods in Applied Mechanics and Engineering*, 193(17-20):1603–1632, 2004.

[62] W. Rudin. *Principle of Mathematical Analysis*. McGraw-Hill, New York, 1976.

[63] A. V. Shapeev. Consistent energy-based atomistic/continuum coupling for two-body potentials in three dimensions, 2011. arXiv:1108.299.

[64] Alexander V. Shapeev. Consistent energy-based atomistic/continuum coupling for two-body potentials in one and two dimensions. *Multiscale Model. Simul.*, 9(3):905–932, 2011.

[65] V. B. Shenoy, R. Miller, E. B. Tadmor, R. Phillips, and M. Ortiz. Quasicontinuum models of interfacial structure and deformation. *Phys. Rev. Lett.*, 80(4):742–745, Jan 1998.

[66] V. B. Shenoy, R. Miller, E. B. Tadmor, D. Rodney, R. Phillips, and M. Ortiz. An adaptive finite element approach to atomic-scale mechanics–the quasicontinuum method. *J. Mech. Phys. Solids*, 47(3):611–642, 1999.

[67] T. Shimokawa, J. J. Mortensen, J. Schiøtz, and K. W. Jacobsen. Matching conditions in the quasicontinuum method: Removal of the error introduced at the interface between the coarse-grained and fully atomistic region. *Phys. Rev. B*, 69:214104, Jun 2004.

[68] Frank H. Stillinger and Thomas A. Weber. Computer simulation of local order in condensed phases of silicon. *Phys. Rev. B*, 31:5262–5271, Apr 1985.

[69] G. Strang and G Fix. *An Analysis of the Finite Element Method*. Wellesley-Cambridge Press, Cambridge, 2008.

[70] E Süli and D. F. Mayers. *An introduction to numerical analysis*. Cambridge University Press, Cambridge, 2003.

[71] B. Van Koten and M. Luskin. Analysis of energy-based blended quasicontinuum approximations. *Siam J. Numer. Anal*, 49(5):2182–2209, 2011.

[72] R. Verfürth. *A Review of A Posterori Error Estimation and Adaptive Mesh-Refinement Techniques*. Wiley-Teubner, Germany, 1996.

[73] Gregory J. Wagner and Wing Kam Liu. Coupling of atomistic and continuum simulations using a bridging scale decomposition. *Journal of Computational Physics*, 190(1):249 – 274, 2003.

[74] H. Wang. A posteriori error estimates for energy-based quasicontinuum approximations of a periodic chain, 2011. arXiv:1112.5480.

[75] S.P. Xiao and T. Belytschko. A bridging domain method for coupling continua with molecular dynamics. *Computer Methods in Applied Mechanics and Engineering*, 193(17-20):1645–1669, 2004.

[76] O. C. Zienkiewicz and J. Z. Zhu. A simple error estimator and adaptive procedure for practical engineerng analysis. *Int. J. Numer. Meth. Engng.*, 24:337357, 1987.

[77] P. F. Zou and R. F. W. Bader. A topological definition of a Wigner–Seitz cell and the atomic scattering factor. *Acta Crystallographica Section A*, 50(6):714–725, Nov 1994.